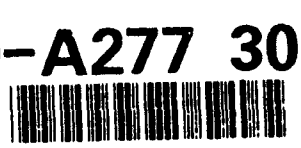

NAVAL POSTGRADUATE SCHOOL
Monterey, California

THESIS

ENSO FORCED VARIATIONS OF THE SEA SURFACE TEMPERATURE AND ADJUSTED SEA LEVEL ALONG THE WEST COAST OF THE UNITED STATES

by

John B. Skillman

December 1993

Co-Advisor: Franklin B. Schwing
Co-Advisor: Curtis A. Collins

REPORT DOCUMENTATION PAGE

Form Approved
OMB No. 0704-0188

1. AGENCY USE ONLY (Leave blank)	2. REPORT DATE	3. REPORT TYPE AND DATES COVERED
	17 December 1993	Master's Thesis

4. TITLE AND SUBTITLE
ENSO Forced Variations of Sea Surface Temperature and Sea Level Along the West Coast of the United States

5. FUNDING NUMBERS

6. AUTHOR(S)
Skillman, John B.

7. PERFORMING ORGANIZATION NAME(S) AND ADDRESS(ES)
Naval Postgraduate School
Monterey, CA 93943-5000

8. PERFORMING ORGANIZATION REPORT NUMBER

9. SPONSORING/MONITORING AGENCY NAME(S) AND ADDRESS(ES)

10. SPONSORING/MONITORING AGENCY REPORT NUMBER

11. SUPPLEMENTARY NOTES

12a. DISTRIBUTION/AVAILABILITY STATEMENT
Approved for public release, distribution is unlimited.

12b. DISTRIBUTION CODE

13. ABSTRACT *(Maximum 200 words)*

Daily coastal surface temperature and adjusted sea level data for the period 1955-1988 were used to characterize the surface temperature and adjusted sea level anomalies, and the propagation of features along the west coast of the United States during El Niño-Southern Oscillation (ENSO). The strong ENSO years examined were 1957-58, 1972-73, and 1982-83. Moderate ENSO years used were 1966, 1976, and 1987. To look at regional differences in the signals, the time series of daily coastal surface temperature and adjusted sea level were divided into three distinct regions: the southern region (i.e., Southern California), the central upwelling region (i.e., Central California), and the northern region (i.e., Northern California, Oregon, and Washington). The anomaly series were compared with cross-spectral analysis. Phase speeds and wavenumbers were estimated from the difference in phase between La Jolla and the other stations as a function of frequency band. These were used to characterize the structure of waves associated with the propagation of the positive surface temperature and adjusted sea level anomalies. These wave characteristics were found to be consistent with coastally trapped internal Kelvin waves, due to their phase speed, wavelength and non-dispersive nature. Phase speeds for frequencies corresponding to 4-20 day periods were 60-100 km/day, based on temperature and sea level. A regression of wavenumber against frequency gives phase speeds of about 65-85 km/day, that is consistent with Kelvin wave theory for typical west coast ocean structure and bathymetry. During ENSO episodes, strong warm surface temperature anomalies were found to exist along the west coast and were supported by high adjusted sea level anomalies. The use of daily observations was advantageous over traditional monthly data for this analysis.

14. SUBJECT TERMS
El Niño, Teleconnection, Internal Kelvin Waves

15. NUMBER OF PAGES
103

16. PRICE CODE

17. SECURITY CLASSIFICATION OF REPORT	18. SECURITY CLASSIFICATION OF THIS PAGE	19. SECURITY CLASSIFICATION OF ABSTRACT	20. LIMITATION OF ABSTRACT
UNCLASSIFIED	UNCLASSIFIED	UNCLASSIFIED	UL

Approved for public release; distribution is unlimited.

ENSO Forced Variations of Sea Surface Temperature and
Sea Level Along the West Coast of the United States

by

John B. Skillman
Lieutenant, United States Navy
B. S., United States Naval Academy, 1986

Submitted in partial fulfillment
of the requirements for the degree of

MASTER OF SCIENCE IN PHYSICAL OCEANOGRAPHY

from the

NAVAL POSTGRADUATE SCHOOL
December 1993

Author: _____
John B. Skillman

Approved By: _____
Franklin B. Schwing, Co-Advisor

_____
Curtis A. Collins, Co-Advisor and Chairman
Department of Oceanography

ABSTRACT

Daily coastal surface temperature and adjusted sea level data for the period 1955-1988 were used to characterize the surface temperature and adjusted sea level anomalies, and the propagation of features along the west coast of the United States during El Niño-Southern Oscillation (ENSO). The strong ENSO years examined were 1957-58, 1972-73, and 1982-83. Moderate ENSO years used were 1966, 1976, and 1987. To look at regional differences in the signals, the time series of daily coastal surface temperature and adjusted sea level were divided into three distinct regions: the southern region (i.e., Southern California), the central upwelling region (i.e., Central California), and the northern region (i.e., Northern California, Oregon, and Washington).

The anomaly series were compared with cross-spectral analysis. Phase speeds and wavenumbers were estimated from the difference in phase between La Jolla and the other stations as a function of frequency band. These were used to characterize the structure of waves associated with the propagation of the positive surface temperature and adjusted sea level anomalies. These wave characteristics were found to be consistent with coastally trapped internal Kelvin waves, due to their phase speed, wavelength and non-dispersive nature. Phase speeds for frequencies corresponding to 4-20 day periods were 60-100 km/day, based on temperature and sea level. A regression of wavenumber against frequency gives phase speeds of about 65-85 km/day, that is consistent with Kelvin wave theory for typical west coast ocean structure and bathymetry. During ENSO episodes, strong warm surface temperature anomalies were found to exist along the west coast and were supported by high adjusted sea level anomalies. The use of daily observations was advantageous over traditional monthly data for this analysis.

TABLE OF CONTENTS

LIST OF TABLES

LIST OF FIGURES

FIGURE PAGE

ACKNOWLEDGMENTS

I would like to thank Patricia Walker and Dr. John McGown, Marine Life Research Group, Scripps Institution of Oceanography for the coastal sea surface temperature data, NOAA for the sea level data and NAVOCEANCOMDET Asheville for the pressure data I required for my analysis. I would also thank Dr. Curt Collins, who provided insights and help from his vast knowledge in the field, and Mr. Paul Jessen, who provided insights into MATLAB programming.

My sincere thanks and appreciation to my advisor Dr. Frank Schwing, who worked untiringly with me until the completion of this project. I could not have had a better mentor. Finally, I must thank my wife, Jacey, who provided the support, love and understanding necessary to keep me in my "ambition room" and complete this thesis.

I. INTRODUCTION

El Niño means change. El Niño is a coupled air-ocean phenomenon which forms in the tropical Pacific and has global climatic and economic ramifications. It may cause severe shifts in the expected weather for large continental regions over the entire Earth. These changes may result in unusual drought or heavy rain conditions that vary the expected agricultural production. Oceanic conditions also change. El Niño is marked by significant changes in water mass characteristics such as warming along the west coast of the Americas. This warming may shift the normal range of various species, drastically changing the composition of the biomass and species diversity for a given region.

The term El Niño originally referred to a warm water current off the coast of Ecuador and Peru. Since this event typically begins around Christmas, it was given a name that means "The Child" (*Rasmusson and Carpenter*, 1981). The term has subsequently been applied to a much stronger and widespread climatic phenomenon, which is "associated with geographically extensive sea surface temperature (SST) anomalies of a standard deviation or more for extended periods of many months to more than a year" (*Enfield*, 1989).

El Niño observations began with the accounts of a 1525-1526 event by Xeres, Secretary to Francisco Pizzaro, in 1534. Accounts of all El Niño-type events have been compiled and analyzed by *Quinn et al.*(1987). They determined that the average period between any El Niño event is 3.8 years, but that the intensity of the event varies radically. In their study, they have broken the events into categories of very strong, strong, moderate and near moderate.

The Southern Oscillation is the atmospheric counterpart of El Niño. Together, they form a coupled system. El Niño/Southern Oscillation (ENSO) consists of a decreased pressure gradient between the Southeast Pacific high and the Indonesian low causing a

weakening of the easterly trade winds. The weakening of the trade wind allows for a cessation of the normal equatorial upwelling in the Eastern Pacific. The oceanic heating center moves equatorward and eastward toward the dateline. Westerly winds cause equatorial Kelvin waves which propagate toward South America. These waves impact the west coast of South America and relay the ENSO signal poleward in both hemispheres in the form of internal Kelvin waves and westward in the form of near-equatorial Rossby waves. These Rossby waves may eventually cause a relaxation of the event (*Enfield*, 1989). The poleward propagating internal Kelvin waves gradually lose energy through the generation of westward Rossby waves.

The purpose of this study is to provide a closer look at the high sea surface temperature and adjusted sea level anomalies, and the propagation of these events associated with the effects of El Niño-Southern Oscillation (ENSO) on the west coast of the United States. To accomplish this, daily coastal surface temperature and adjusted sea level data are used to characterize the temperature and adjusted sea level anomalies associated with ENSO. The regional differences for the anomalies are identified along the west coast of the United States. Phase speeds are estimated to characterize the waves associated with the propagation of the warm surface temperature and high adjusted sea level anomalies. This study also provides an exploratory look at applications for daily sea surface temperature data.

The analysis covers the period 1955-1988. Known strong ENSO years, moderate ENSO years and, non-ENSO years based on *Quinn et al.* (1987) were selected for analysis and comparison. The strong ENSO years used are 1957-58, 1972-73, and 1982-83. Moderate ENSO years used are 1966, 1976, and 1987.

Time series of daily coastal surface temperature and adjusted sea level are divided into three distinct regions for the west coast: the southern region (i.e., Southern California), the central upwelling region (i.e., Central California), and the northern region (i.e., Northern California, Oregon, and Washington).

A. BACKGROUND

The most useful research related to this study was by *Robinson* (1972), who used daily sea surface temperatures, *Smith* (1978), who observed waves of 4-20 day periods off Peru during ENSO events, and *Enfield and Allen* (1980), *Huyer and Smith* (1985), and *Norton et al.* (1985), who focused on the teleconnection of the ENSO signal between the equator and the west coast of the United States. Unpublished data from *Francisco Chavez,* provides direct evidence of the presence of internal Kelvin waves in a high resolution temperature time series.

Robinson (1972) was an early attempt at using the long-term daily coastal temperature data set to draw conclusions concerning the interannual variability of the west coast of North America. Her study provides a general overview and makes only limited statements concerning "highly anomalous" signals corresponding to the El Niño events of 1953 and 1957-58. This was the first description of these data and only a cursory examination was undertaken.

Enfield and Allen (1980) showed the behavior and relationship of the anomalies of monthly mean sea level and monthly coastal sea surface temperature. Data used were from 1950-1974 for stations from Yakutat, Alaska (59°N) to Valparaiso, Chile (33°S). The analysis showed that the sea level anomalies had a well-defined lag with respect to the occurrence of the event at the equator. This lag supports poleward coastal propagation. They argue that the observed features were internal Kelvin waves. Phase speeds for lagged cross-correlations between Northern and Southern Hemisphere stations were 180±100 km/day. They compared phase spectra of sea level station pairs in the interannual band (2-5 years) and found phase speeds of 75 km/day. Temperature was less coherent for spatial variations. The temperature record lagged the sea level record by two to six months. This lag was attributed to coastal influences on the record.

Smith (1978) found evidence of shorter than annual frequencies off Peru during ENSO events. These frequencies correspond to 4-20 day periods. This frequency band is used for the analysis in this study of event propagation and phase speed determination of the events. He also observed stronger upwelling-favorable winds off Peru during an El Niño. The observed thickening of the warm water layer prevented nutrients from being upwelled.

Huyer and Smith (1985) focused on the 1982-83 ENSO off the coast of Oregon. Their analysis was similar to *Enfield and Allen* (1980). They found a lagged cross-correlation phase speed of approximately 140 km/day.

Norton et al. (1985) primarily focused on the 1982-83 event off Baja and Alta California. The analysis supports the coastally trapped internal Kelvin wave mechanism for oceanic teleconnection of the ENSO. They use the Pacific/North American (PNA) index to explain atmospheric teleconnection of the ENSO to California. They define a California El Niño as the teleconnected signal of the tropical ENSO to the west coast of the United States. The associated rises in sea surface temperature and sea level are caused by either the atmospheric or oceanic teleconnection, or both. From the oceanic teleconnection, the coastally trapped internal Kelvin wave activity causes a depression of the thermocline along the coast leading to an associated northward counter-current flow. This alteration of the California Current System (CCS) brings warmer water in toward the coast. The atmospheric teleconnection may foster downwelling-favorable winds, with associated Ekman convergence at the coast, which would enhance the northward counter-current flow. They also explain how basin-wide forces act to force subarctic water away from the CCS, allowing warmer water to be transported to the coast.

Francisco Chavez (personal communication) found direct evidence of internal Kelvin waves based on high resolution temperature time series for an extended length of time during an ENSO event. Using a thermister chain moored over Monterey Canyon, northwest of Pacific Grove, two warm events were observed throughout the chain depth

in 1992. These events were attributed to the passage of internal Kelvin waves and were compared with events in equatorial time series and found to be consistent with the internal Kelvin wave phase speeds.

B. EL NIÑO TELECONNECTION THEORY

Teleconnections are any climatic anomaly geographically removed from, but associated with the fundamental interactions occurring equatorially. All the effects, such as high sea level and warm sea temperature, that are observed along the west coast of the United States, could be teleconnections or remote consequences of the ENSO (*Enfield*, 1989). The nature of the effects of an ENSO along the west coast may be characterized by two dominant regimes or their combination. Events may be characterized by a southeastward shift of the Aleutian Low leading to a change in the California Current system from the north via direct atmospheric forcing (e.g., changes in storm tracks and seasonal wind patterns). This shift in the low is frequently an indirect ramification of El Niño. The phenomenon is labeled an Atmospheric El Niño. A reversal of the California Current system from an equatorward to a poleward regime as occurred in 1972-73 is called an Oceanic El Niño, because the signal propagates from the equator to higher latitudes via internal ocean waves, hence is a subsurface feature. It may be limited in poleward extent.

The type of regime called a Combined El Niño has produced the strongest recent events (*Enfield*, 1989). The very strong event years of 1957-1958 and 1982-1983 caused large-scale changes not only in the physical forcings, but of the biological make-up of the region, and were formed by as combination of the two regimes (*Wooster and Fluharty*, 1985). These teleconnections are important concerning this study because they dictate how each of the three regions selected will be affected by a given event.

II. ANALYSIS METHODS

A. SURFACE TEMPERATURE DATA

1. Data Assimilation and Editing

Surface temperature time series were provided by Patricia Walker and Dr. John McGowan, Marine Life Research Group, Scripps Institution of Oceanography. The series are based on daily temperature measurements at several locations along the west coast of the United States. Data were analyzed from seven stations in three geographic regions: La Jolla and Balboa, California in the Southern Region, Pacific Grove and Farallon Islands, California in the Central Region, and Crescent City, California, Charleston, Oregon and Neah Bay, Washington in the Northern Region (Figure 1). The period of analysis is from 1955 to 1988. The exception is the Charleston series, which began in 1966. This time span provided records with minimal data gaps and insured an adequate number of stations for comparison. This period also includes several strong and moderate ENSO events.

The series have been subdivided into eight three-year periods to capture three strong ENSO events (1956-58, 1971-73 and 1981-83) and three moderate ENSO events (1964-66, 1974-76 and 1986-88). Two non-ENSO events (1960-62 and 1978-80) are evaluated for comparison.

2. Data Gap Removal

The data contained numerous gaps that were primarily of a few days duration. These data gaps were bridged using a linear fit. The Farallon Islands station contained many gaps that were of up to a month duration, mainly during January and February due to the difficulty of sampling during those months. A linear regression of Farallon Islands and nearby Bodega Bay was performed for each of the three-year periods to estimate missing Farallon Islands values from Bodega Bay temperatures available during those

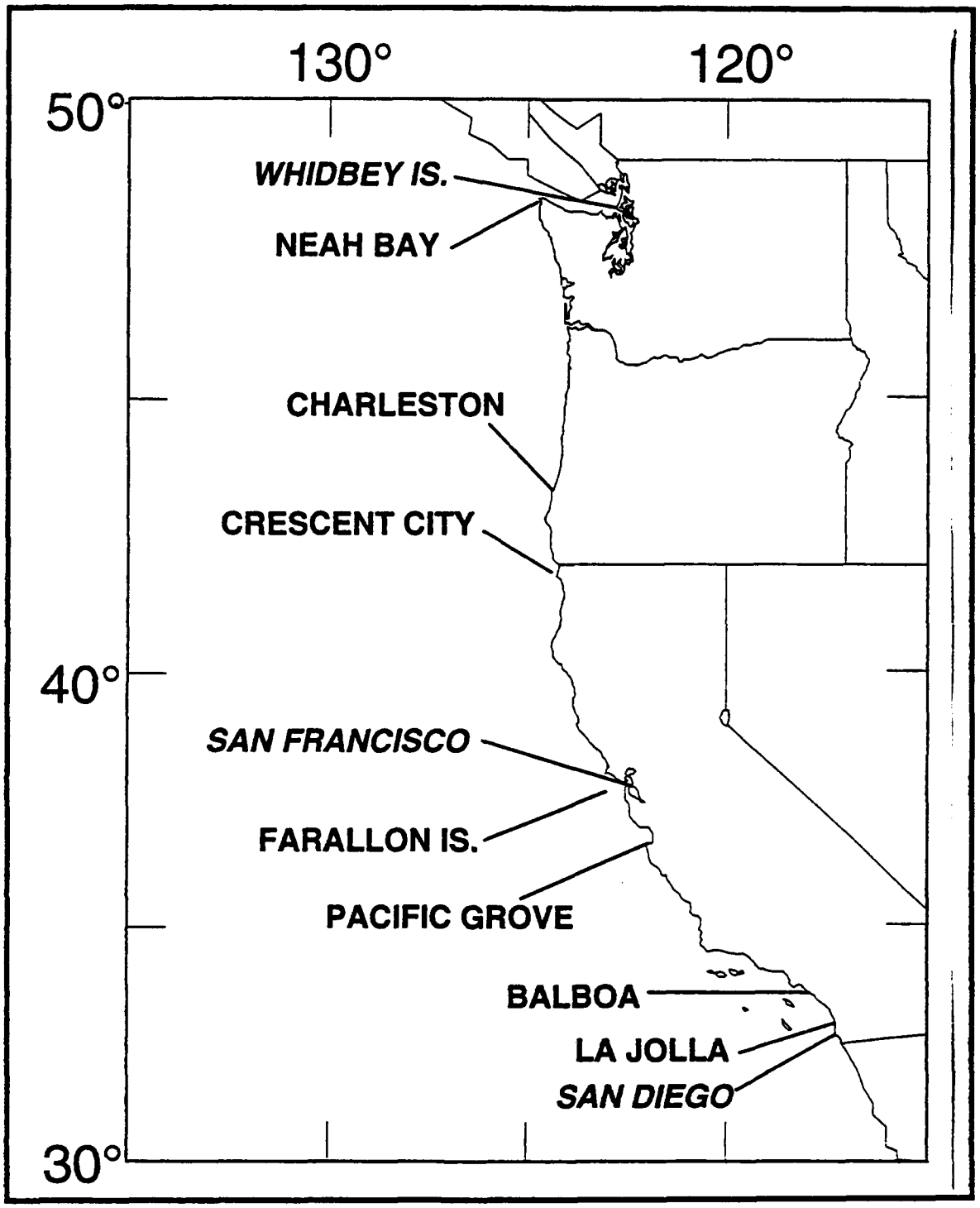

Figure 1. Daily Surface Temperature, Sea Level and Pressure Stations.
Stations along west coast of the United States.

gaps. A detailed description of this process, the amount it was used, and its accuracy is found in the Appendix.

Two stations have very long data gaps. Measurements were not taken at Pacific Grove from early 1975 through 1977, and at Crescent City during 1975 and 1976. Analyses of these stations omitted these years.

3. Mean Signal Extraction, Filtering and Temperature Anomaly Formulation

The average annual signal was extracted from the data records following gap filling. This was accomplished by dividing the entire 34-year record into individual years and deriving a mean temperature for each calendar day of the year (Figure 2a-c). The averaging at Pacific Grove omitted 1975-77 (31 years) and at Crescent City omitted 1975-76 (32 years). The Charleston average is a 22 year period from 1966-1988. Each average annual series was lowpass filtered using a Chebyshev type I digital filter with .01 dB ripple in the bandpass and a half-power period of 40 days to remove higher frequency variability associated with the non-stationary synoptic events. This filter, designated **cheby1** is found in the Signals Toolbox of the Matrix Laboratory (MATLAB) software version 4.0 (*Little and Shule*, 1992).

The MATLAB function **cheb1ord** was first applied to select the order for the filter. (*Little and Shule*, 1992) Inputs to this function were that no more than 3 dB would be lost in the passband and that 10 dB at a minimum of attenuation would be applied in the stopband. The range of the passband (0 to 0.05) and the stopband (0.1 to 1.0), scaled by the Nyquist Frequency, were also input. Output for use by **cheby1** was the lowest order (n=2) for the filter which the previous conditions support.

The filtered annual average signal was then subtracted from each year of the gap-filled data record to form a time series of daily temperature anomalies for each station. The gap-filled data series were not filtered prior to removing the annual signal since the daily variations in the temperature anomaly are of interest in this study. The temperature anomalies were filtered using the lowpass Chebyshev type I digital filter of second order

and natural frequency corresponding to a half-power period of forty days. The bandpass ripple was enlarged to 3 dB. This filter adequately removes the visual biasing due to the daily excursions inherent in the temperature anomaly series. The filtered temperature anomaly series are displayed for presentation purposes and are not the bases of any further analysis.

B. SEA LEVEL AND PRESSURE DATA

1. Data Assimilation and Editing

Sea level time series were provided by NOAA for La Jolla, San Francisco, and Neah Bay, Washington (Figure 1). These series are based on hourly tide gauge measurements at these stations. The National Geodetic Vertical Datum of 1929 (NGVD) for each site and period was removed. The series were converted to centimeters of water. Atmospheric pressure series were furnished by the National Climatic Center via NAVOCEANCOMDET Asheville. Data were available for San Diego, San Francisco, and Whidby Island, Washington (Figure 1) at three-hourly sample intervals. The pressure series were demeaned and converted to centimeters of water.

2. Pressure Signal Correction and Filtering

The sea level series were decimated to a three-hourly format, and the coincident pressure series were added to remove the "inverse barometer effect." These adjusted sea level series were then filtered using a ninth-order, 20-hour lowpass Chebyshev-type I filter for tide signal removal. The 1300 PST sea level for each day was extracted to create a series of daily adjusted sea level analogous to the daily surface temperature series.

3. Data Gap Removal

The raw sea level series contained numerous short gaps. Following filtering and decimation to daily values, the gaps were filled using a linear fit of the data. A very long data gap existed for Neah Bay during the 1974-76 period, so no analysis was performed

for this station during this period. No analysis was performed on La Jolla from 1971-76, because the data were not provided by NOAA.

4. Mean Signal Extraction, Filtering and Sea Level Anomaly Formulation

The average annual signal was extracted from the data records at each station in the same manner as the temperature series, except the adjusted sea level yearly series length were based on 24 years of data, corresponding to the eight selected three-year periods. The averaging at La Jolla omitted 1971-76 (18 years) and at Neah Bay omitted 1974-76 (21 years). Each average annual series was lowpass-filtered using the identical Chebyshev type I filter described for average annual temperature signal filtering. The filtered annual average signal was then subtracted from each year of the gap-filled data record to form a time series of adjusted sea level anomalies for each station. These series were used for the spectral analysis.

The adjusted sea level anomalies were lowpass filtered again using the Chebyshev type I digital filter of second order and natural frequency corresponding to a half-power period of forty days. The band-pass ripple was increased to 3dB. This filter adequately removes the visual biasing of short duration events inherent in the adjusted sea level anomaly series.

C. FREQUENCY DOMAIN ANALYSIS

Discrete Fourier transforms (**FFT**) converted the time series of temperature and sea level anomalies to the frequency domain for spectral analysis. The MATLAB function **spectrum** was used to compute spectral characteristics of the time series (*Little and Shule*, 1992). This function performed FFT analysis of the series using the Welch method of power spectrum estimation (*Oppenheim and Schafer*, 1975). Each time series was divided into equal length, overlapping sections based on the "power of two"-point FFT to be used and the length of the series. Each section was successively Hanning windowed, Fourier transformed and accumulated to form the power spectrum estimation of the series.

Since the length of each window was a power of two, a fast radix-2 fast Fourier transform algorithm was used.

1. Autospectra

Power spectral densities for the entire series were calculated using a 4096-point FFT at low frequencies ($\omega<0.00586$ cpd) and a 256-point FFT at high frequencies ($0.00586\leq\omega<0.3425$ cpd). These curves were fitted together by commencing the 256-point FFT at the 1.5 point ($\omega\approx0.00586$ cpd) to remove the energy aliased onto the first point by the lower frequency energy of the whole series. The break point between the two series is visible and close in energy level.

Single-year (365 day) series for the period July 1, year 2 to June 30, year 3 were extracted from the three-year series and defined as the ENSO years. A 128-point FFT analysis was used to generate power spectral density for these one-year series.

2. Cross Spectra

Cross-spectral analysis was performed on each ENSO year versus all years in the temperature and adjusted sea level anomaly series. The **spectrum** function was used to calculate autospectra for each ENSO year and for all years, the transfer function for both magnitude and phase, and the coherence.

Cross-spectral analysis was also performed on the temperature anomalies versus the adjusted sea level anomalies for each ENSO year and for all years. The autospectra for temperature and sea level, the transfer function and the coherence were determined and graphically displayed.

Phase speed determination in the frequency domain required cross spectra of La Jolla versus all of the other stations. The phase speed $\left(c\left(\frac{\text{km}}{\text{day}}\right)=\frac{2\pi\cdot\Delta y\cdot\omega}{\Delta\phi+\left(2\pi\cdot n\right)}\right)$ was estimated at each frequency band ω, where $\Delta\phi$ is the phase at each station relative to La Jolla, Δy is the distance between each station and La Jolla, and n is the number of cycles

added. The number of cycles, where $n \geq 1$, is based on an objective fit to the theoretical phase speed for an internal Kelvin wave and the fact that the distance between stations is much greater than the wavelength at high frequencies. The phase speed was plotted in the form of day versus station distance from La Jolla. Coherence was calculated to determine whether results are statistically significant.

The wavelengths $\left(L_{\omega(\mathrm{km})} = \frac{c}{\omega} \right)$ were calculated from phase speed. The mean and standard deviation of the wavenumber, k, (inverse of the wavelength) were calculated for each frequency band from all La Jolla-station pairings . These values were plotted in ω-k space for comparison to theoretical estimates of non-dispersive coastal waves.

III. RESULTS

A. TIME SERIES ANALYSIS

1. Lowpass Filtered Mean Annual Signal

a. Southern Region

The average annual temperature signals for La Jolla and Balboa are very similar (Figure 2a). La Jolla shows a minimum temperature of 14°C at the end of January and a maximum of 21°C in mid-August. Corresponding values for Balboa are 14°C in early February and 19.5°C also in mid-August. Both series show a slow warming until March and then a rapid warming commencing the first week of March. La Jolla cools following the temperature maximum in August. Balboa shows cooling at a reduced rate until early October when the slope corresponds with La Jolla.

The average annual adjusted sea level for La Jolla drops from a height of 12 cm at the beginning of the year to a minimum of 1 cm in early May (Figure 2a). The minimum coincides with the timing of maximum equatorward wind stress at this latitude (*Nelson*, 1977). Adjusted sea level rises to a plateau of 11 to 14 cm which lasts from mid-August to January. Adjusted sea level appears to lag the temperature with the major height reduction in the spring following the large temperature decrease of late fall and winter. Warming commences in March, apparently in response to seasonal atmospheric warming, but the corresponding rise in adjusted sea level does not occur until June, when equatorward wind stress begins to decrease (*Nelson*, 1977). The lagged relationship between temperature and sea level suggests that the set-down in sea level associated with increased equatorward wind stress does not result in coastal upwelling of cooler water to the surface. Further, it suggests that steric effects are not reflected in coastal sea surface temperature.

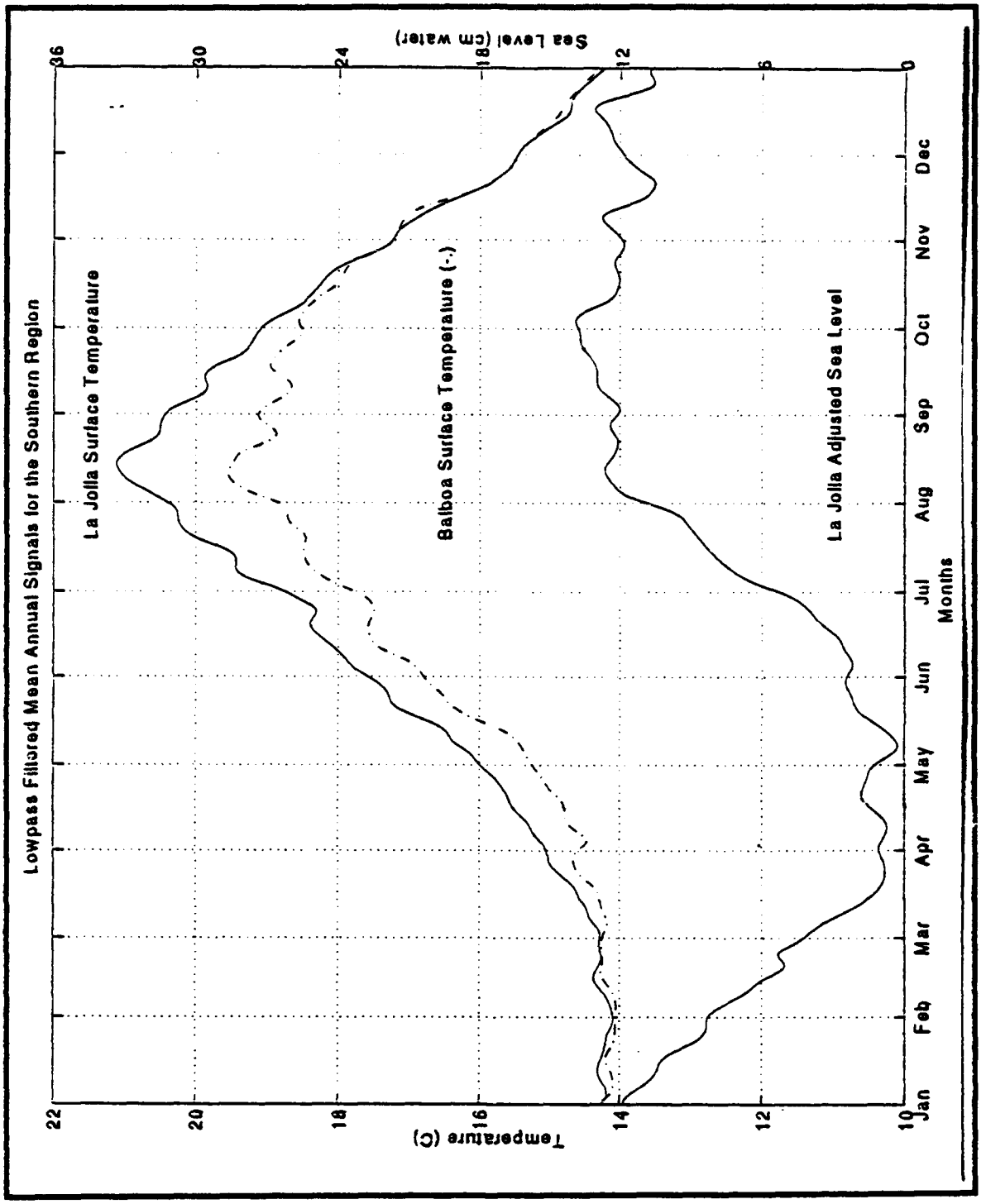

Figure 2a. Lowpass Filtered Average Annual Signals for the Southern Region.
The first day of each month is marked with the name of the month.

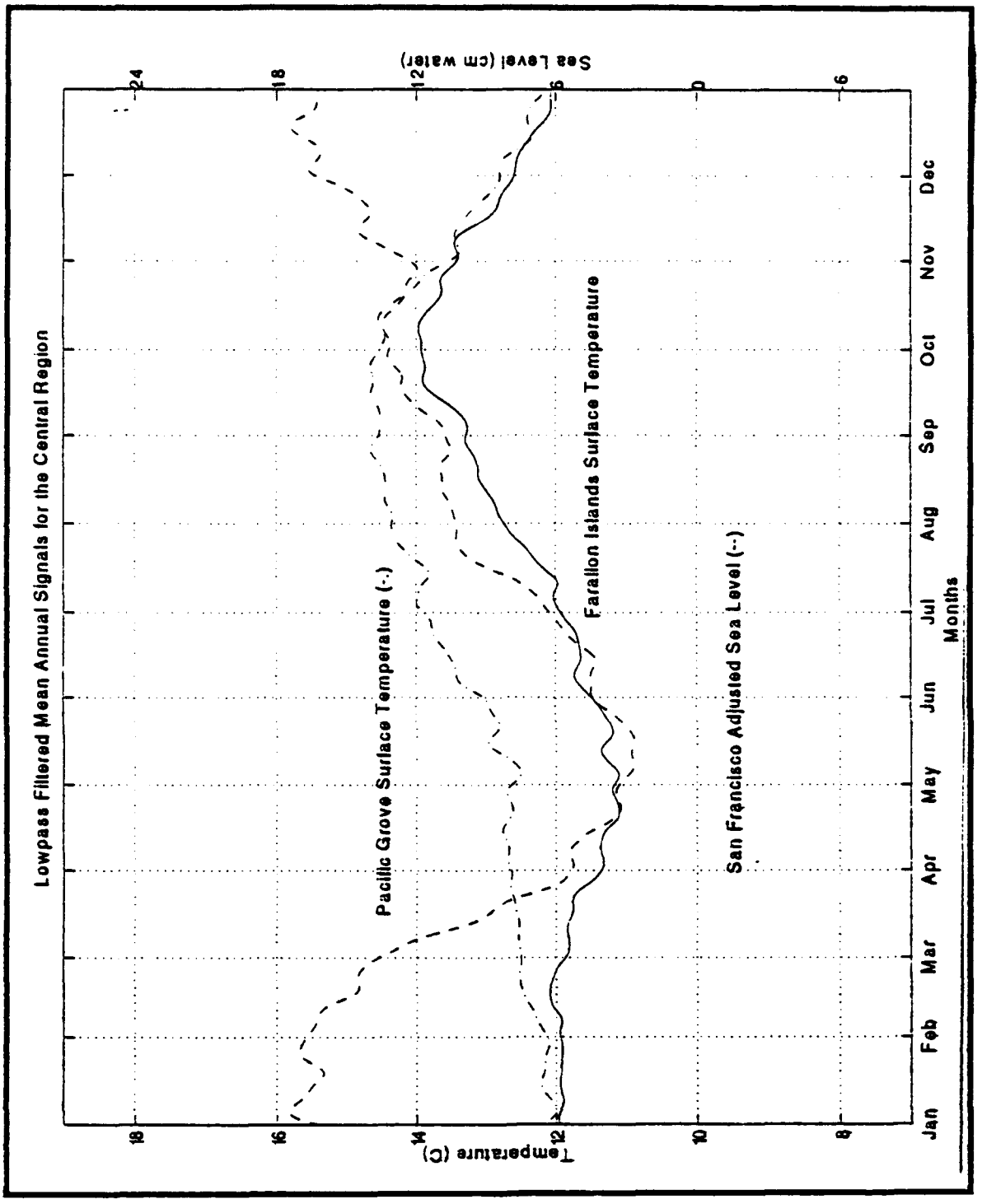

Figure 2b. Lowpass Filtered Average Annual Signals for the Central Region.
The first day of each month is marked with the name of the month.

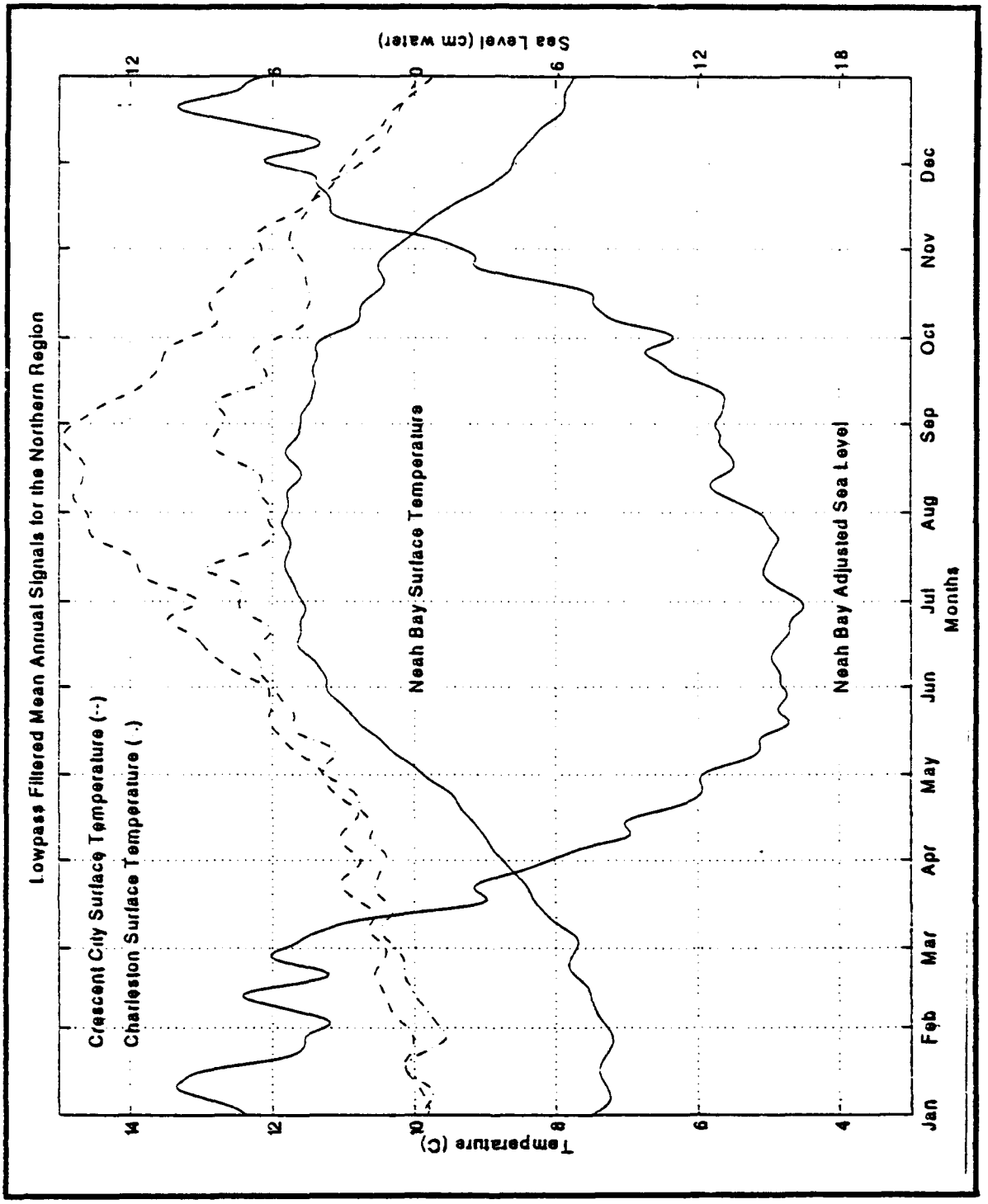

Figure 2c. Lowpass Filtered Average Annual Signals for the Northern Region. The first day of each month is marked with the name of the month.

b. Central Region

The average annual temperature signals for Pacific Grove and the Farallon Islands do not resemble the signals for the Southern Region (Figure 2b). Pacific Grove has a minimum temperature of 12°C in early January and a maximum of 14.6°C in late September. Farallon Islands has a minimum of 11°C in early May and a maximum of 14.0°C in early October. Secondary maximum and minimum occur in early October and January, respectively. Pacific Grove warms slowly from January until May, then more rapidly warming until the maximum temperatures are reached in September. Cooling is much more regular from September to January. The cooling phase timing appears to be similar to the Southern Region stations, except the range is greatly reduced to only 2.6°C. Farallon Islands does not show a steadily rising temperature, but a pronounced cooling from late March until early May, when a more characteristic warming occurs. The cooling phase is similar to the other stations. The spring cooling exhibited in Farallon Islands is associated with increased coastal upwelling following the Spring Transition and is manifested only by a temperature plateau in the Pacific Grove series. The protected Pacific Grove site is located in Monterey Bay, and is less exposed to the oceanic influences seen at Farallon Islands.

The average annual adjusted sea level for San Francisco is 17 cm during December and January and falls from February to mid-May to a height of 3 cm (Figure 2b). This sea level reduction is associated with the Spring Transition and upwelling period prevalent off the central coast. The adjusted sea level rises steadily to its December maximum. Adjusted sea level changes generally lead surface temperature changes. Adjusted sea level reflects a much larger change throughout the water column from the effects of upwelling than is shown by the surface characteristics. As at La Jolla, the adjusted sea level minimum in the spring is associated with the period of greatest

equatorward wind stress, which has a larger annual amplitude off central California (*Nelson*, 1977).

c. Northern Region

The average annual temperature signals for Crescent City, Charleston, and Neah Bay resemble the Southern Region in shape and timing of the maximum and minimum. (Figure 2c). Crescent City has a minimum value of 9.8°C at the beginning of January and a maximum of 14.8°C the last week of August. Minimum and maximum values for Charleston are 9.6°C at the end of January and 13°C in mid-July. Minimum and maximum values for Neah Bay are 7°C is late January and 12°C is late July. Crescent City closely resembles the southern stations in pattern, except the temperatures are colder and the range is smaller (5.0°C versus 5.5°C and 7.0°C for Balboa and La Jolla, respectfully). Charleston has a similar, but slightly cooler pattern than Crescent City until early May, then becomes highly variable. Between mid-July and mid-August, the record actually cools by 1°C. Charleston may have higher variability on shorter scales since it has eleven fewer years sampled than the other stations. Charleston also has a very small seasonal temperature range. Neah Bay warms from January to June, then plateaus from the June to October, when all temperatures are between 11.6°C and 12°C. The seasonal cooling commences over a month later at Neah Bay than at Crescent City, even though Neah Bay is farther north.

The annual average adjusted sea level for Neah Bay has maximum heights in December and January at 10 cm (Figure 2c). Sea level falls from the end of February until the end of June when a minimum of -16.5 cm is reached. A slow rise in sea level occurs from July through mid-September when a more rapid rise takes place until December. The adjusted sea level appears to be approximately out of phase with temperature. The shape both surface temperature and adjusted sea level are similar, but offset temporally with the minimum sea level leading the maximum temperature by about two months. Unlike the other regions, where monthly mean wind stress is equatorward throughout the

year, the stress at these latitudes is poleward during September to April (*Nelson*, 1977). The sea level minimum at Neah Bay coincides with the timing of the equatorward wind stress. Neah Bay has a much greater variability of sea level than the other stations at 26.5 cm compared to 14 cm for San Francisco and 13 cm for La Jolla, corresponding to a relatively larger annual amplitude in alongshore wind stress (2.43 dynes cm^{-2} versus 1.34 dynes cm^{-2} at 35°N and 0.88 dynes cm^{-2} at 36°N; *Nelson*, 1977). The timing of the temperature cycle suggests that it is dominated by seasonal warming, not upwelling.

The seasonal variations of the California Current System may significantly impact the adjusted sea level. The development of a nearshore equatorward flow in April replaces the winter poleward flow prevalent off the coast of Washington (*Hickey*, 1979). This flow reversal in the California Current System corresponds with the observed reduction in average annual adjusted sea level and denotes a denser, cooler water column. The surface temperature would not be affected by this current shift, since it is not a surface current or upwelling feature.

2. Gap-Filled Surface Temperature and Adjusted Sea Level Signals

The gap-filled daily time series plots (Figure 3a-g) consist of linear temperature plots for eight three-year periods for each of the seven stations. The gap-filled daily plots of adjusted sea level (Figure 4a-c) are of three-year periods for three stations. These plots are arranged by either strong, moderate or non-ENSO periods. Each series analyzed shows considerable variability on synoptic time scales, associated with the passage of atmospheric pressure systems. Interannual variability is readily apparent in all series.

a. Southern Region

Over the eight periods evaluated here, La Jolla temperature varies between 10 and 25°C (Figure 3a). The three strong ENSO periods (1957-58, 1972-73 and 1982-83) have unseasonably warm winters (circa day 800). The moderate ENSO periods do not show any strong trends. The non-ENSO periods have one period which looks ENSO-like for the winter of 1979-80 (approximately day 800). The Balboa signal is nearly identical

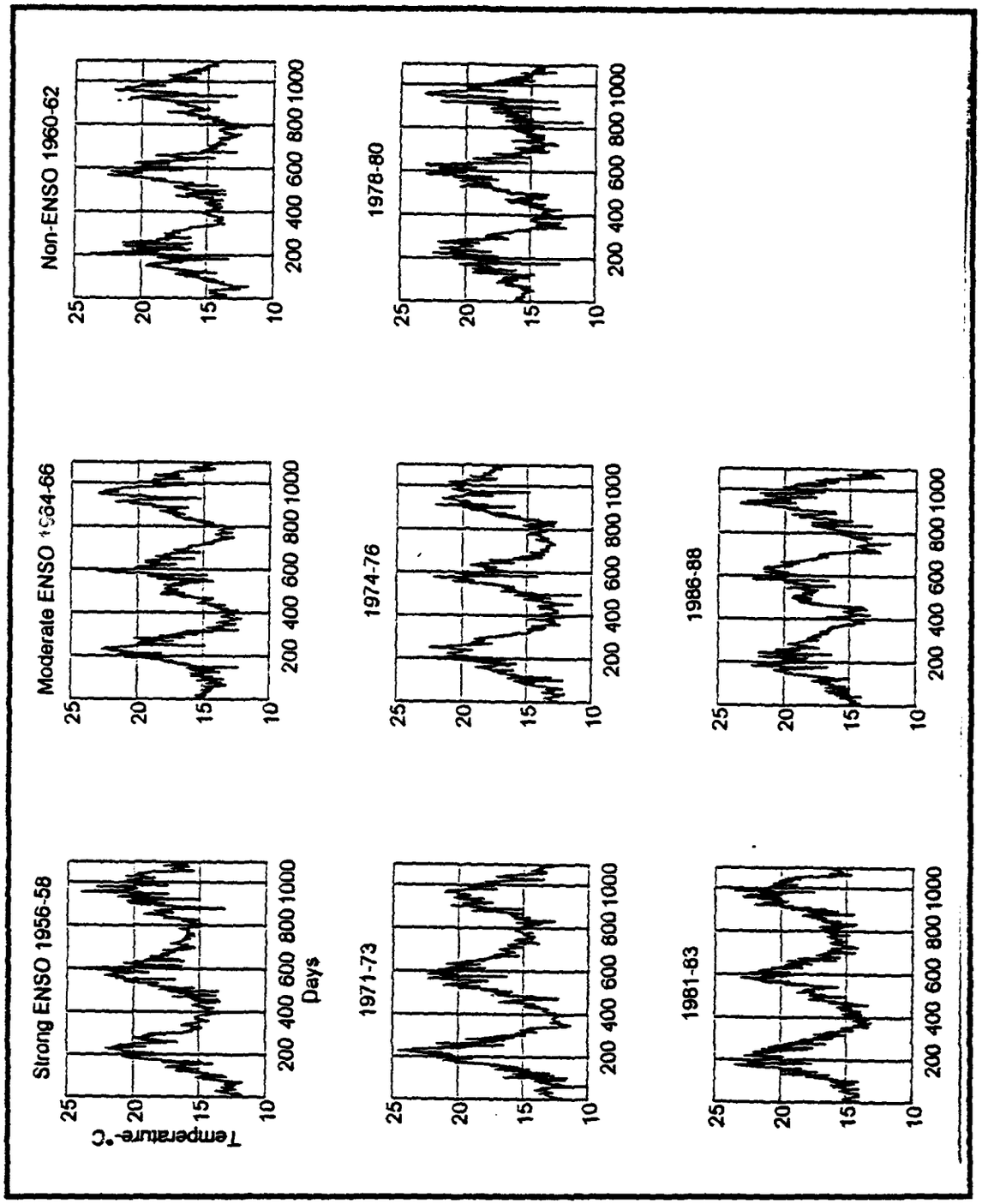

Figure 3a. Gap-Filled Surface Temperature Series for LaJolla.
For each x-axis, day 0 is January 1 of the first year of the three-year period.

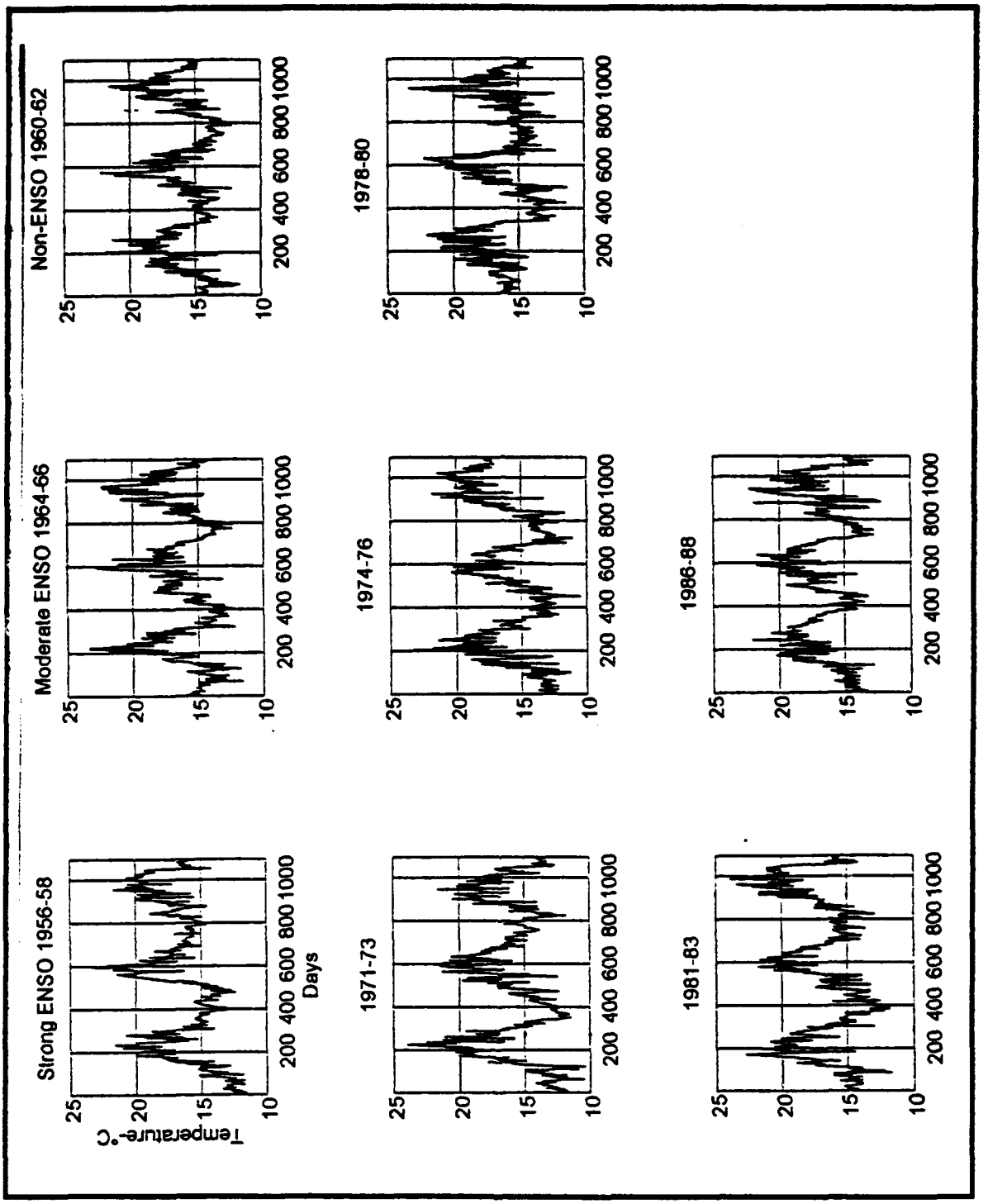

Figure 3b. Gap-Filled Surface Temperature Series for Balboa.
For each x-axis, day 0 is January 1 of the first year of the three-year period.

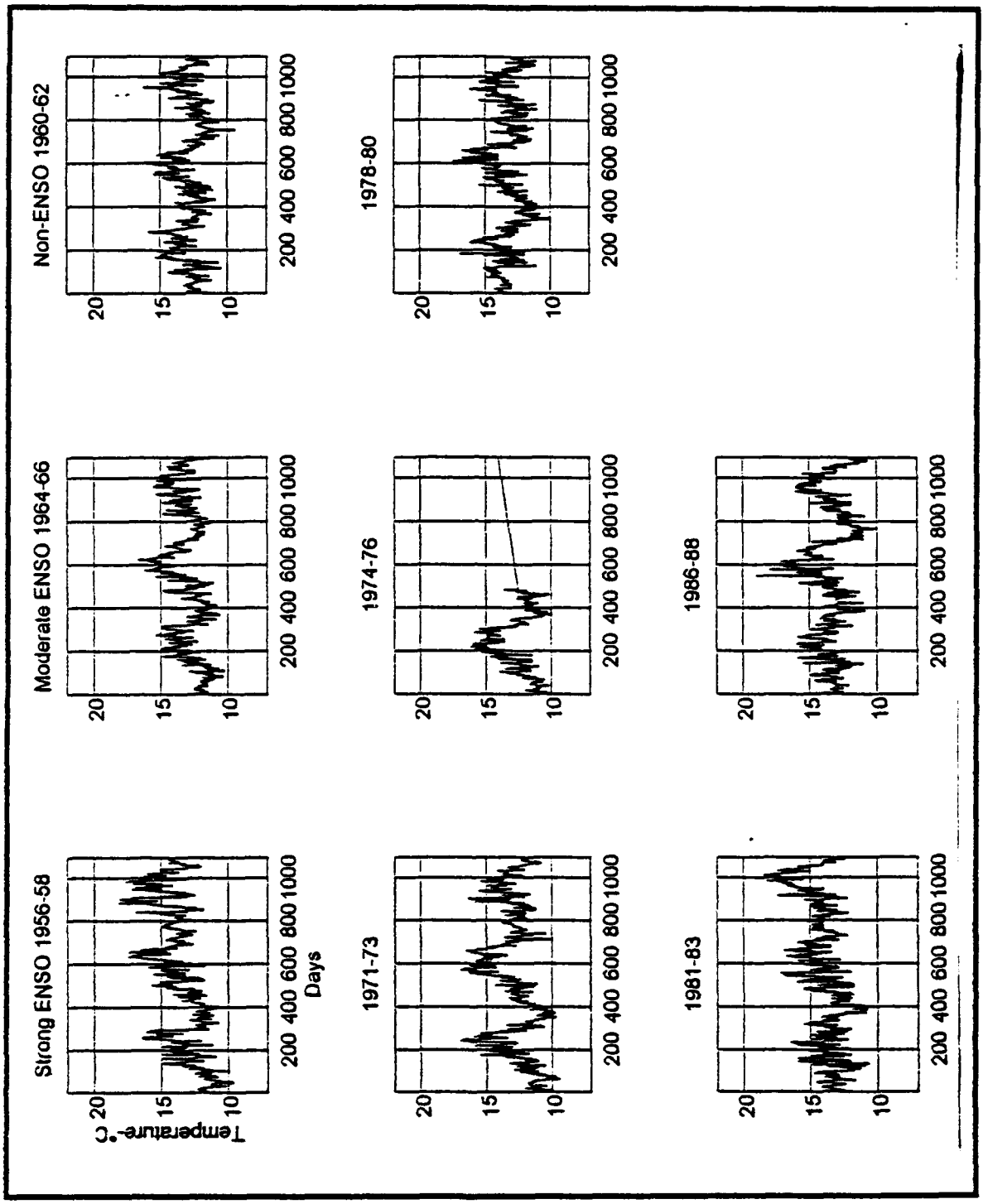

Figure 3c. Gap-Filled Surface Temperature Series for Pacific Grove.
For each x-axis, day 0 is January 1 of the first year of the three-year period.

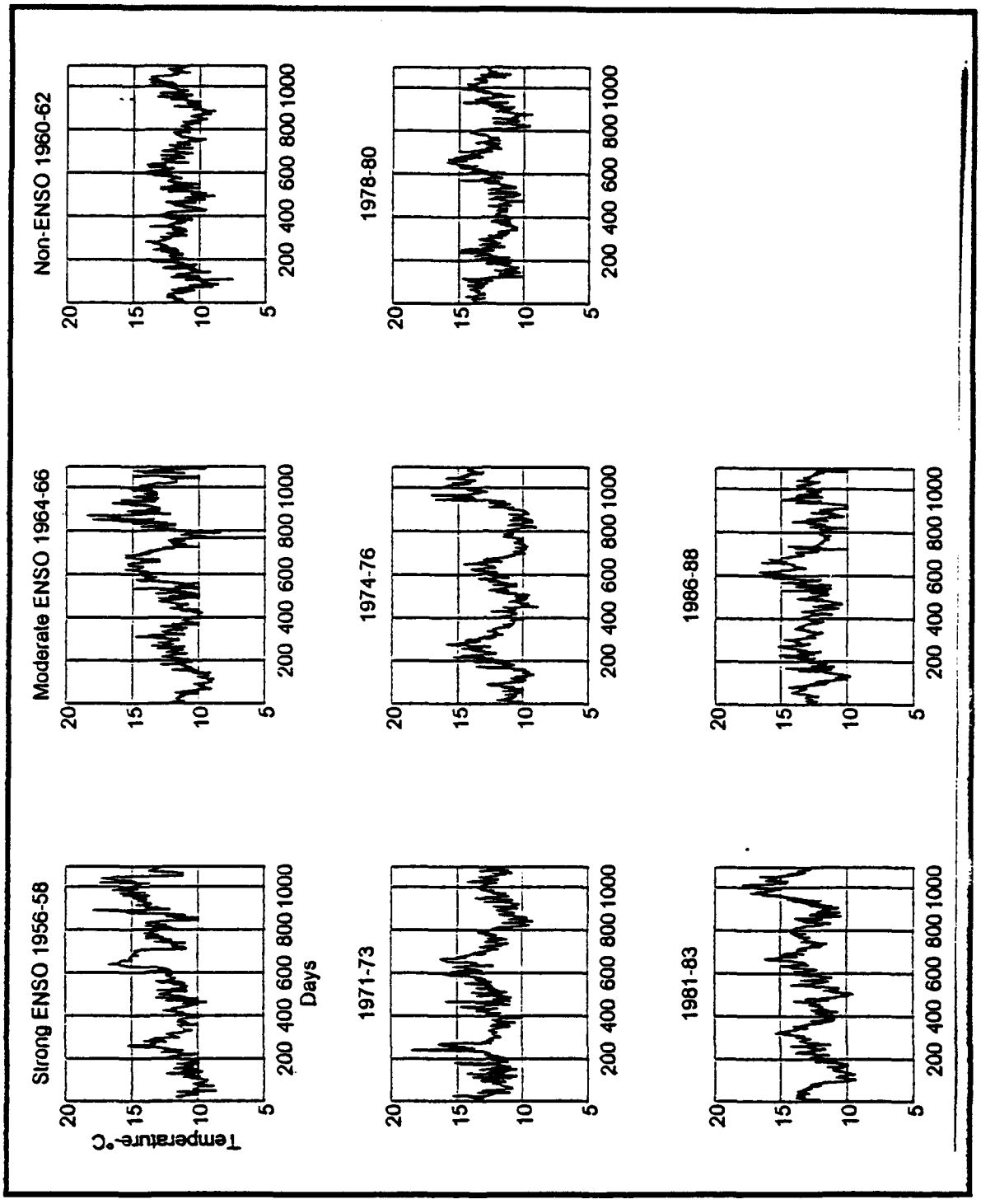

Figure 3d. Gap-Filled Surface Temperature Series for Farallon Islands.
For each x-axis, day 0 is January 1 of the first year of the three-year period.

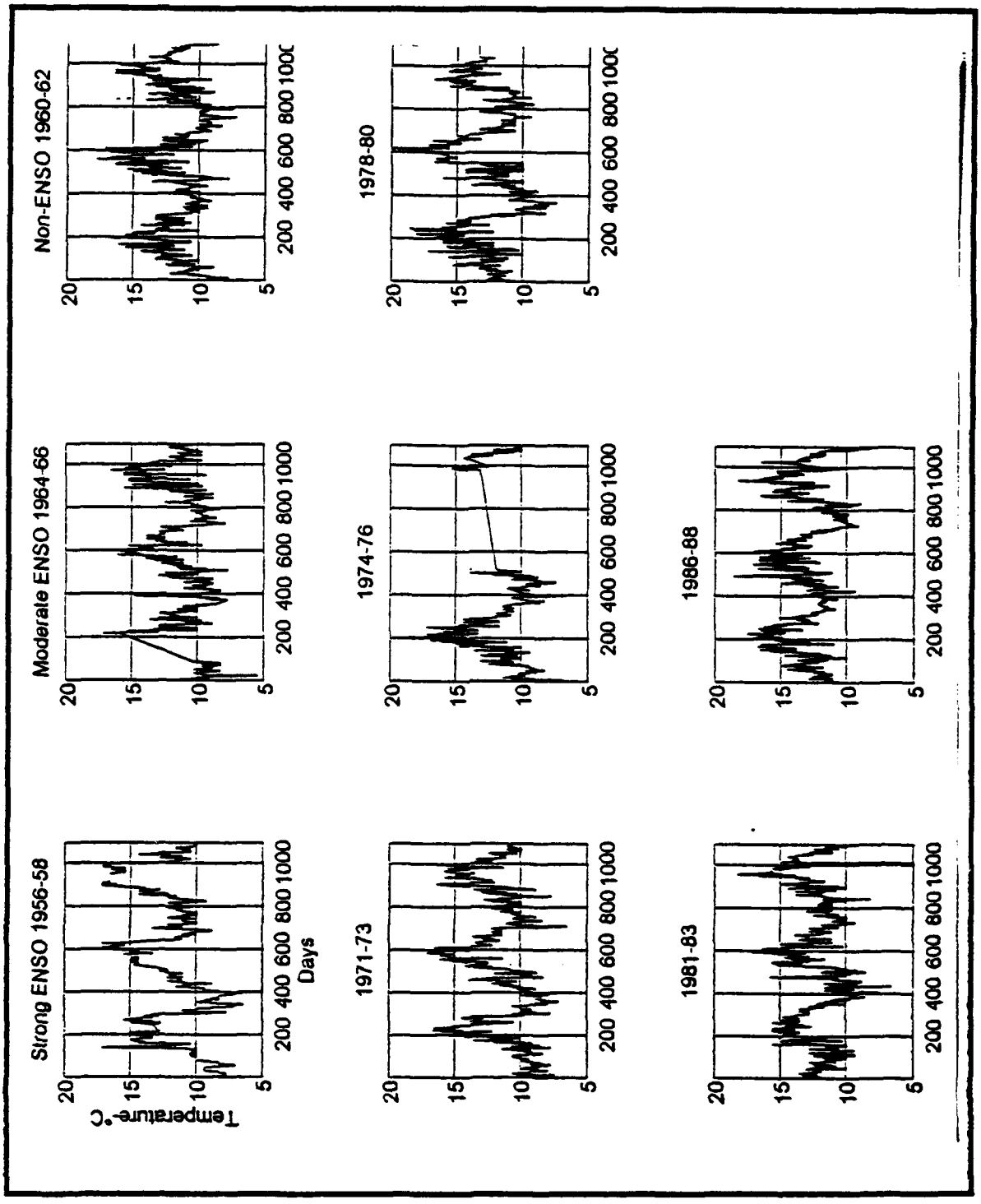

Figure 3e. Gap-Filled Surface Temperature Series for Crescent City.
For each x-axis, day 0 is January 1 of the first year of the three-year period.

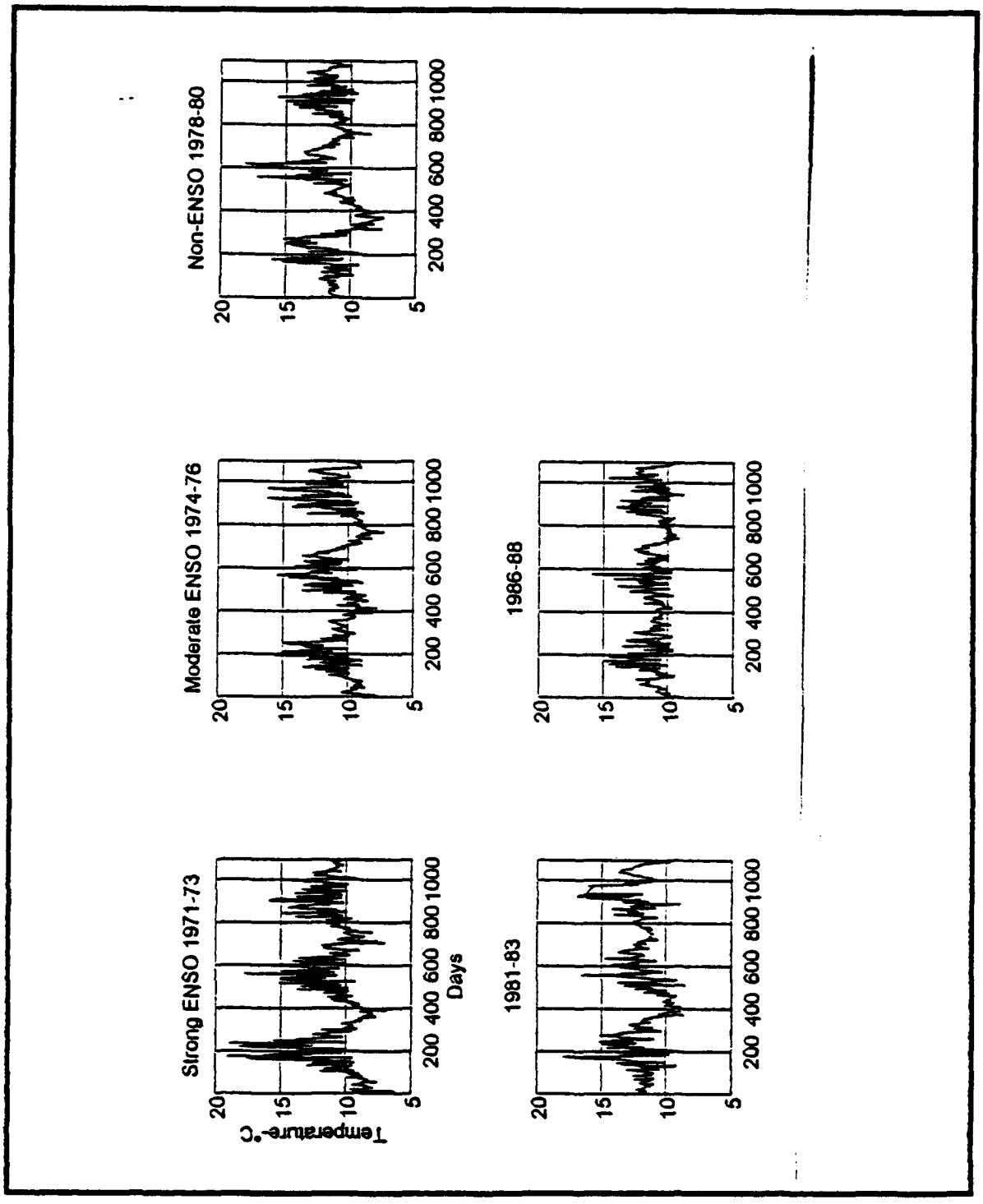

Figure 3f. Gap-Filled Surface Temperature Series for Charleston.
For each x-axis, day 0 is January 1 of the first year of the three-year period.

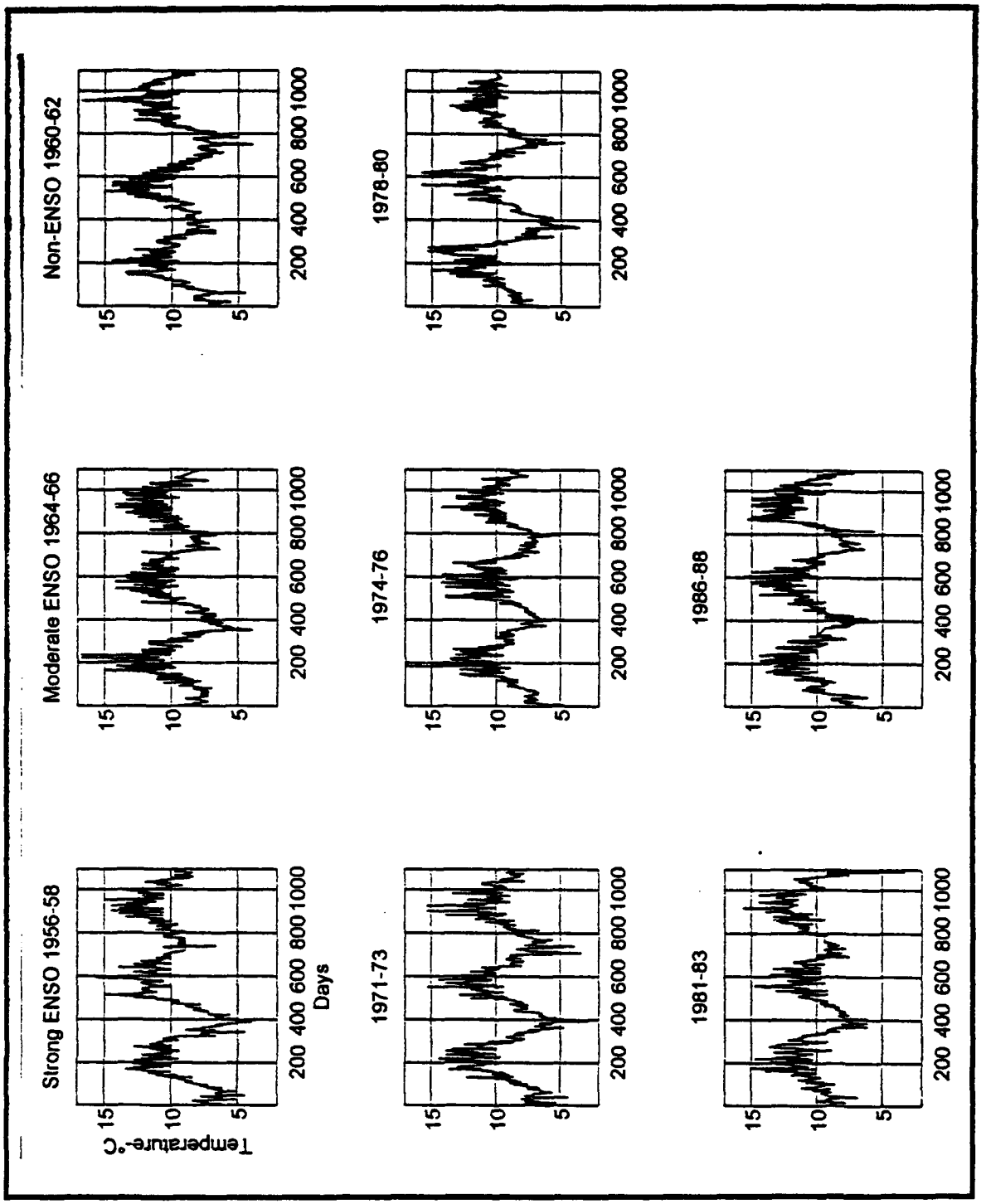

Figure 3g. Gap-Filled Surface Temperature Series for Neah Bay .
For each x-axis, day 0 is January 1 of the first year of the three-year period.

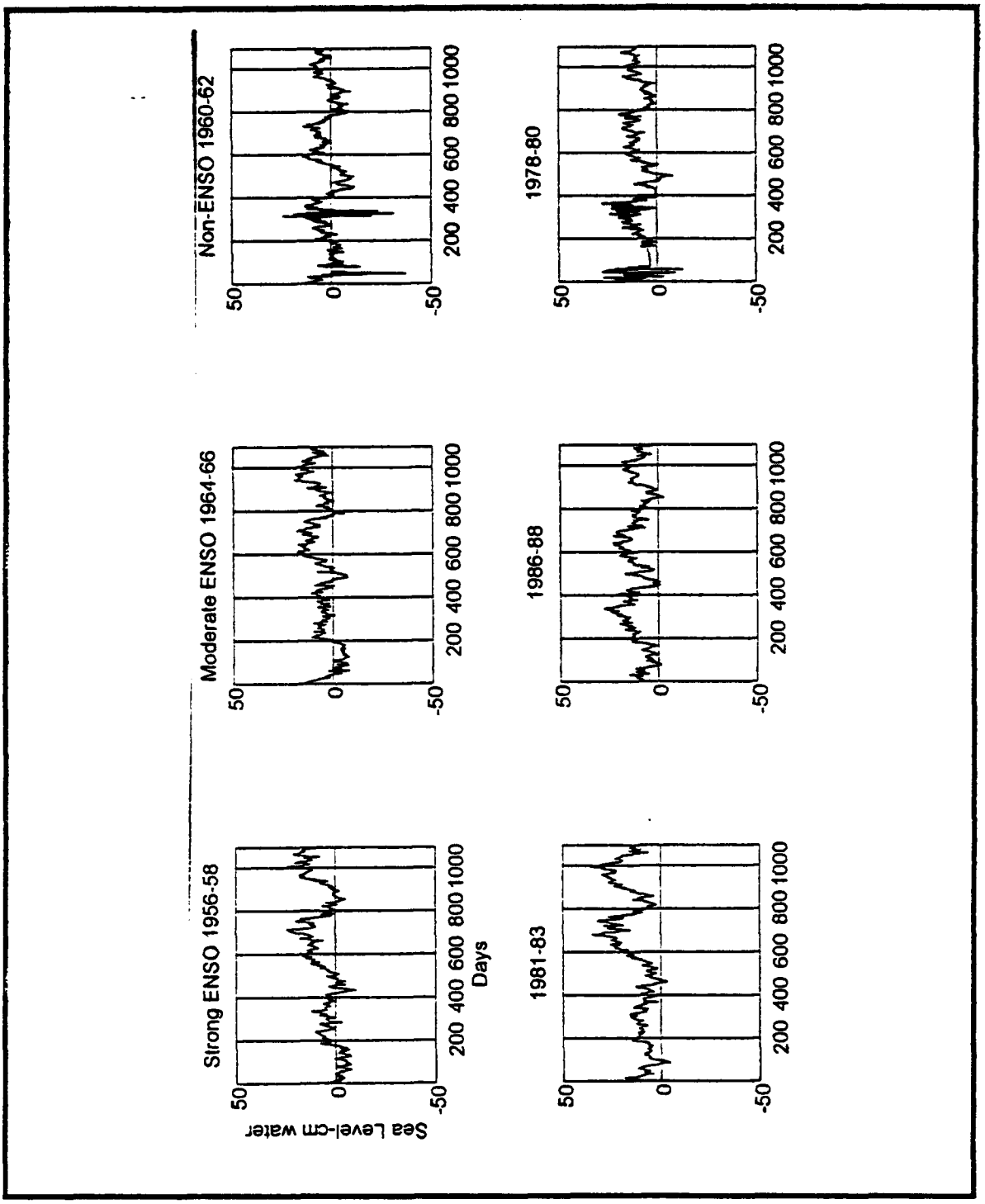

Figure 4a. Gap-Filled Adjusted Sea Level Series for La Jolla.
For each x-axis, day 0 is January 1 of the first year of the three-year period.

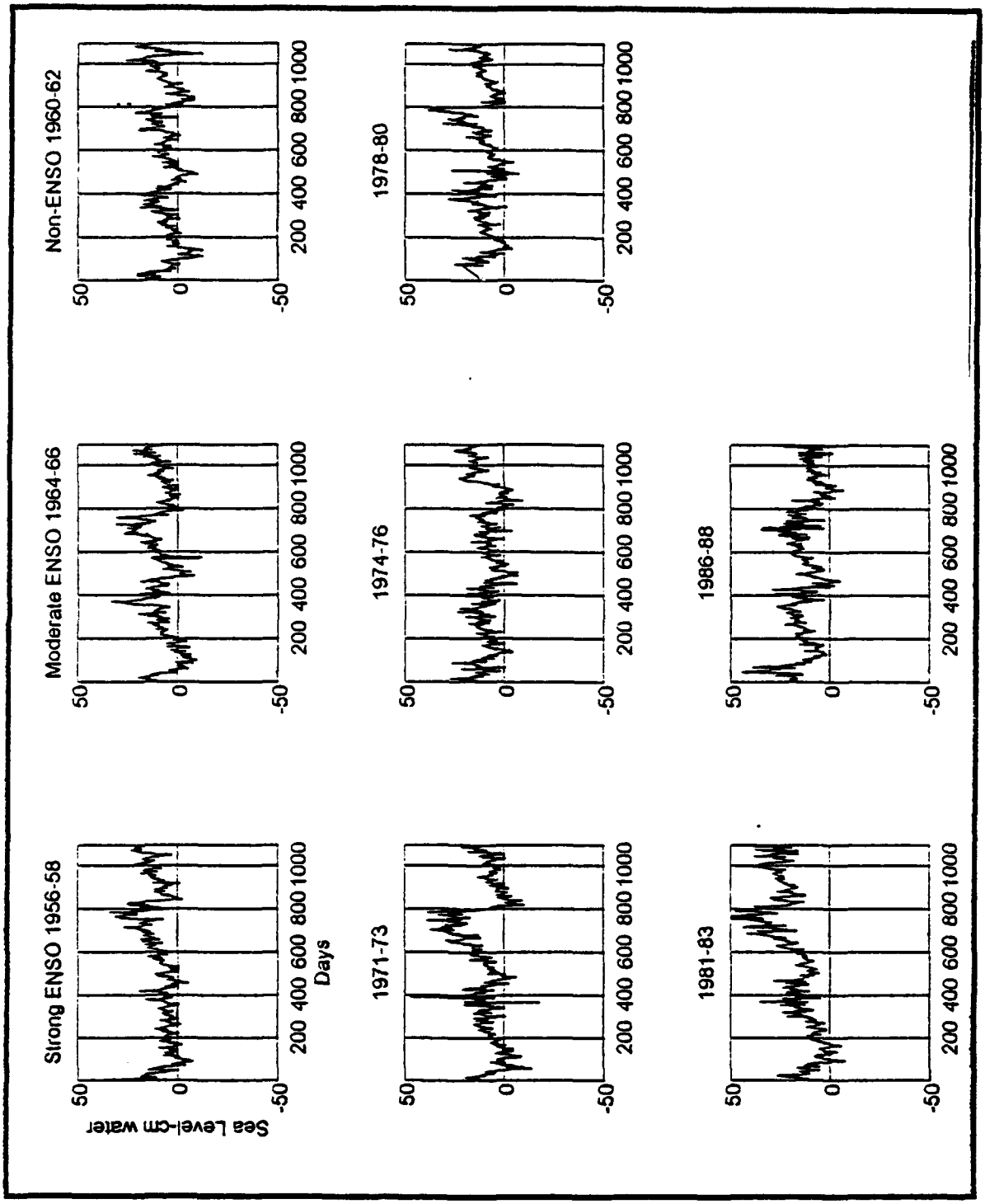

Figure 4b. Gap-Filled Adjusted Sea Level Series for San Francisco.
For each x-axis, day 0 is January 1 of the first year of the three-year period.

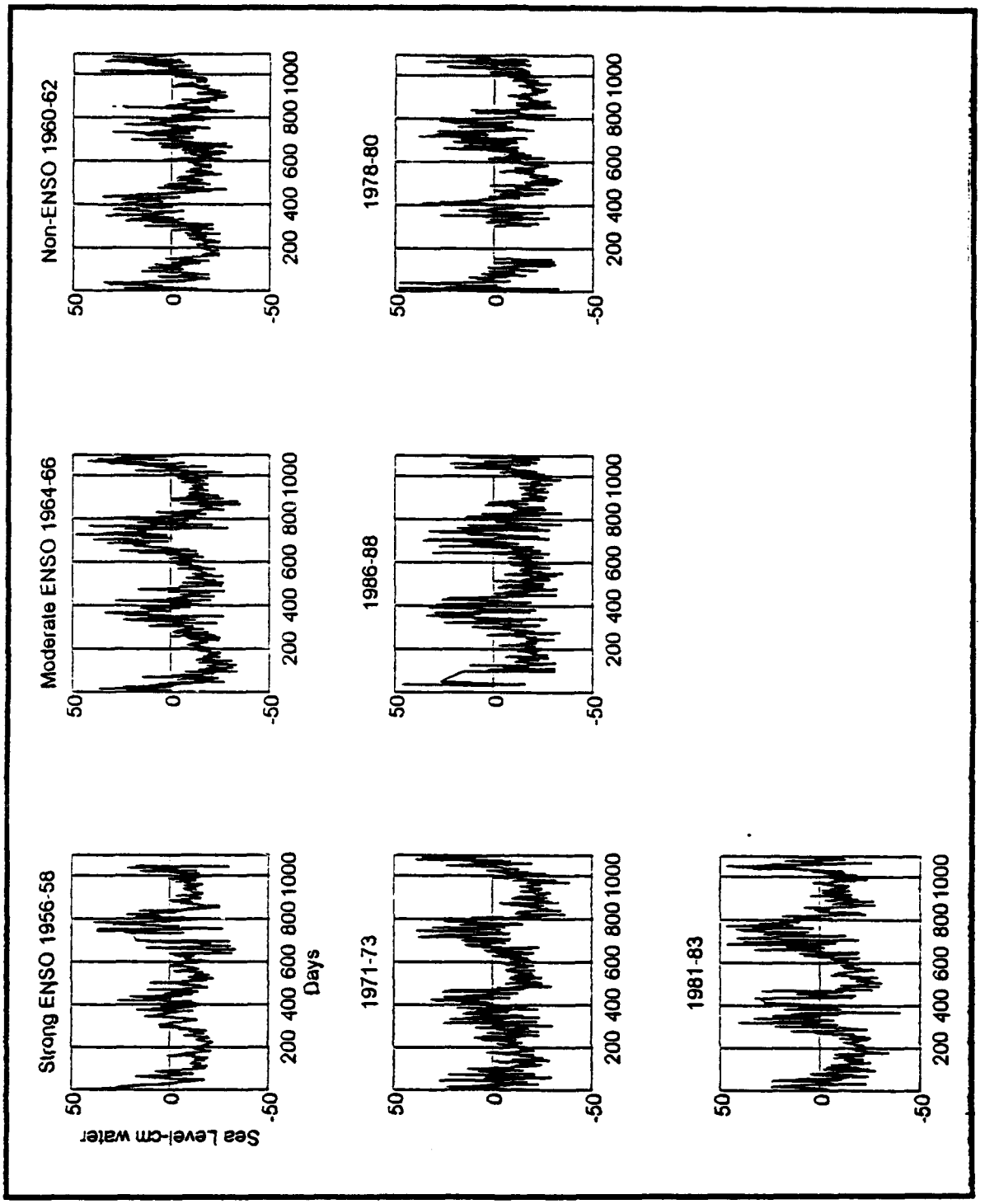

Figure 4c. Gap-Filled Adjusted Sea Level Series for Neah Bay.
For each x-axis, day 0 is January 1 of the first year of the three-year period.

to La Jolla (Figure 3b). Minor differences include consistently lower temperatures at Balboa.

Only six periods of La Jolla adjusted sea level were available for evaluation (Figure 4a). Adjusted sea level varies between 35 cm and -35 cm for La Jolla. The plotting scale was selected for the larger magnitudes present for Neah Bay. The strong ENSO periods show high sea levels with 1981-1983 standing out as the highest, especially during the actual ENSO year of 1982-83. Higher sea levels are expected for ENSO years at this station due to the steric volume increase. The steric volume increase is caused by the warming of the entire water column by the teleconnection of the ENSO from the equator. The adjusted sea level lags surface temperature at this station as was seen for the mean annual signals. The warm ENSO winters cited in the preceding paragraph correspond with the high sea levels found for the same period.

b. Central Region

Pacific Grove temperature varies between 9 and 18°C (Figure 3c). A warm winter pattern similar to La Jolla and Balboa was found for the strong ENSO periods and 1979-80. A data collection gap is apparent in 1975-76. Farallon Islands varies between 8 and 18°C (Figure 3d). It has a much more variable signal due partially to the gap-filling process. Farallon Islands and Pacific Grove are visually dissimilar, due in part to the physical proximity of the Farallon Islands to the open ocean, while Pacific Grove is more protected in Monterey Bay.

San Francisco adjusted sea level varies between -15 cm and 40 cm (Figure 4b). Again, the adjusted sea level is higher during the strong ENSO periods and the winter of 1979-80. 1981-83 has the highest levels. San Francisco adjusted sea level varies at the synoptic time scales than does La Jolla.

Comparison of the adjusted sea level and the surface temperature signals for this region shows the influences of upwelling. The temperature signal is higher for the strong ENSO periods than for the other periods, but it is not a large change. Sea level is clearly

higher for strong events. For the strong event of 1982-83, the sea level rise corresponds to the expansion of the entire water column and is readily apparent, while the surface temperature is only slightly higher than usual. Reduced upwelling, possibly associated with ENSO, produces a significant effect on adjusted sea level at this analysis level, and on surface temperature. The moderate ENSO events may or may not show a rise in sea level or a warming temperature depending on the effect of the ENSO on upwelling.

c. Northern Region

Crescent City, Charleston, and Neah Bay have elevated temperatures during the strong ENSO periods. Crescent City has two large data gaps for 1964 and 1975-76, and 1956-58 was extensively filled. Crescent City varies from 6 and 19°C (Figure 3e). Beginning with the 1971-73 period, Charleston varies between 7 and 17°C (Figure 3f). Neah Bay has a very regular annual pattern which varies between 4 and 16°C(Figure 3g). These stations are similar, but an exception is Charleston (1986-88) which looks very different from the other two northern stations.

Neah Bay adjusted sea level signal has great variability on synoptic scales, presumably in response to the passage of atmospheric pressure systems. The heights vary between -35 cm and 45 cm (Figure 4c). The ENSO periods have higher sea levels, except for 1971-73. At day 800 (mid-March 1973), the sea level falls much lower than it does for the other strong periods. This low level corresponds to 1972-73 being an oceanic ENSO which was not teleconnected to Neah Bay, via the more southern stations. The other ENSO's are reflected in the Neah Bay series through atmospheric forcing also (*Norton et al.*, 1985). The relationship between adjusted sea level and surface temperature is in line with the mean annual signal with sea level lagging temperature.

d. Summary of ENSO Impact

Oceanic ENSO events cause warm surface temperature and high sea level anomalies in all regions to which the signal is teleconnected. 1972-73 is the best example of this type with regional limitations such that the signal did not reach Neah Bay.

The ENSO may be manifested along the west coast by a cessation or reduction of upwelling favorable winds. This change to the upwelling favorable winds causes lower adjusted sea level and warm temperature anomalies for all regions. The temperature anomaly for the Central Region is most noticeably warmer due to the greater change from the reduction in upwelling than for any other region.

The California Current System (CCS) may also be directly affected by the ENSO. The result of modifying the CCS may be higher or lower anomalies for adjusted sea level and surface temperature.

3. Filtered Surface Temperature and Adjusted Sea Level Anomaly Series

Temperature (Figures 5a-g) and adjusted sea level (Figures 6a-c) anomaly series were formed by subtracting the lowpass-filtered annual series from the gap-filled raw series. These anomaly series were filtered using a second-order, 40-day lowpass Chebyshev type I filter to provide a smooth record for visual comparisons. Each of the eight three-year periods are displayed by station. The year designated for use in single ENSO year (1 July-30 June) spectra have been shaded for reference. The anomaly only varies between 2 and -2°C, and the range is generally smaller than 2°C. The strong ENSO periods have more events that appear to propagate between the stations than either the moderate or non-ENSO periods, especially in the shaded ENSO year. Adjusted sea level anomalies vary between -10 cm and 15 cm. Generally, the ENSO years appear to have more positive anomalies, and have more propagating features than non-ENSO years. Interestingly, a large decrease occurs in the adjusted sea level anomaly plots for all years at approximately the 750-800 day mark.

a. Southern Region

La Jolla surface temperature anomalies have anomalously warm periods during the winter of 1957-58, 1972-73 and 1983-83, corresponding to the development of the strong ENSO events (Figure 5a). The 1958 and 1983 series appear to be the most similar.

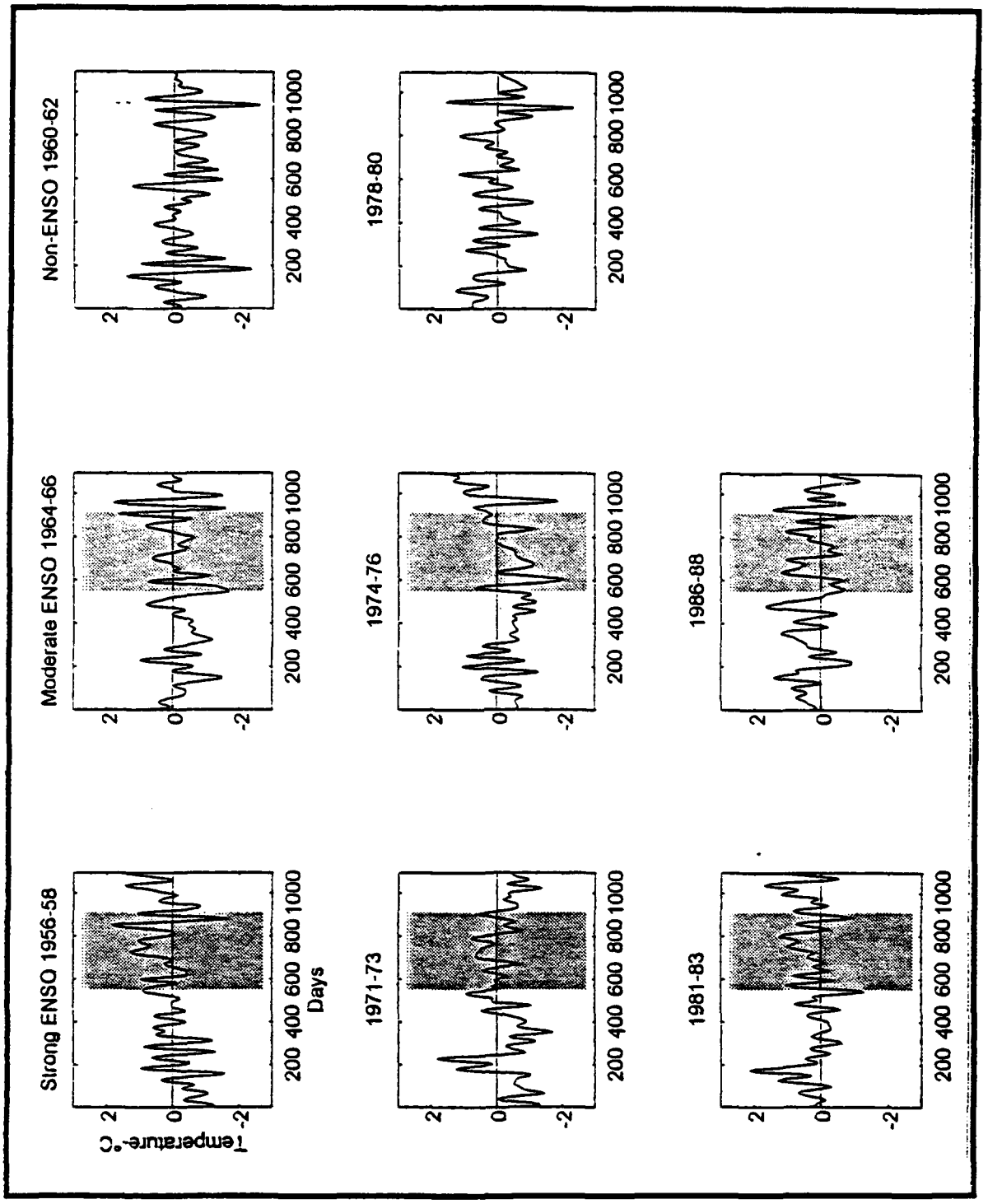

Figure 5a. Filtered Surface Temperature Anomaly Series for La Jolla.
For each x-axis, day 0 is January 1 of the first year of the three-year period. The shaded region corresponds to July 1, year 2, to June 30, year 3.

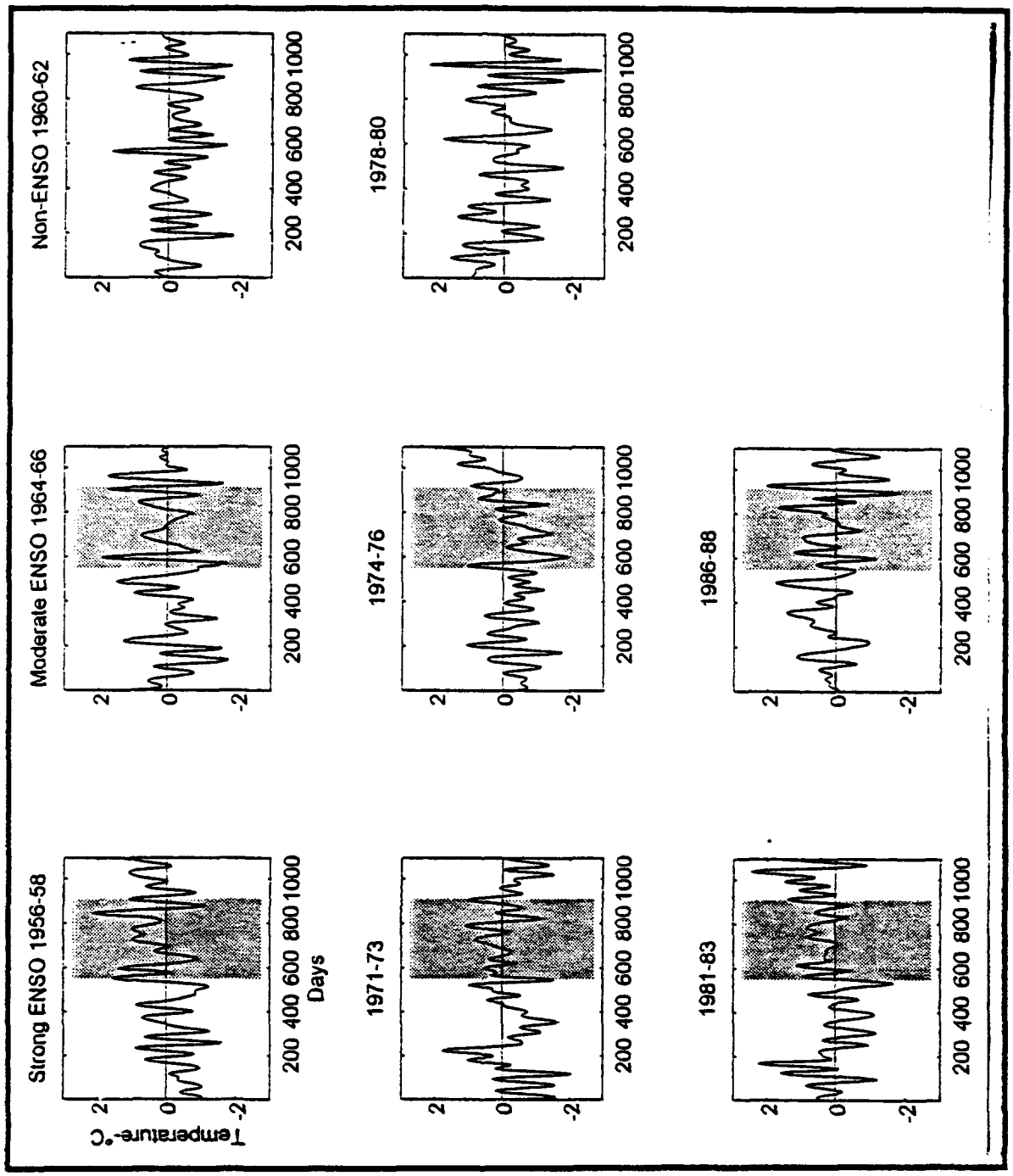

Figure 5b. Filtered Surface Temperature Anomaly Series for Balboa.
For each x-axis, day 0 is January 1 of the first year of the three-year period. The shaded region corresponds to July 1, year 2, to June 30, year 3.

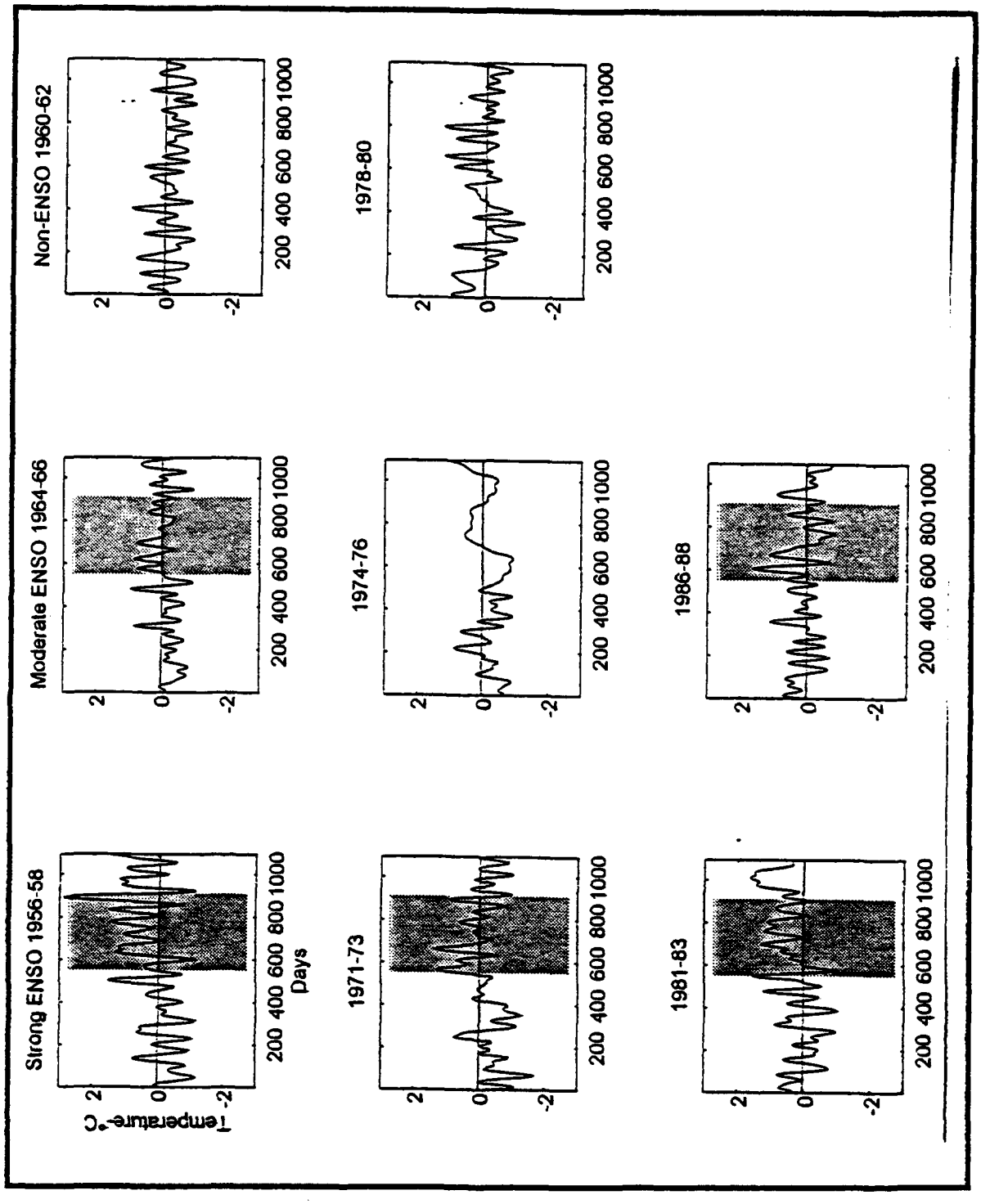

Figure 5c. Filtered Surface Temperature Anomaly Series for Pacific Grove.
For each x-axis, day 0 is January 1 of the first year of the three-year period. The shaded region corresponds to July 1, year 2, to June 30, year 3.

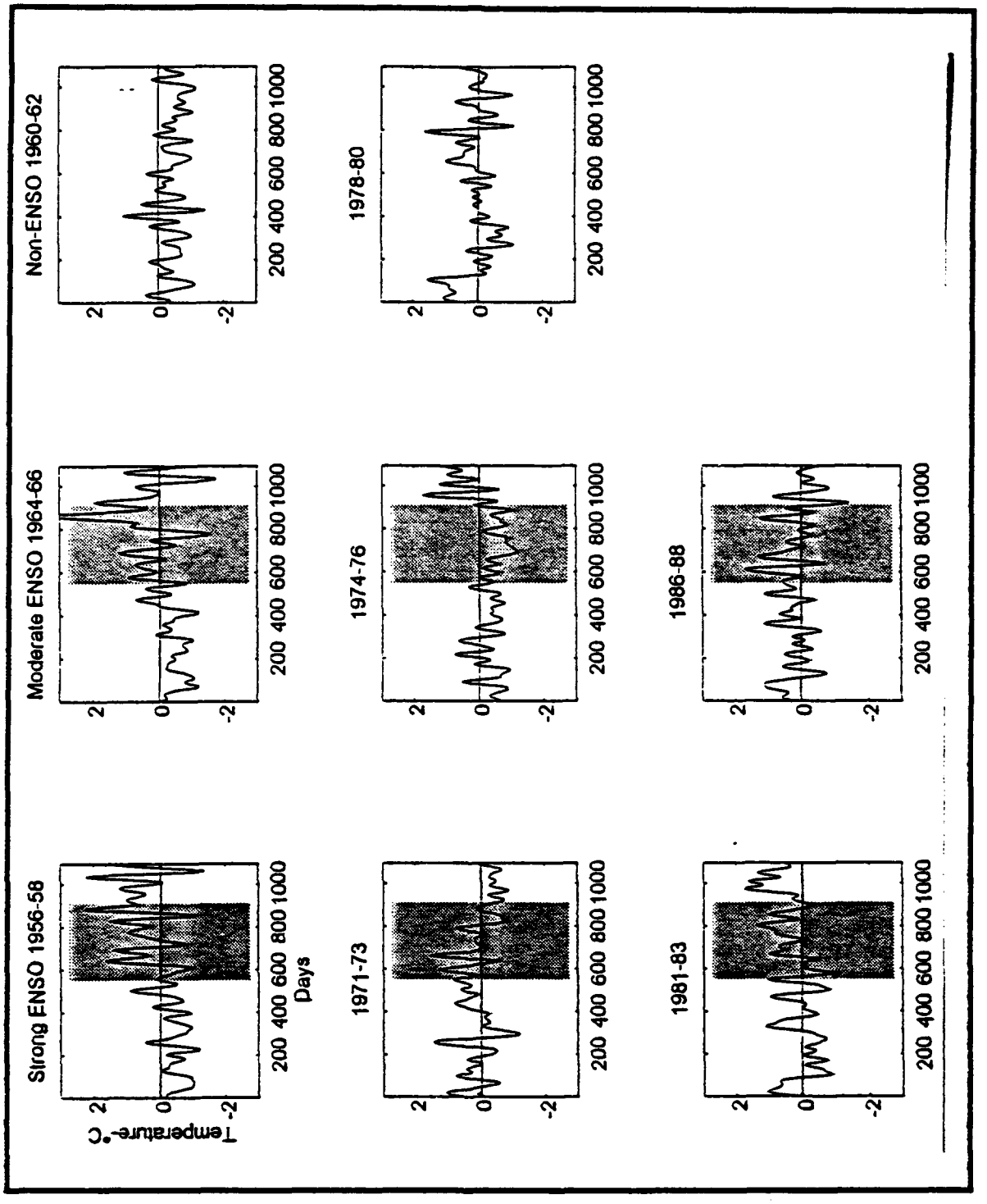

Figure 5d. Filtered Surface Temperature Anomaly Series for Farallon Islands. For each x-axis, day 0 is January 1 of the first year of the three-year period. The shaded region corresponds to July 1, year 2, to June 30, year 3.

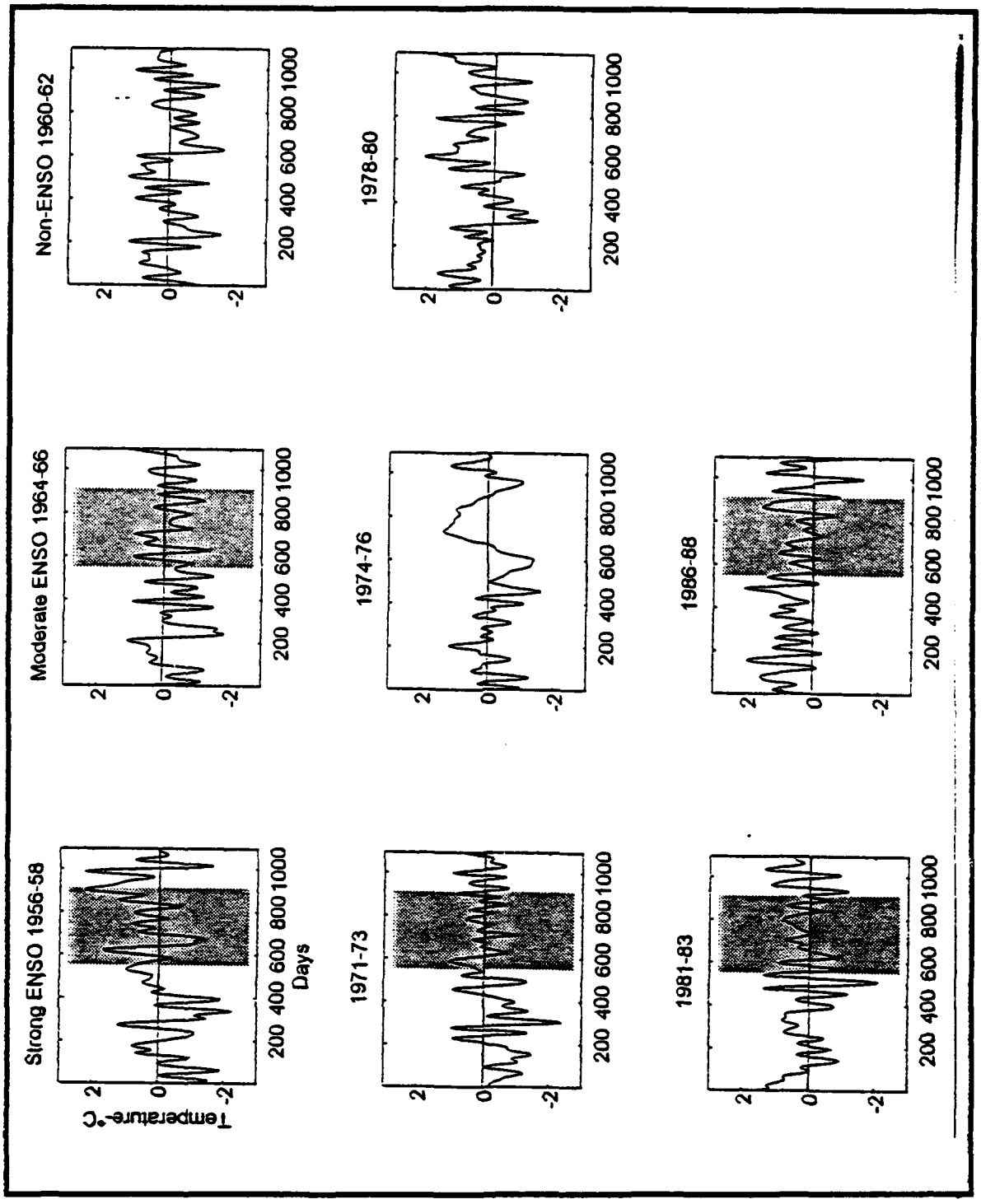

Figure 5e. Filtered Surface Temperature Anomaly Series for Crescent City.
For each x-axis, day 0 is January 1 of the first year of the three-year period. The shaded region corresponds to July 1, year 2, to June 30, year 3.

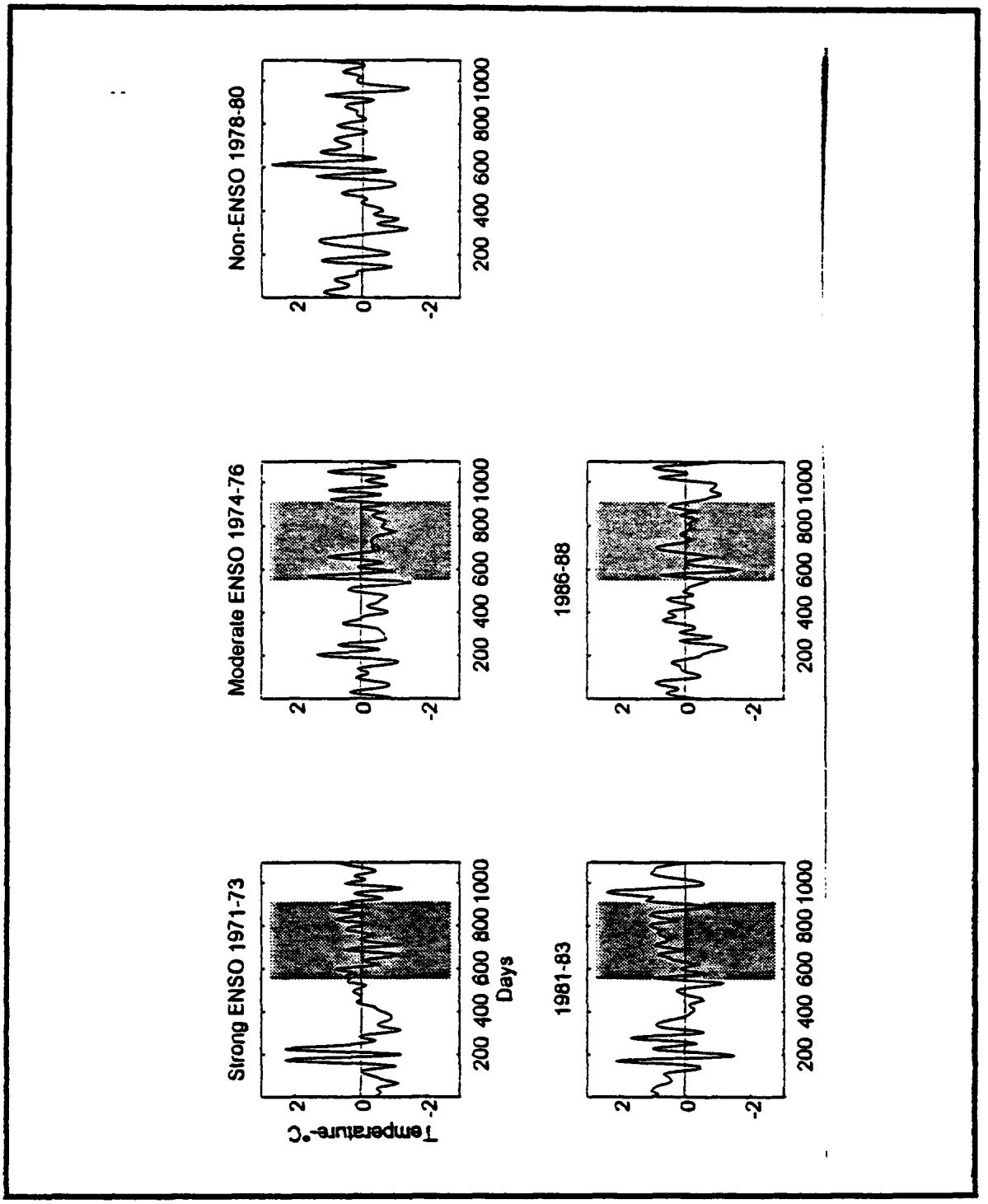

Figure 5f. Filtered Surface Temperature Anomaly Series for Charleston.
For each x-axis, day 0 is January 1 of the first year of the three-year period. The shaded region corresponds to July 1, year 2, to June 30, year 3.

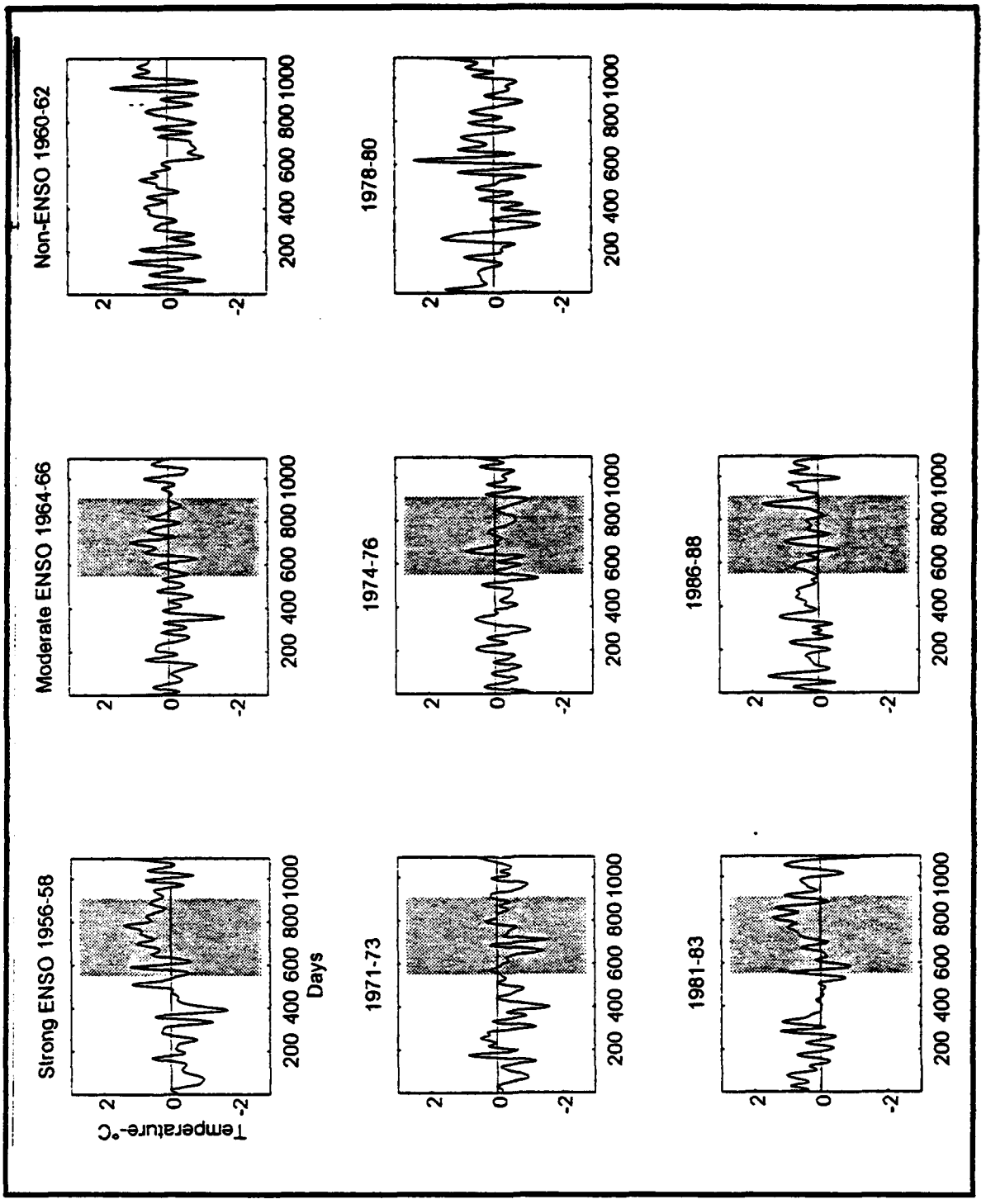

Figure 5g. Filtered Surface Temperature Anomaly Series for Neah Bay.
For each x-axis, day 0 is January 1 of the first year of the three-year period. The shaded region corresponds to July 1, year 2, to June 30, year 3.

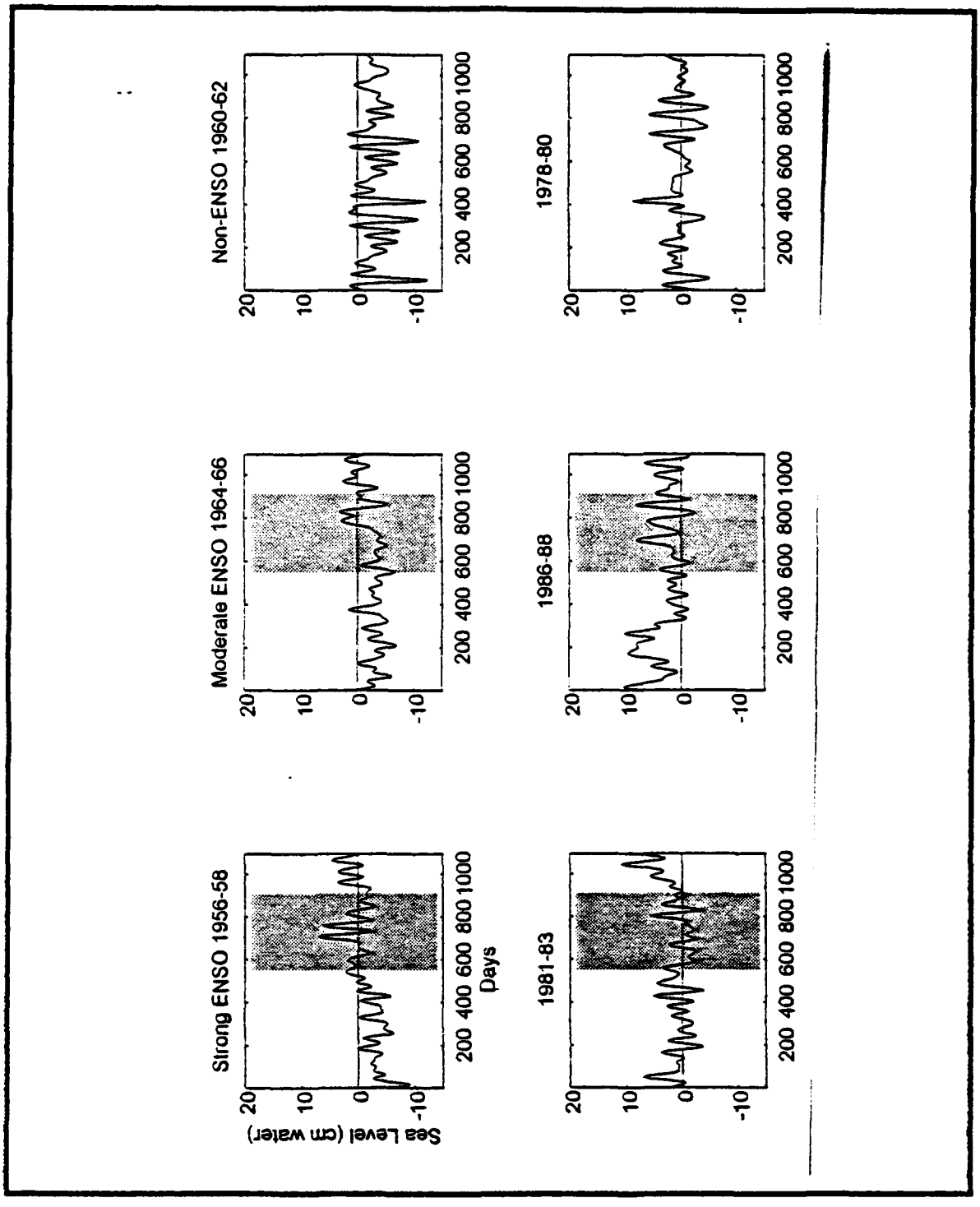

Figure 6a. Filtered Adjusted Sea Level Anomaly Series for La Jolla.
For each x-axis, day 0 is January 1 of the first year of the three-year period. The shaded region corresponds to July 1, year 2, to June 30, year 3.

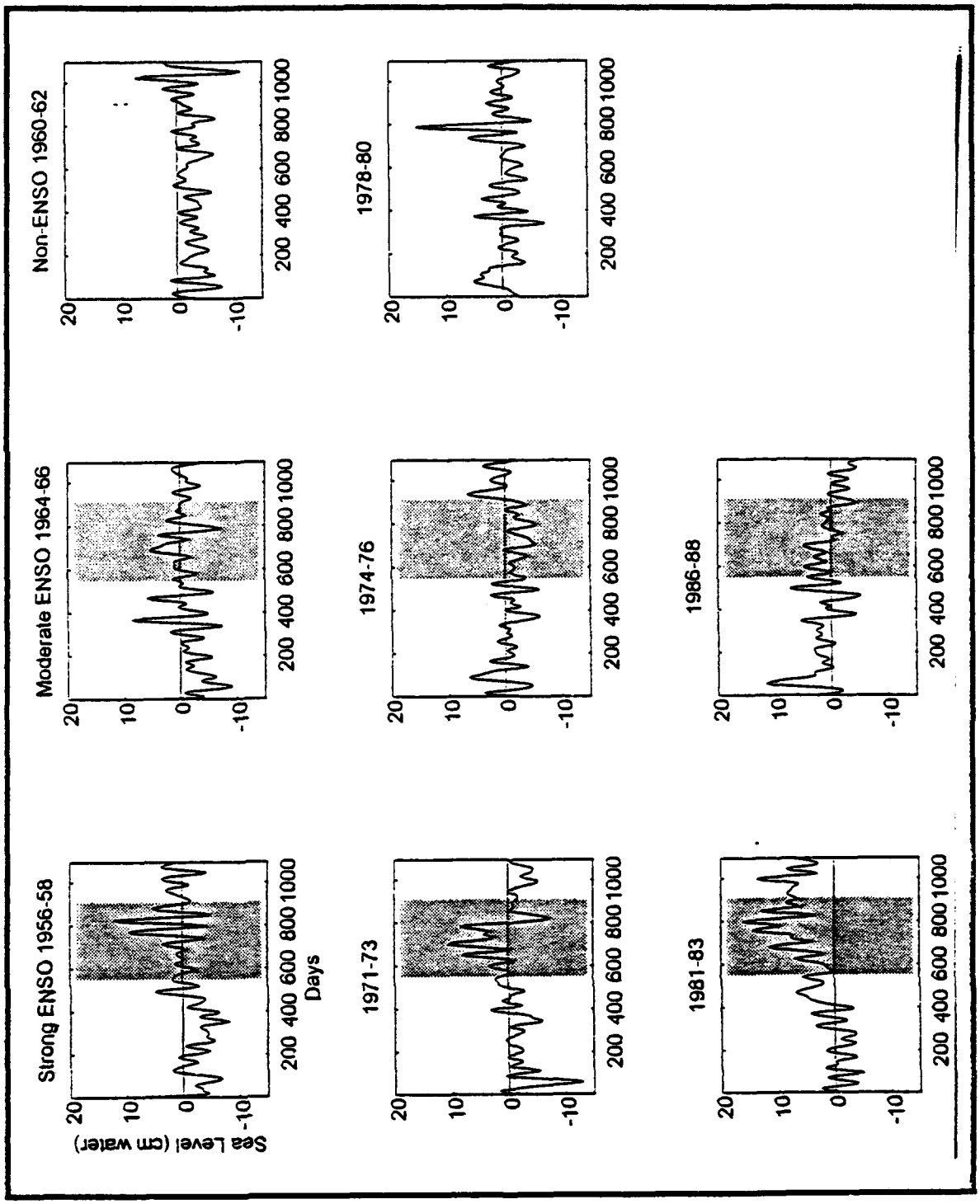

Figure 6b. Filtered Adjustes Sea Level Anomaly Series for San Francisco.
For each x-axis, day 0 is January 1 of the first year of the three-year period. The shaded region corresponds to July 1, year 2, to June 30, year 3.

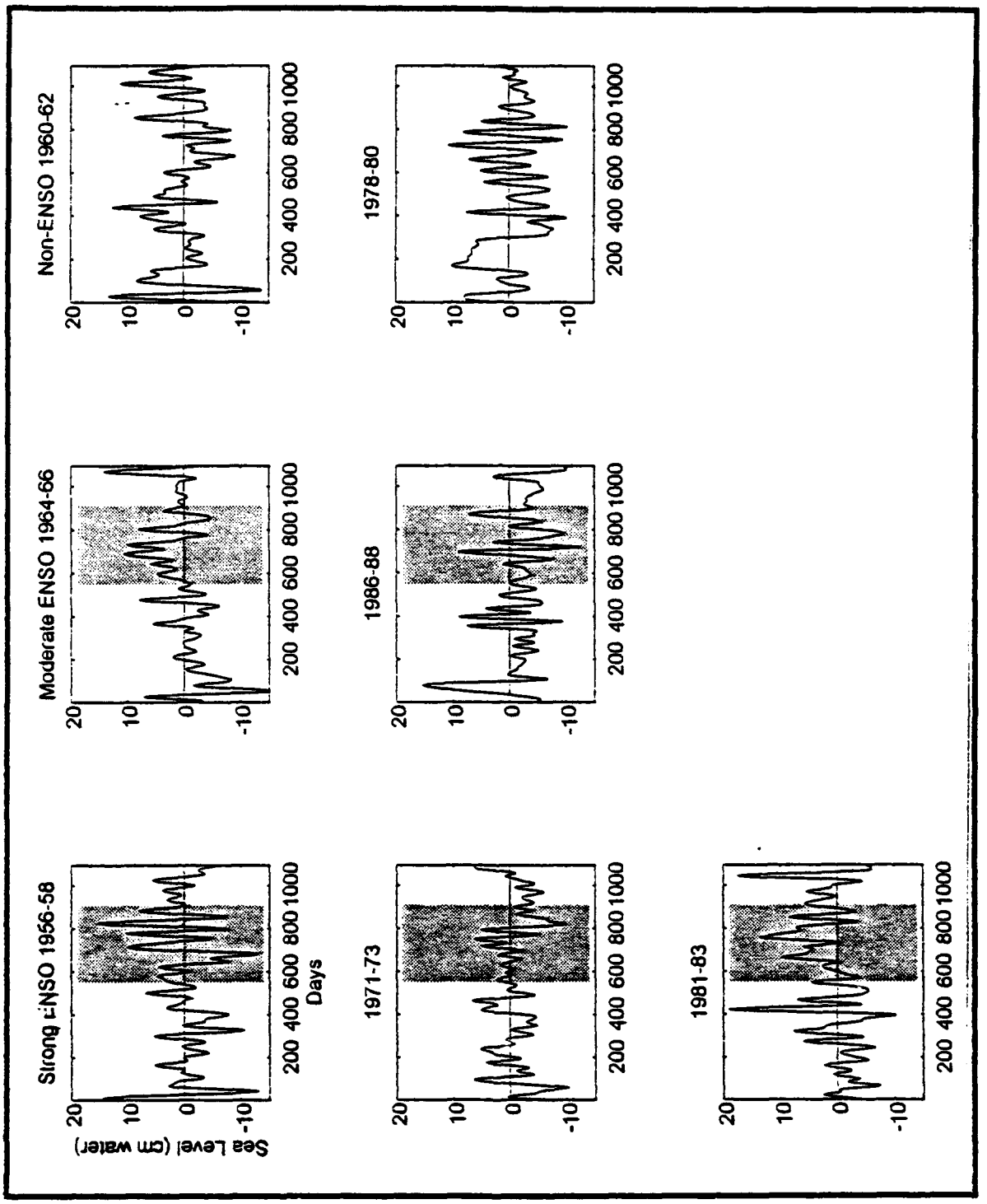

Figure 6c. Filtered Adjusted Sea Level Anomaly Series for Neah Bay.
For each x-axis, day 0 is January 1 of the first year of the three-year period. The shaded region corresponds to July 1, year 2, to June 30, year 3.

Moderate ENSO years of 1966 and 1976 actually appear to have anomalously low temperatures. Balboa (Figure 5b) is consistent with La Jolla for all of these periods.

La Jolla adjusted sea level anomalies (Figure 6a) have a small range. The highest period is 1986-88 and the lowest is from 1960-62. The shaded 1982-83, 1957-58, and 1987-88 show the higher sea levels expected of strong ENSO periods. The only segment of time which is consistently higher for all the ENSO periods is from day 750 to 850 (mid-January to May).

b. Central Region

Pacific Grove and the Farallon Islands surface temperature anomalies have the largest warm anomalies during the strong ENSO periods (Figure 5c-d). 1956-58 and 1981-83 are by far the warmest periods for both stations. 1971-73 is not as warm for either station and does not appear to be similar to the other strong ENSO events. Both of these stations are similar for most events, but the moderate event in 1964-66 for the Farallon Islands shows a large warm anomaly not present at Pacific Grove or any other station.

San Francisco (Figure 6b) has high sea level anomalies during the strong ENSO periods. The shaded year is higher than the corresponding period for the non-ENSO years, except for 1974-76 which appears low. These strong ENSO years standout as very different signals from the moderate event years and the non-ENSO years. A sudden drop in sea level in early 1966 precedes the dramatic warm anomaly noted previously at Farallon Islands.

c. Northern Region

Neah Bay surface temperature anomalies have warm temperatures for the 1956-58 and 1981-83 periods, with the 1971-73 series being similar to the non-ENSO series (Figure 5e). The moderate events are warm, but show no marked features. Crescent City is warm for the 1956-58 and 1981-83 periods (Figure 5f). The 1971-73 series for Crescent City looks like the Neah Bay 1971-73 record. The extensive gap-

filling of the 1956-58 record can be seen. Charleston was warm in 1981-83 with a similar pattern as Neah Bay (Figure 5g).

Neah Bay adjusted sea level anomalies (Figure 6c) have much more variability than either La Jolla or San Francisco. It tends to have a higher sea level during the ENSO periods, especially within the shaded portion. Exceptions are 1986-88 which is low in the shaded period, and 1960-62 which tends to be high in the shaded period. The record for 1960-62 is a marked change from the small variability and low heights of the other two stations for this period. The 1971-73 period has low sea levels and supports an oceanic-type ENSO event which was evident at San Francisco, but did not extend north to Neah Bay.

d. Propagating Events

Propagation of surface temperature anomalies are especially pronounced within the single, shaded ENSO years. The shaded 1982-83 event shows an initial peak in June-July 1982 (about day 550) with the central region leading the northern and southern regions slightly (Figure 5a-g). The double-humped peak prevalent through all stations from January to March 1983 (day 730-day 800) is least pronounced at Crescent City (Figure 5f). The shaded 1972-73 event is marked by more spatial variation and the loss of the warm anomaly at Neah Bay (Figure 5e). The shaded 1957-58 event is anomalously warm for all stations. It has a significant propagating peak from mid-March to April 1958 (day 800-day 815) for all stations. It is extremely difficult to track any events through the entire domain in the non-ENSO (non-shaded) years.

Propagating events for adjusted sea level anomalies are more difficult to determine. For 1956-58, a three events can be found at approximately day 725 (December 1957) to day 825 (April 1958) which appear to be propagating. Another event may be the positive anomaly near day 775 (February 1983) during 1981-83. These propagating events are much less pronounced than the temperature events, but roughly line up with them.

4. Filtered Single Year ENSO Anomaly Series

A second set of lowpass filtered temperature and sea level anomaly series was created using the Chebyshev type I digital filter of second order and natural frequency corresponding to a half-power period of ten days and a band pass ripple of 3 dB. Plotting these anomaly series together after offsetting the origin of each series proportional to the distance between each station allows examination of the series for propagating events in the 1982-83 ENSO year. (Figures 7 and 8). For the 1982-83 event, all series are visually well correlated. Adjacent stations such as La Jolla and Balboa are extremely similar. Interestingly, the variability is damped during the warmest period from day 200 to day 250 (mid-January to March 1983). Propagating features can be found from these series. Phase speeds are estimated from station separation and the lag of the event, assuming a theoretical speed range of 60-100 km/day, shown by phase spectra comparison to be the propagation speeds of alongshore anomalies (*Enfield and Allen*, 1980). Five events are shown with phase speed lines between 74 and 98 km/day.

Since there are only three stations for adjusted sea level anomalies, the progression of the signal from south to north is not as easily tracked as it was for surface temperature. Even with these differences and shortcomings, propagating features can be selected. Five such events were selected and phase speed lines were drawn with speeds of between 68 and 84 km/day. Subsequent cross-spectral analysis will support the propagation of these events and for phase speeds of this order.

B. FREQUENCY DOMAIN ANALYSIS

Autospectra and cross-spectra of the unfiltered surface temperature and adjusted sea level anomaly series are analyzed to determine energetic frequencies in the signals and estimate propagation of the alongshore waves.

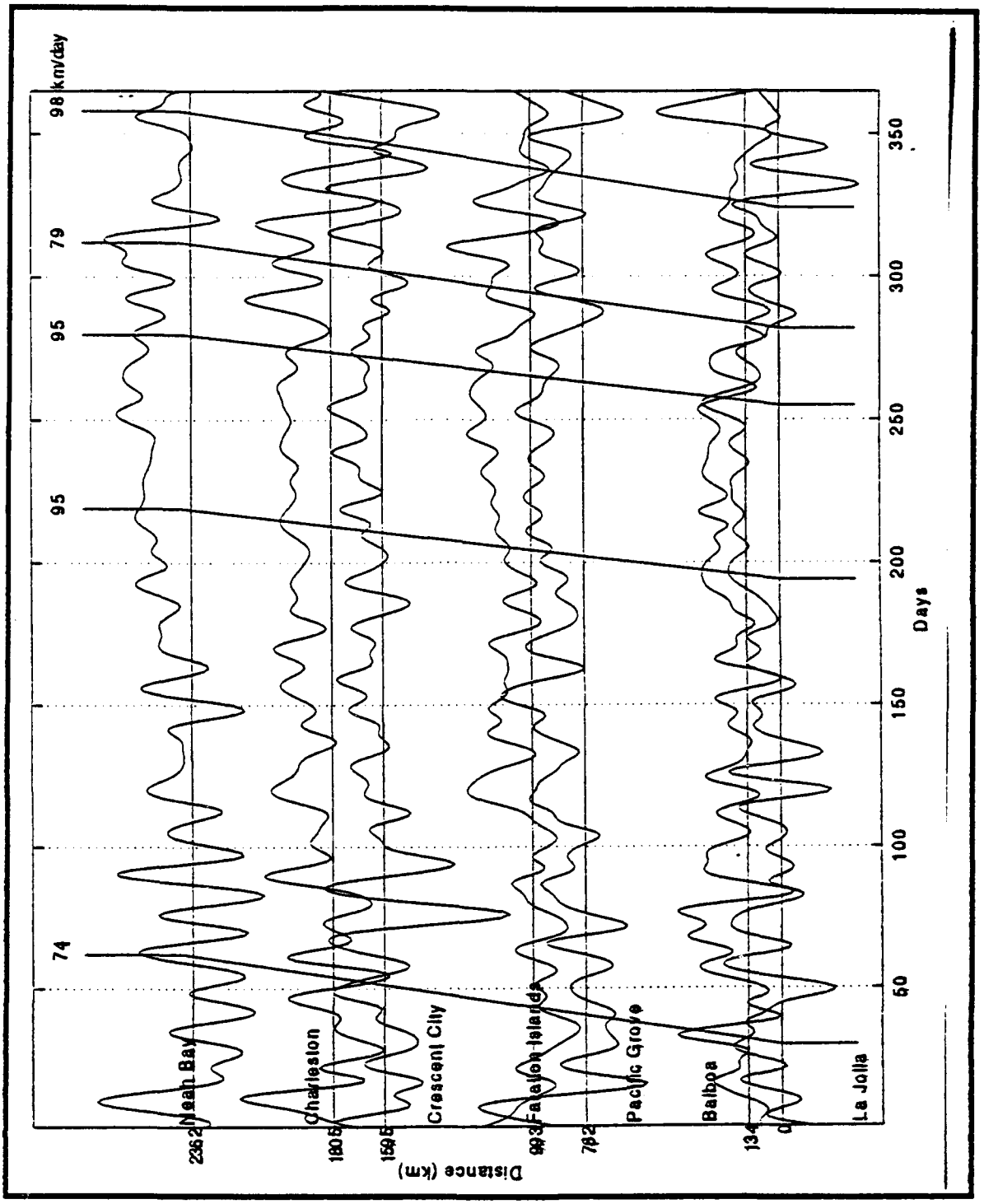

Figure 7. Filtered Surface Temperature Anomaly Series for Propagating Events.
For the x-axis, day 0 is July 1, 1982, and day 365 is June 30, 1983.
The slope of the lines is the phase speeds for the intersected events.

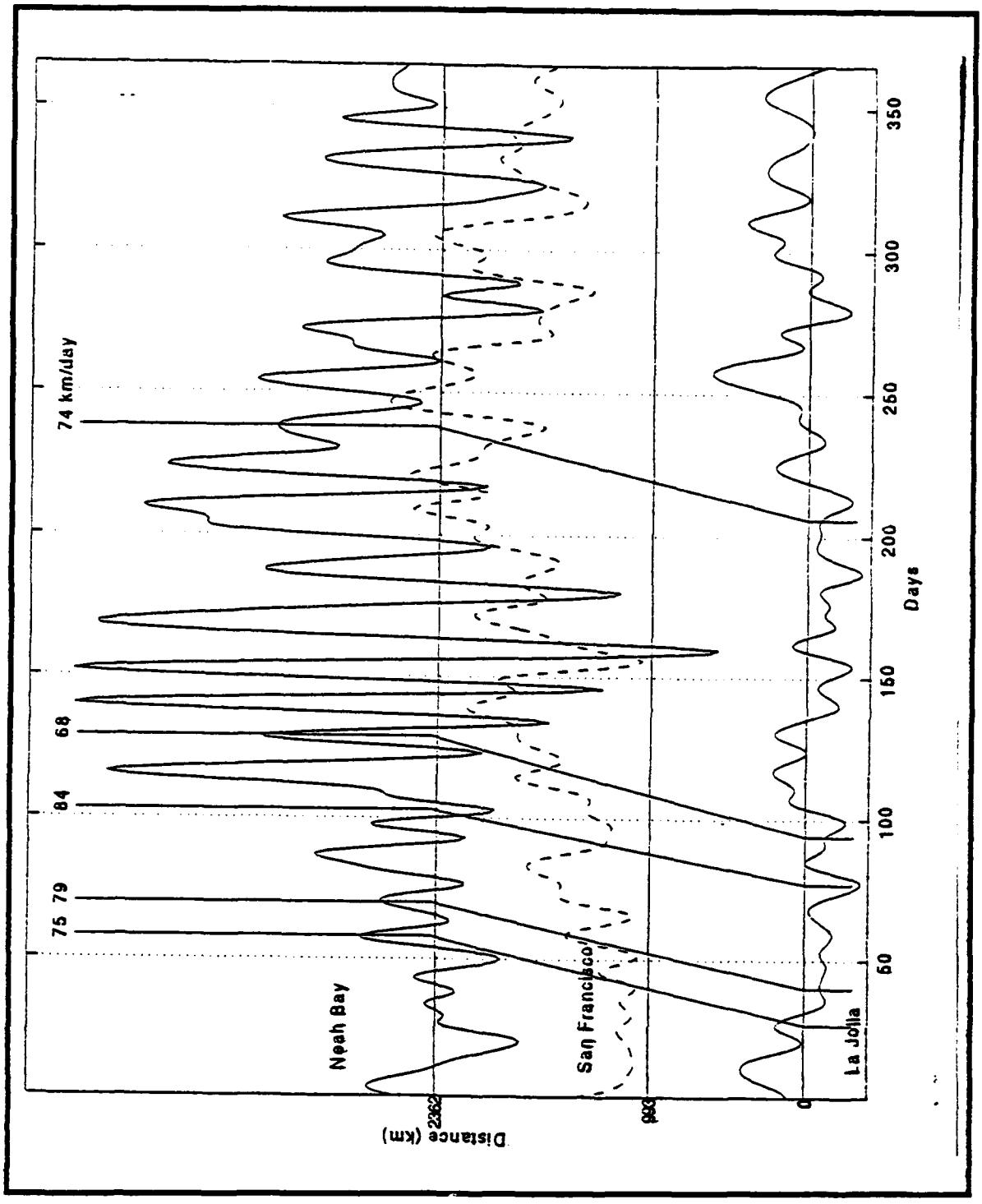

Figure 8. Filtered Adjusted Sea Level Anomaly Series for Propagating Events.
For the x-axis, day 0 is July 1, 1982, and day 365 is June 30, 1983.
The slope of the lines is the phase speeds for the intersected events.

1. Entire Series Autospectra for Temperature Anomaly and Sea Level Anomaly

Autospectra of the entire anomaly series for both the surface temperature and adjusted sea level is performed to find frequency bands of high power spectral density. The autospectra are plotted by region as power spectral density versus frequency in cycles per day (cpd) (Figure 9a-c). A 4096-point FFT was used for periods longer than 6 months. A 256-point FFT was used for periods from the 6 months to 3 days. 95% confidence intervals are plotted on the 256-point FFT spectra at representative frequencies for the primary station in each region. The 95% confidence intervals do not provide meaningful information due to the small number of windows available and large variability in the energetics at lower frequencies. The surface temperature anomaly series is 34 years long, while the adjusted sea level series varies between 18 and 24 years long. The shorter series will provide an overestimate of power spectral density with respect to a longer series, but the location and relative magnitudes will be accurate.

a. Southern Region

For the 4096-point FFT spectrum, La Jolla surface temperature anomaly (Figure 9a) has energy at the 1-year period (0.0027 cpd), but the largest peak with respect to background noise is at 300 days (0.0034 cpd). Monthly temperature data (*Cayan et al.*, 1988) confirms a less than 1 year "annual" cycle for this station. The 256-point FFT commences at approximately the same energy as the 4096-point FFT ended. Frequencies with power spectral density peaks are 0.034 cpd (29-day period), 0.074 cpd (13.5 days), 0.100 cpd (10 days), 0.124 cpd (8 days), 0.143 cpd (7 days), and 0.171 (6 days). The 29- and 13.5-day period energies may be associated with residual tidal energy at the fortnightly and MF periods in the series. Balboa has a very similar spectrum, which is expected due to the similarity of the original anomaly series to La Jolla. Substantial interannual variability in these and all other series is denoted by high spectral energy at periods longer than one year.

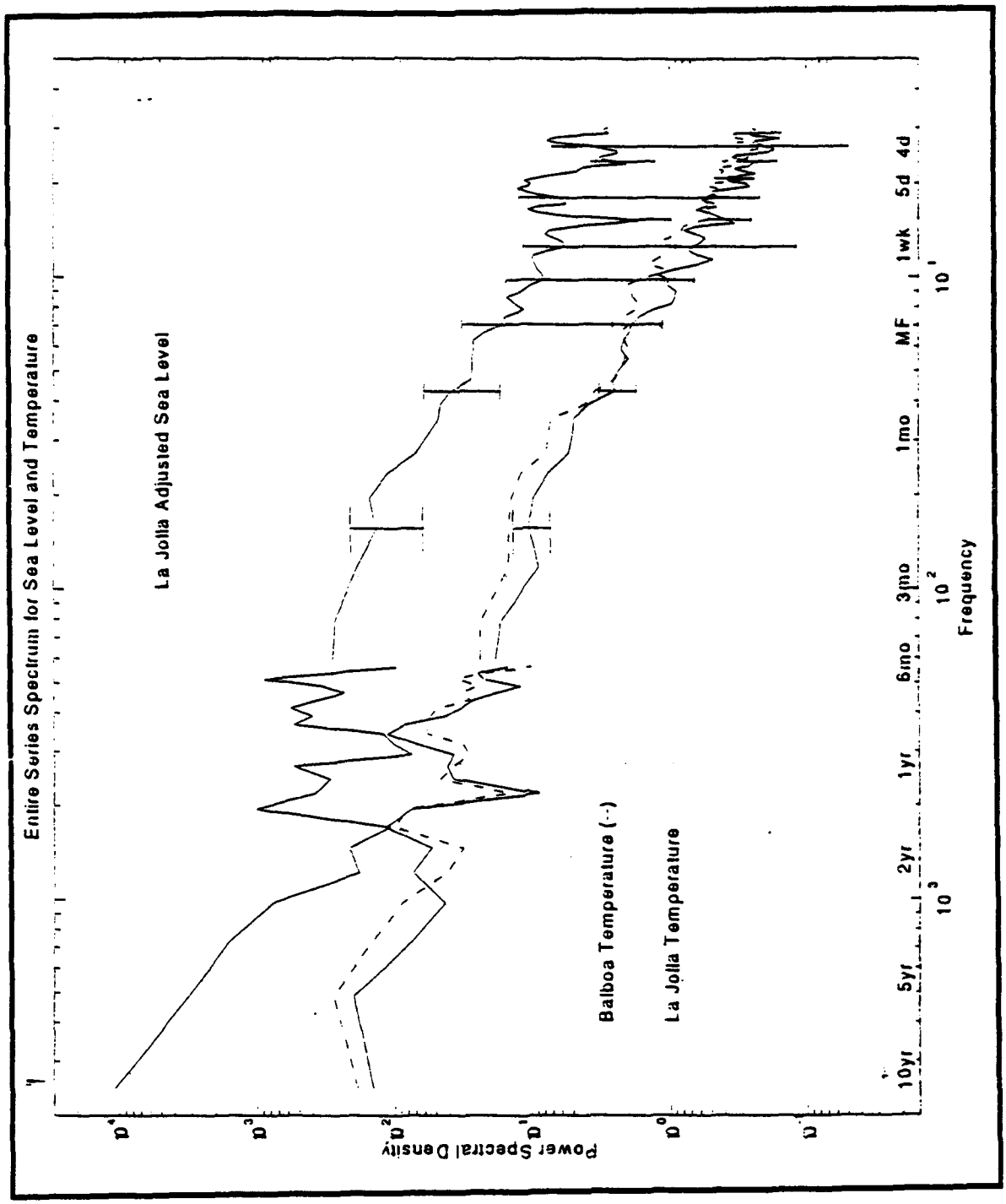

Figure 9a. Entire Series Spectra for Sea Level and Temperature Anomalies for the Southern Region: $(°C^2/cpd)$ and (cm^2/cpd) are power spectral density units for temperature and sea level, respectively.

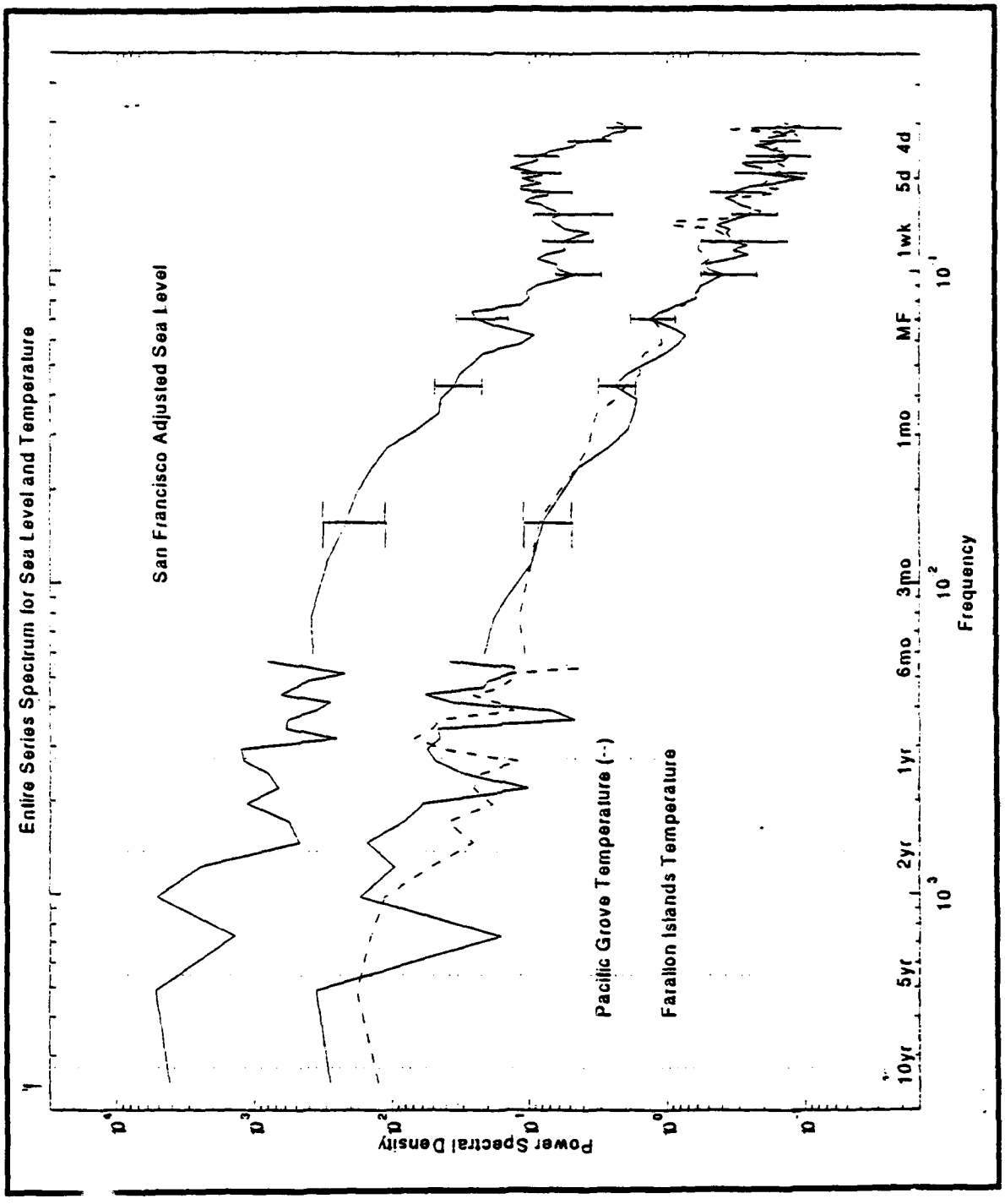

Figure 9b. Entire Series Spectra for Sea Level and Temperature Anomalies for the Central Region: $(°C^2/cpd)$ and (cm^2/cpd) are power spectral density units for temperature and sea level, respectively.

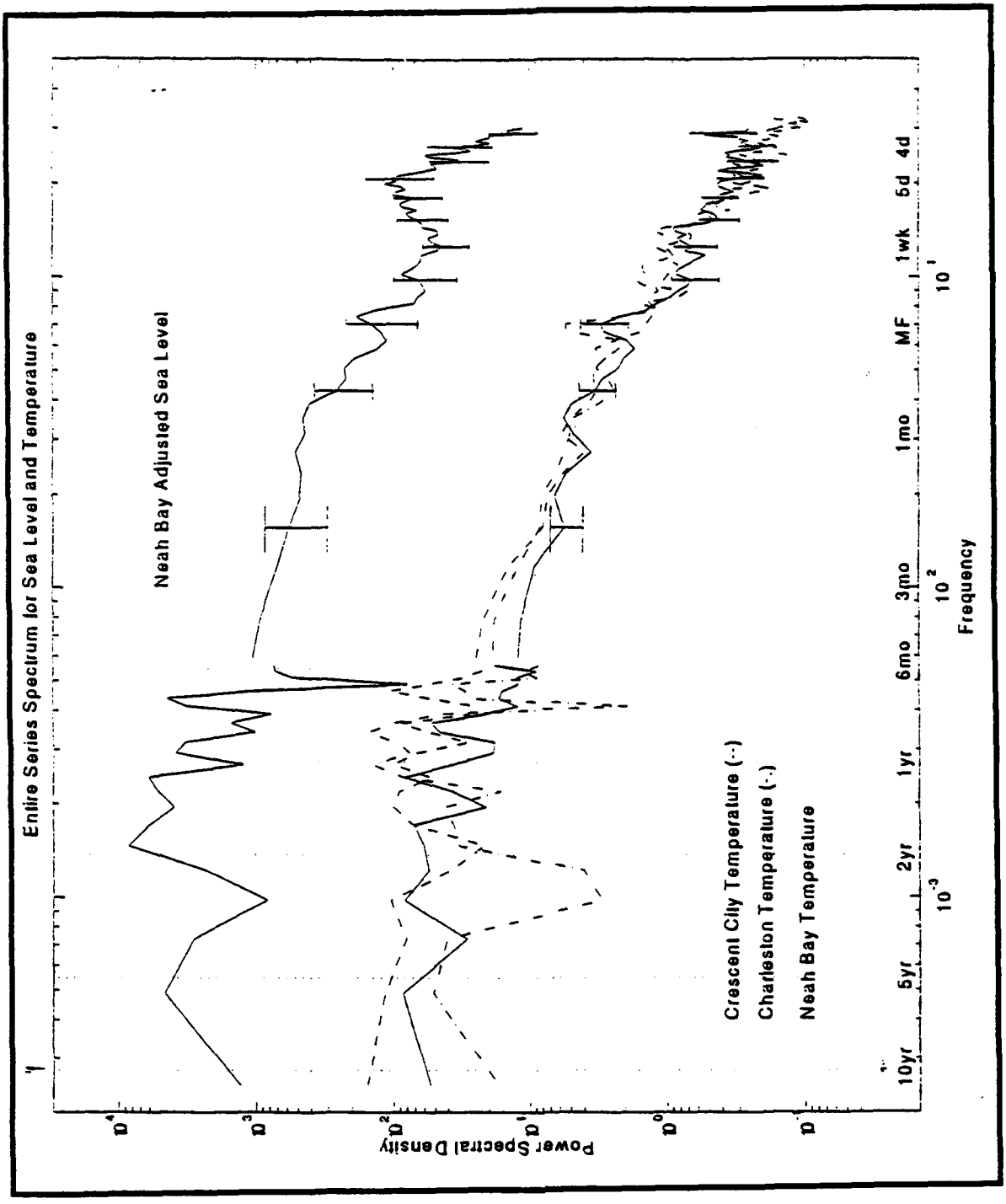

Figure 9c. Entire Series Spectra for Sea Level and Temperature Anomalies for the Northern Region: $(°C^2/cpd)$ and (cm^2/cpd) are power spectral density units for temperature and sea level, respectively.

The La Jolla adjusted sea level anomaly spectrum (Figure 9a) is based on a series length of 18 years compared to 34 years for the surface temperature series. The energy cascade is similar for both sea level and temperature spectra. For the 4096-point FFT, peaks exist at the 1-year period, and also at approximately 300 days to match temperature. In the 256-point FFT spectrum, the tidal frequencies appear to be effectively filtered. Peaks coincide with the temperature spectra at the 7-and 6-days. The adjusted sea level anomaly has relatively more high frequency (ω>0.1 cpd) energy than the surface temperature anomaly.

b. Central Region

Farallon Islands surface temperature anomaly spectrum (Figure 9b) has an annual signal peak at 1-year for the 4096-point FFT. For the 256-point FFT spectra, peaks are 0.044 cpd (22 days), 0.074 cpd (13.5 days), 0.100 cpd (10 days), 0.143 cpd (7 days), and 0.174 cpd (5.75 days). No fortnightly peak exists, but the MF peak is more pronounced than at La Jolla. The 10 day, 7 day and 6 day periods match La Jolla.

The energy cascade of the San Francisco adjusted sea level anomaly spectrum (Figure 9b) is similar to that of the Farallon Islands surface temperature anomaly spectrum. The 4096-point FFT spectrum is very similar in peaks and shape to the Farallon Islands spectrum.. The 1-year period is a peak. For the 256-point FFT, peaks correspond for 13.5 days, 10 days and 7 days. No peak is present at 22 days. The rising energy level from 4 to 7 days, peaking at 4.8 days, may mask any energy at the 6 day period. The San Francisco sea level spectrum is based on 24 years of data, compared to 34 years for the temperature series.

c. Northern Region

For the 4096-point FFT, Neah Bay surface temperature anomaly spectrum (Figure 9c) has a peak at approximately 400 days, but not at 1-year. Both Charleston and Crescent City have peaks at 1-year. The series length for Charleston is only 15 years, so the energy is slightly overestimated. The 4096-point FFT spectra for these three stations

have similar energy levels, but dissimilar shape. For the 256-point FFT, peaks are 0.0196 cpd (51 days), 0.0348 cpd (29 days), 0.0740 cpd (13.5 days), 0.100 cpd (10 days), and 0.143 cpd (7 days). Both the fortnightly and MF peaks are significant. Again, the 10 day and weekly periods stand out. Crescent City and Charleston closely resemble Neah Bay for the 256-point FFT spectra.

The Neah Bay 4096-point FFT adjusted sea level anomaly spectrum (Figure 9c) is dissimilar from its surface temperature equivalent. The series length is only 21 years compared to 34 years for the surface temperature series. The "annual" peak appears at about 400 days. The 256-point FFT spectra for both adjusted sea level and surface temperature have the same energy cascade until the adjusted sea level anomaly spectra rises at the 7 day mark until 4.5 days. All three stations for adjusted sea level anomaly exhibit this feature, which probably corresponds to short duration storms. The reason a similar pattern does not appear in the temperature spectrum is unclear. Peaks in Neah Bay adjusted sea level anomaly spectrum occur at 0.0274 cpd (36.5 days), 0.0353 cpd (28 days), 0.0560 cpd (18 days), 0.0790 cpd (12.7 days), 0.143 cpd (7 days), and 0.181 cpd (5.5 days). The fortnightly and MF periods are significant. Of these, only the weekly peak corresponds to surface temperature spectral peaks.

2. Cross- Spectra for Temperature Anomaly Versus Sea Level Anomaly

The ENSO year of 1982-83 is the interval selected for the cross-spectral analysis of the surface temperature anomaly to the adjusted sea level anomaly. Results are shown for the primary station in each region (Figure 10a-c). A 128-point FFT was selected for the analysis. The surface temperature spectra ($^{\circ}C^2$/cpd) and sea level spectra (cm^2/cpd) are plotted versus frequency (cpd) in the upper left subplot of each figure. Coherence between the two series is plotted with a 95% confidence (.77) in the upper right subplot. The transfer function magnitude or gain is the lower left subplot. Gain greater than 1 means that the surface temperature anomaly spectral energy is less than the adjusted sea

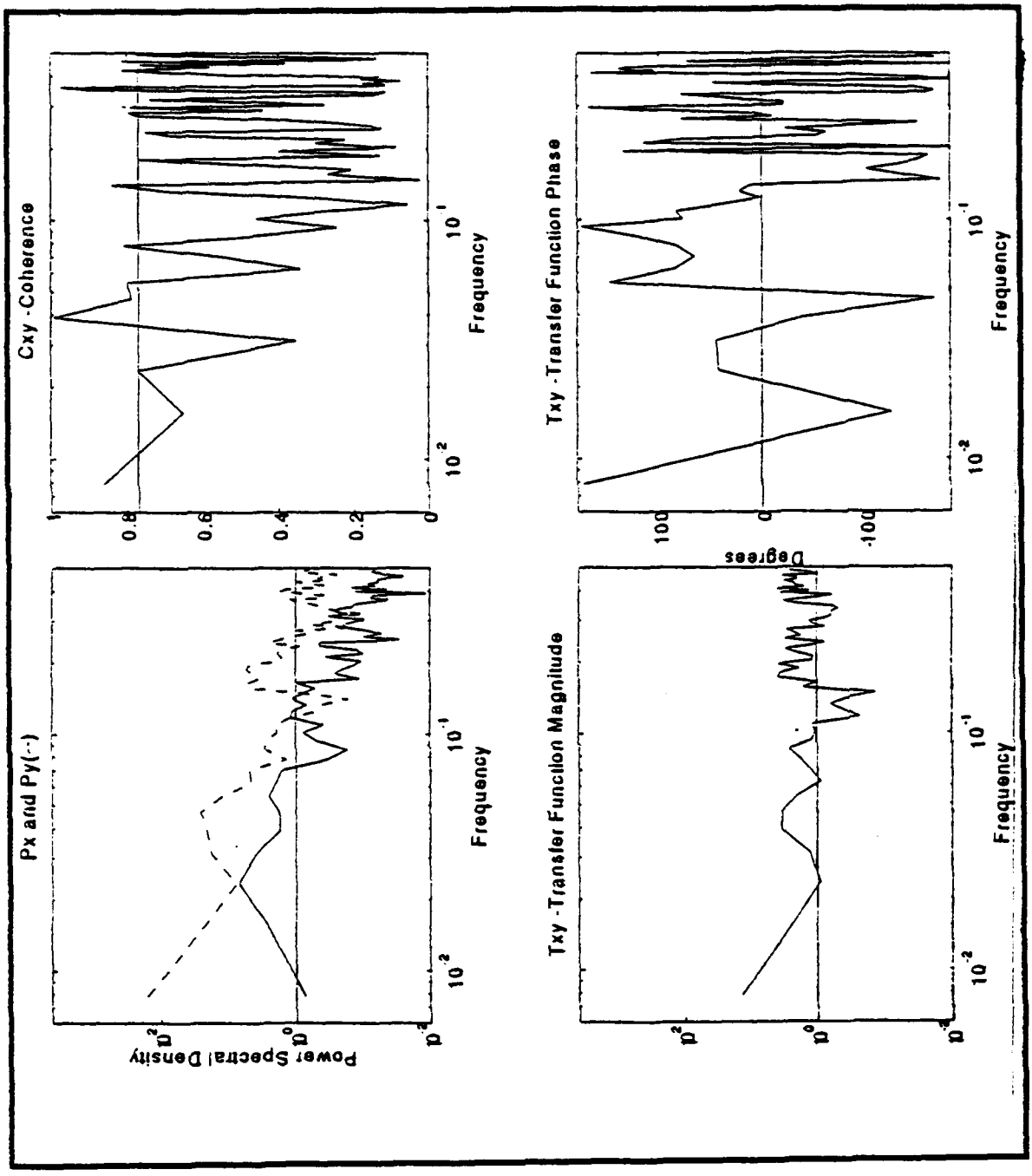

Figure 10a. 1982-83 Temperature Anomaly Versus Sea Level Anomaly Cross-Spectral Plots for La Jolla.

Power spectral density units are: $\left(°C^2/\text{cpd}\right)$ and $\left(\text{cm}^2/\text{cpd}\right)$. Frequency is in (cpd). The 95% confidence level (0.77) is plotted on the Coherence subplot.

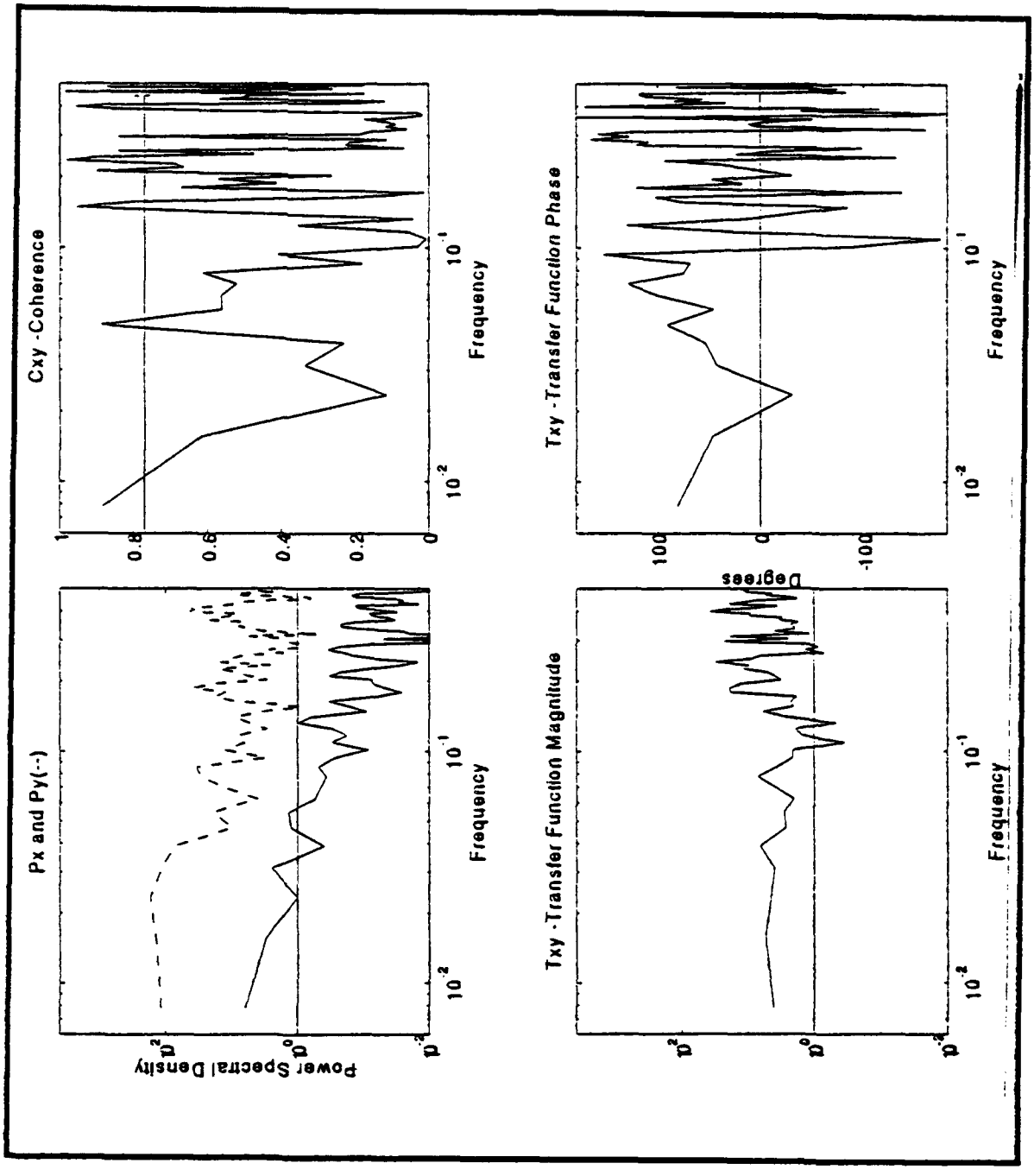

Figure 10b. 1982-83 Temperature Anomaly Versus Sea Level Anomaly Cross-Spectral Plots for Farallon Islands/San Francisco.

Power spectral density units are: $\left(°C^2/\text{cpd}\right)$ and $\left(\text{cm}^2/\text{cpd}\right)$. Frequency is in (cpd). The 95% confidence level (0.77) is plotted on the Coherence subplot.

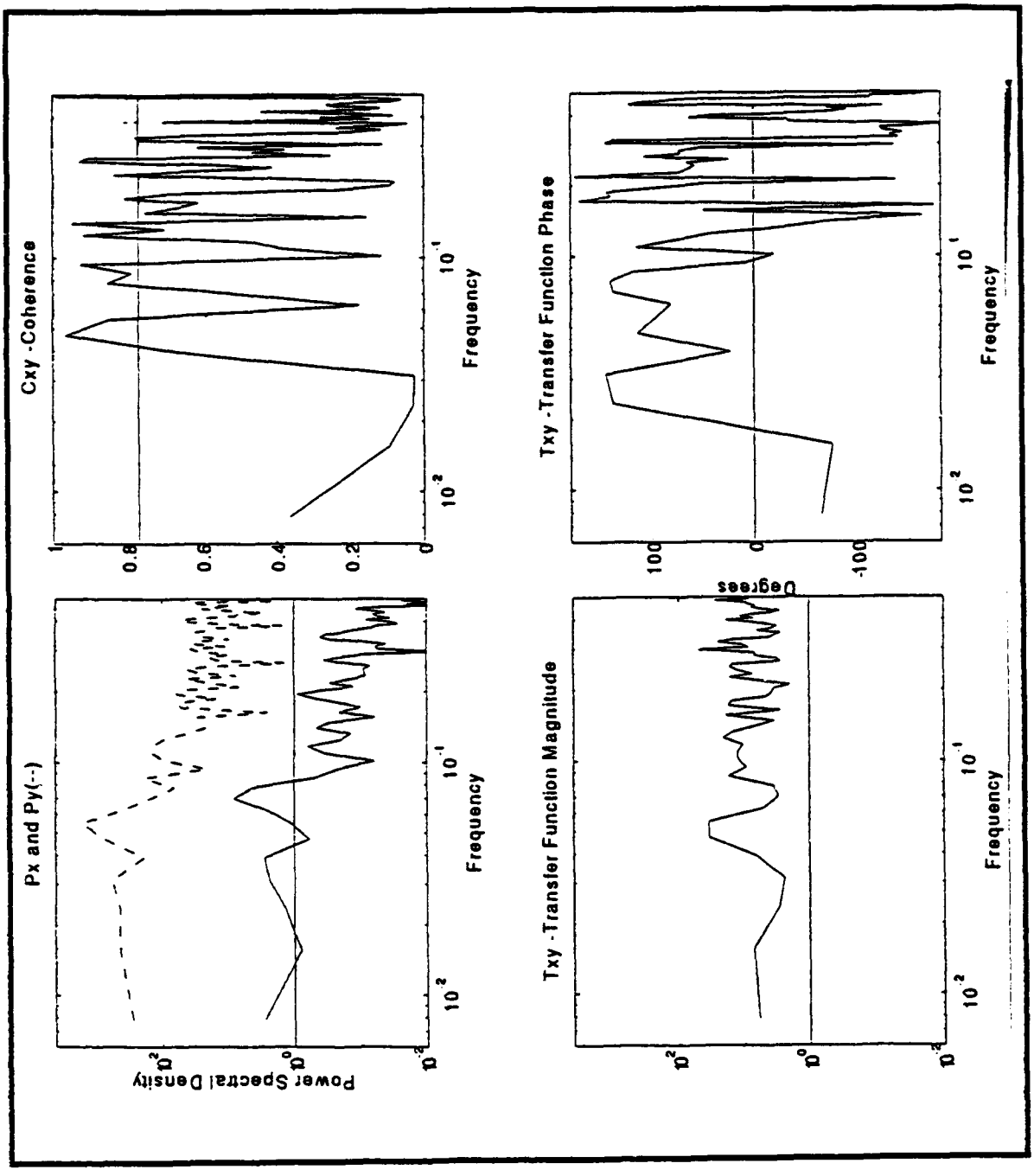

Figure 10c. 1982-83 Temperature Anomaly Versus Sea Level Anomaly Cross-Spectral Plots for Neah Bay.

Power spectral density units are: $\left(°C^2/\text{cpd}\right)$ and $\left(\text{cm}^2/\text{cpd}\right)$. Frequency is in (cpd). The 95% confidence level (0.77) is plotted on the Coherence subplot.

level anomaly spectral energy. The transfer function phase, in degrees, is the lower right subplot. Positive phases for surface temperature anomaly leads adjusted sea level anomaly.

a. Southern Region

La Jolla surface temperature anomaly autospectrum (solid) (Figure 10a) peaks include 0.0210 cpd (48 days), 0.0700 cpd (14 days), 0.110 cpd (9 days), 0.140 cpd (7 days) and 0.210 cpd (4.8 days). Adjusted sea level anomaly autospectrum (broken) peaks include 0.0480 cpd (21 days), 0.0700 cpd (14 days), 0.0900 cpd (11 days), 0.140 cpd (7 days), and 0.210 cpd (4.8 days). Coherent peaks include 128 days, 25 days, 12.5 days, 7 days, 3.6 days, and 3.2 days. The gain is greater than one, for all coherent peaks except 7 days. Except for the 25 day period, surface temperature leads adjusted sea level at coherent frequencies.

b. Central Region

The Farallon Islands surface temperature anomaly autospectrum (solid) (Figure 10b) peaks include 0.0300 cpd (33 days), 0.0540 cpd (18.5 days), 0.0820 cpd (12 days), and 0.140 cpd (7 days) San Francisco adjusted sea level anomaly autospectrum (broken) peaks include 0.0540 cpd (18.5 days), 0.0820 cpd (12 days), 0.140 cpd (7 days), and 0.0180 cpd (5.5 days). Coherent periods are 128 days, 21 days, 7 days, and 4.8 days. Gain is consistently greater than 1 for the coherent frequencies. As was for La Jolla, only the 25 day period has adjusted sea level leading surface temperature in phase.

c. Northern Region

Neah Bay surface temperature anomaly autospectrum (solid) (Figure 10c) has peaks at 0.0300 cpd (33 days), 0.0700 cpd (14 days), 0.105 cpd (9.5 days), 0.200 cpd (5 days), and 0.280 cpd (3.6 days). Neah Bay adjusted sea level anomaly autospectrum (broken) has peaks at 0.0300 cpd (33 days), 0.050 cpd (20 days), 0.105 cpd (9.5 days), 0.200 cpd (5 days), and 0.280 cpd (3.6 days). Coherent periods include 21 days, 14 days, 11 days, 9 days, 8 days, and 3.7 days. The coherent periods have high gains with the 14

day period being relatively low. Temperature leads sea level in phase for all of these periods except for 8 days.

d. Summary

Coherent bands are fairly consistent for the stations. These bands are 21-25 days, 12-14 days and 4-5 days. The 7 day peak is not prevalent for Neah Bay as it was for the other stations. This analysis confirms spectrally the interrelationship of surface temperature and adjusted sea level anomalies.

3. ENSO-Year Cross- Spectra of La Jolla Versus All Other Stations

La Jolla surface temperature and adjusted sea level anomalies were compared cross-spectrally to all other stations for the strong ENSO-year of 1982-83, to examine the propagation of events along the coast. Internal Kelvin waves with periods of 4-20 days were of special interest, based on the research of *Enfield and Allen* (1980) and *Smith* (1978). 1982-83 was also compared to the moderate ENSO year 1965-66. A 128-point FFT was employed. The most coherent frequencies were then selected for further analysis to insure statistical confidence in the phase speeds.

a. Surface Temperature Anomaly

For 1982-83, the periods of 16.0, 9.1, 6.1, and 4.9 days were chosen since they are generally highly coherent and thus more representative of reasonable phase differences (Figure 11). Phase speeds between La Jolla and each station were used to estimate the travel time along the coast (Figure 12). The phase speeds were adjusted by increments of 2π until the estimated phase speed was the closest to 80 km/day based on phase speeds determined by *Enfield and Allen* (1980). This adjustment of the phase speed accounts for the fact that the distance between stations was often greater than the internal Kelvin wavelength, based on theoretical estimates for the west coast. This method may lead to ambiguity at higher frequencies, since for each additional cycle added only a small amount of phase speed is gained allowing the number of cycles $\pm$ 1 cycle to fall within the phase speed range of 60-100 km/day. However, wavelengths for the lower frequencies

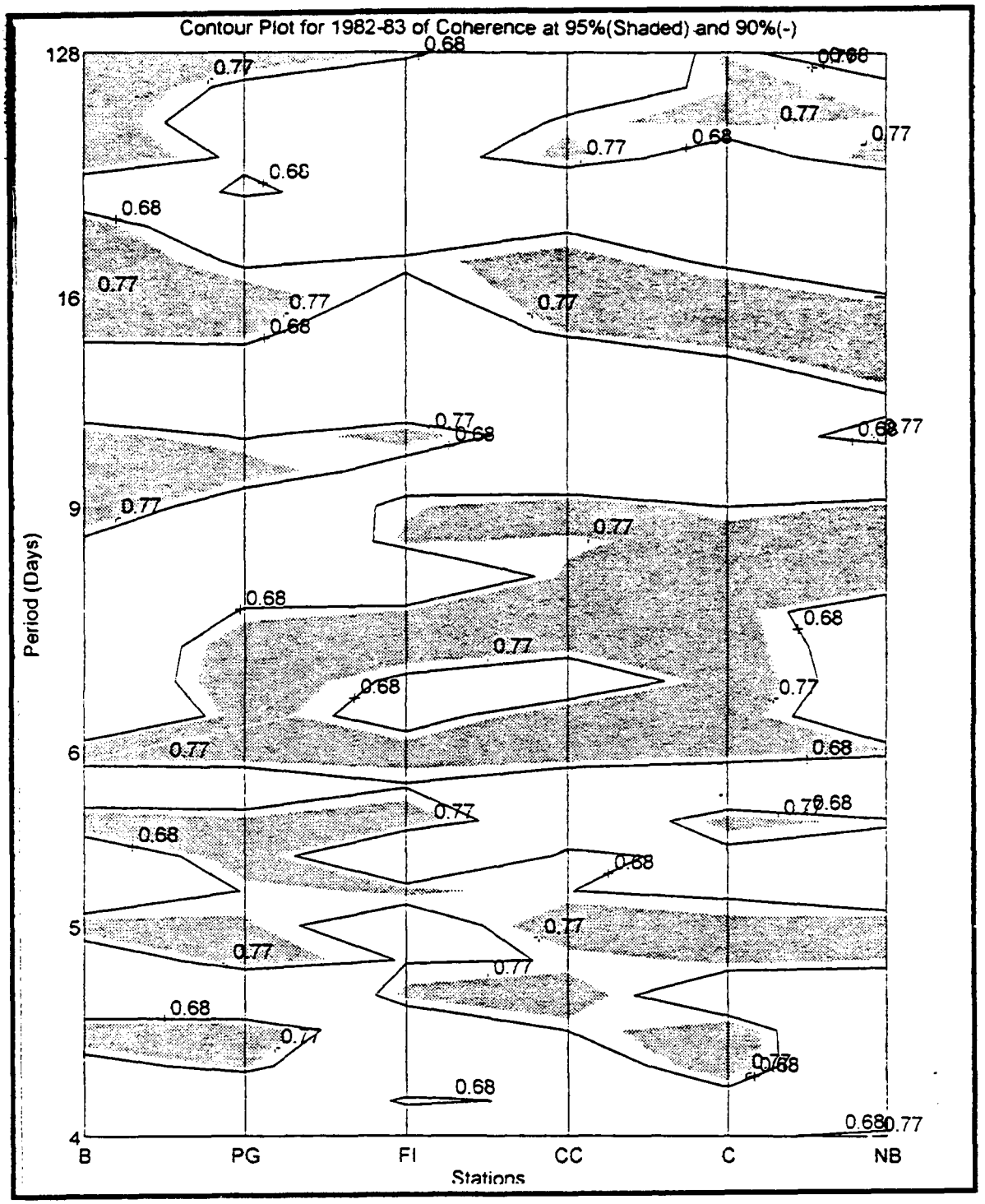

Figure 11. 1982-83 Surface Temperature Anomaly Coherence Contour Plot. Shaded regions correspond to 95% confidence level (0.77), while contour lines are for 90% confidence level (0.68).

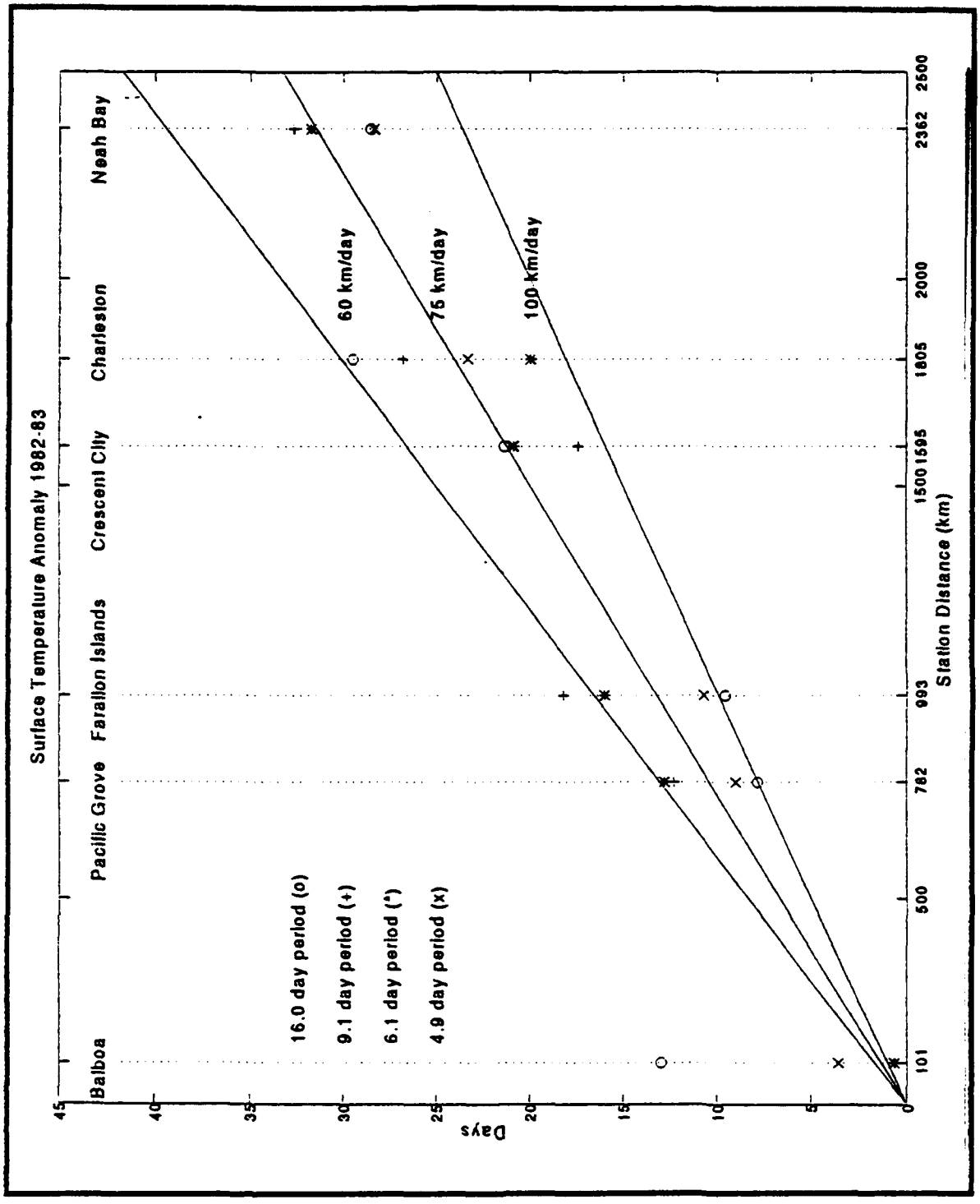

Figure 12. 1982-83 Surface Temperature Anomaly Phase Travel Times from La Jolla to the Other Stations for Selected Periods.

are close to the distance between La Jolla and the northern stations, so the lower frequency solutions for phase speed cannot be ambiguous. In all the analysis, when incremented by 2π, there is a systematic progression up the coast such that estimated wavelength at each frequency point for each station is reasonable when compared to the theoretical estimates. The cycles added to each period and the coherence are shown in Table 1.

TABLE 1. 1982-83 SURFACE TEMPERATURE ANOMALY CROSS-SPECTRA: This table lists the complete cycles added per period for each station and the respective coherence.

Period in Days	Pacific Grove		Farallon Islands		Crescent City		Charleston		Neah Bay	
	n	Coh	n	Coh	n	Coh	n	Coh	n	Coh
16.0	0	0.88	0	0.60	1	0.88	1	0.91	1	0.73
9.1	1	0.43	1	0.74	1	0.98	2	0.68	3	0.82
6.1	2	0.94	2	0.89	3	0.98	3	0.86	5	0.78
4.9	1	0.81	2	0.44	4	0.96	4	0.84	5	0.97

As seen in Table 1, the number of additional cycles (full wavelengths) increases steadily with distance from La Jolla and for increasing frequency (shorter wavelengths). For example, for the 16.0 day period wave, a full wavelength for the internal Kelvin wave was not reached until Crescent City and less than two wavelengths were reached by Neah Bay.

These waves propagate between 60 to 100 km/day (Figure 12). Outliers for Balboa are probably associated with its geographical proximity to La Jolla. This analysis was also run with respect to Neah Bay instead of La Jolla, giving more reasonable phase speeds for Balboa, which were very similar to those determined by the Neah Bay/La Jolla pair.

For 1965-66, the coherence is not as high as for 1982-83. Although the phase speeds fall generally within 60 to 100 km/day, there are many outliers, especially 18.3 days (Figure 13). These outliers can be attributed to the reduced coherence of the series. Table 2 shows the number of cycles added and the coherence for the periods selected for 1965-66.

TABLE 2. 1965-66 SURFACE TEMPERATURE ANOMALY CROSS-SPECTRA: This table lists the complete cycles added per period for each station and the respective coherence.

Period in Days	Pacific Grove		Farallon Islands		Crescent City		Neah Bay	
	n	Coh	n	Coh	n	Coh	n	Coh
18.3	1	0.96	1	0.32	1	0.78	1	0.02
10.7	0	0.19	1	0.06	1	0.66	3	0.72
6.4	1	0.91	2	0.06	3	0.77	5	0.27
5.6	1	0.89	2	0.32	3	0.41	4	0.65

At virtually all frequencies and stations, the number of cycles added is the same for 1965-66 as for 1982-83 with a few differences of one cycle. The number of complete cycles added increases with distance from La Jolla and with increasing frequency (shorter periods) as expected from previously analyzing 1982-83. The patterns for increasing cycles to be added with increasing distance from La Jolla and increasing frequency as shown in Tables 1 and 2 are evident at less coherent frequencies as well.

Wavenumbers were calculated for each frequency and station from the phase speeds and distance relative to La Jolla. The wavenumber $\left(k_i\right)$ for each station (i) is:

$\left(k_i = \frac{\omega}{c} = \frac{\Delta\phi_i + 2\pi n}{2\pi\Delta y_i}\right)$, where c is the phase speed, $\Delta\phi_i$ is the phase difference from La Jolla to station (i), n is the number of cycles added, and Δy_i is the distance separating La Jolla from station (i). The mean and standard deviation wavenumbers based on all

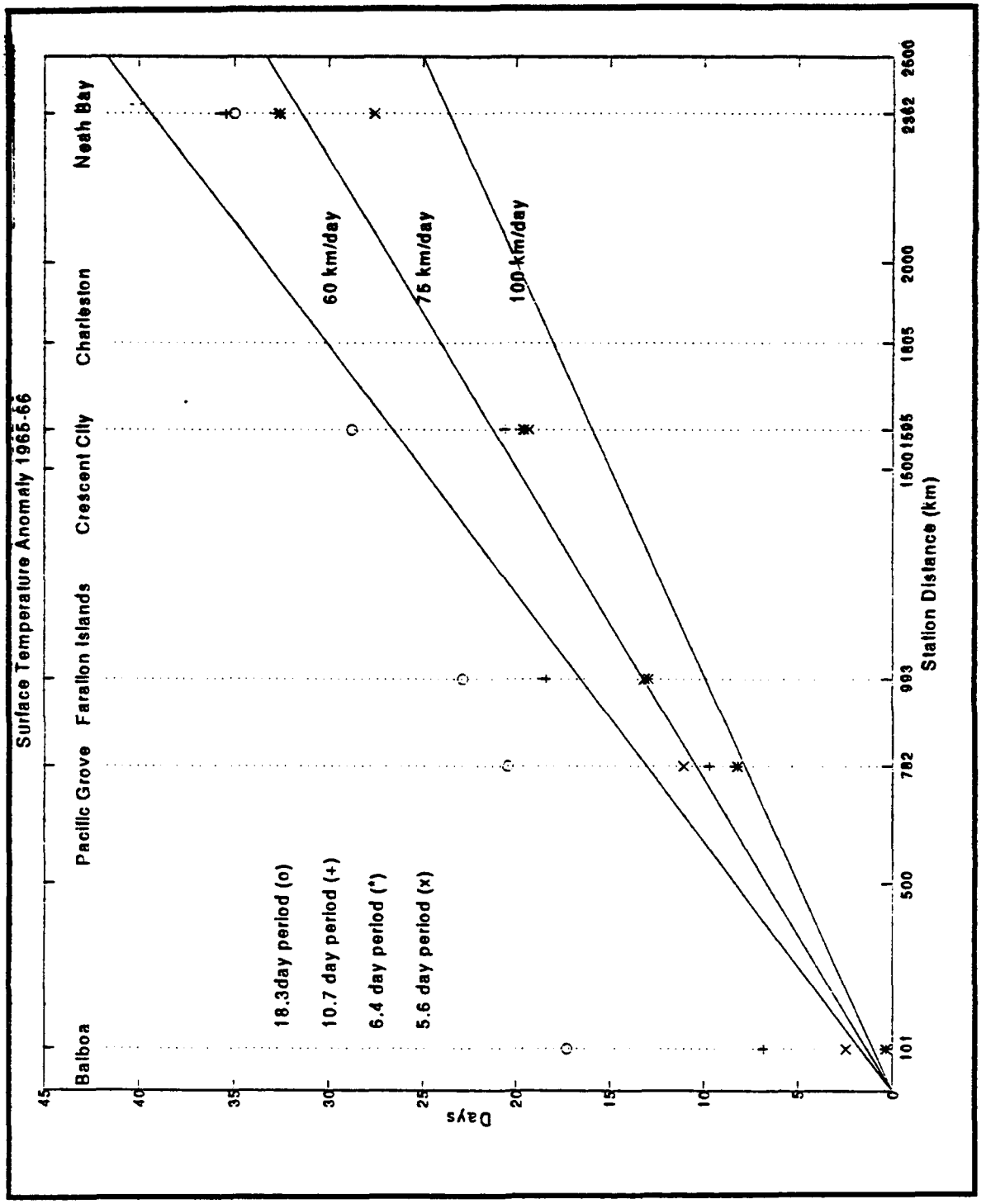

Figure 13. 1965-66 Surface Temperature Anomaly Phase Travel Times from La Jolla to the OtherStations for Selected Periods.

stations, except Balboa, were determined at each frequency. The mean wavenumber $\left(\bar{k}(\omega)\right)$ and the standard deviation wavenumber $\left(k_{std}(\omega)\right)$ are:

$\left(\bar{k}(\omega) = \sum_{i=1}^{5} k_i(\omega) \Big/ 5\right)$ and $\left(k_{std}(\omega) = \left[\sum_{i=1}^{5}\left(k_i(\omega) - \bar{k}_i(\omega)\right)\right]^2 \Big/ 4\right)$, respectively.

The results were plotted on a dispersion diagram (frequency versus wavenumber) for all 63 of the frequencies. The dispersion diagram for 1982-83 is shown as Figure 14. The standard deviation of the wavenumber is given by the horizontal error bars. A regression $\left(r^2 = 0.89\right)$ was performed and the slope of the least squares fit line is 65.7±8.2 km/day with a y-intercept of 0.015±0.016 cpd. Corrected to a zero y-intercept as per *Enfield and Allen* (1980), the slope is 72.4 km/day. *Enfield and Allen* (1980) calculated a 75 km/day phase speed using monthly sea level records. The placement of these points suggests that the represented waves are non-dispersive. Similar analysis to estimate the lowest mode shelf wave speeds (*Denbo and Allen*, 1987), which for the west coast is ~250 km/day (*Clarke and Brink*, 1985) provided unrealistic, poorly correlated results.

Frequency versus wavenumber for 1965-66 surface temperature is plotted on Figure 15. A regression $\left(r^2 = 0.98\right)$ was performed and the slope of the least squares fit line is 86.2±4.5 km/day with a y-intercept of -0.020±0.009 cpd. The plot is similar to the 1982-83 plot (Figure 14), further supporting the idea that these waves are non-dispersive.

b. Adjusted Sea Level Anomaly

The adjusted sea level anomaly employs only three stations. For 1982-83, the highly coherent periods of 14.2, 9.1, 6.4, and 5.3 days are plotted as travel times to each station (Figure 16). The phase speeds again fall in the 60 to 100 km/day range, with the actual phase speed being closer to 75 to 80 km/day. Adjusted sea level anomaly phase

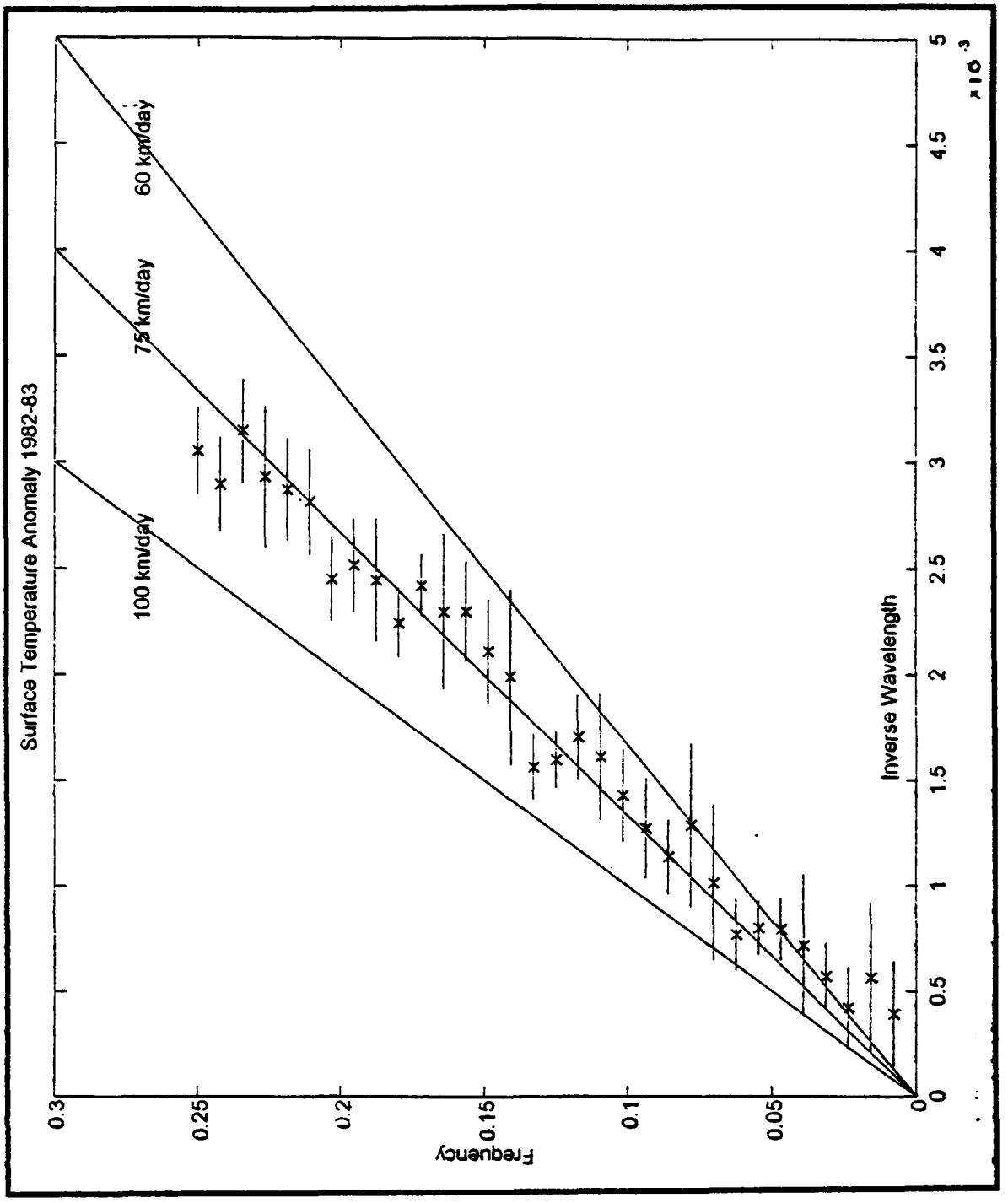

Figure 14. 1982-83 Surface Temperature Anomaly Dispersion Diagram. Frequency (ω) has units of (cpd), and the wavenumber (k) or inverse wavelength has units of (km^{-1}). The errorbars correspond to the standard deviation of the wavenumber.

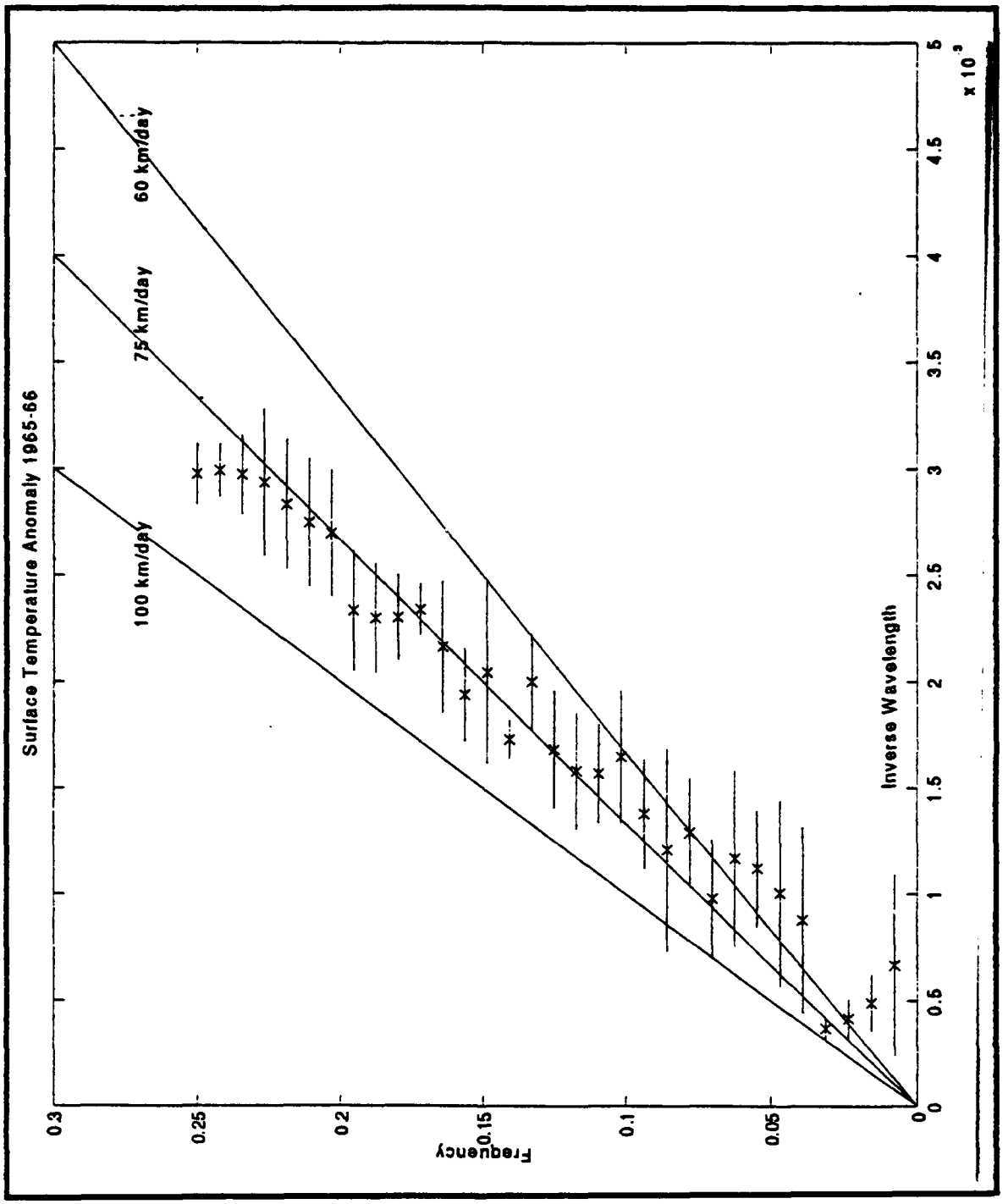

Figure 15. 1965-66 Surface Temperature Anomaly Dispersion Diaagram. Frequency (ω) has units of (cpd), and the wavenumber (k) or inverse wavelength has units of (km^{-1}). The errorbars correspond to the standard deviation of the wavenumber.

speeds are supportive of the surface temperature anomaly results. Table 3 shows the number of cycles added for the selected periods and the associated coherence values.

TABLE 3. 1982-83 ADJUSTED SEA LEVEL ANOMALY CROSS-SPECTRA: This table lists the complete cycles added per period for each station and the respective coherence.

Period in Days	Farallon Islands		Neah Bay	
	n	Coh	n	Coh
14.2	0	0.91	1	0.69
9.1	1	0.95	3	0.72
6.4	2	0.05	4	0.87
5.3	2	0.74	5	0.81

Table 3 shows that the number of additional cycles, indicative of the wavelength, are nearly identical to those for 1982-83 surface temperature anomalies.

The 1965-66 plot (Figure 17) is very similar to the 1982-83 plot. Although the 1965-66 sea level anomaly coherence is generally lower than for 1982-83 sea level anomaly, they are greater than for the 1965-66 surface temperature anomaly. Again complete cycles were added to the phase speeds as appropriate. The highly coherent periods used and the cycles added are shown in Table 4.

TABLE 4. 1965-66 ADJUSTED SEA LEVEL ANOMALY CROSS-SPECTRA: This table lists the complete cycles added per period for each station and the respective coherence.

Period in Days	Farallon Islands		Neah Bay	
	n	Coh	n	Coh
16.0	0	0.69	1	0.69
9.8	1	0.56	3	0.65
6.4	2	0.98	5	0.64
4.9	2	0.83	5	0.85

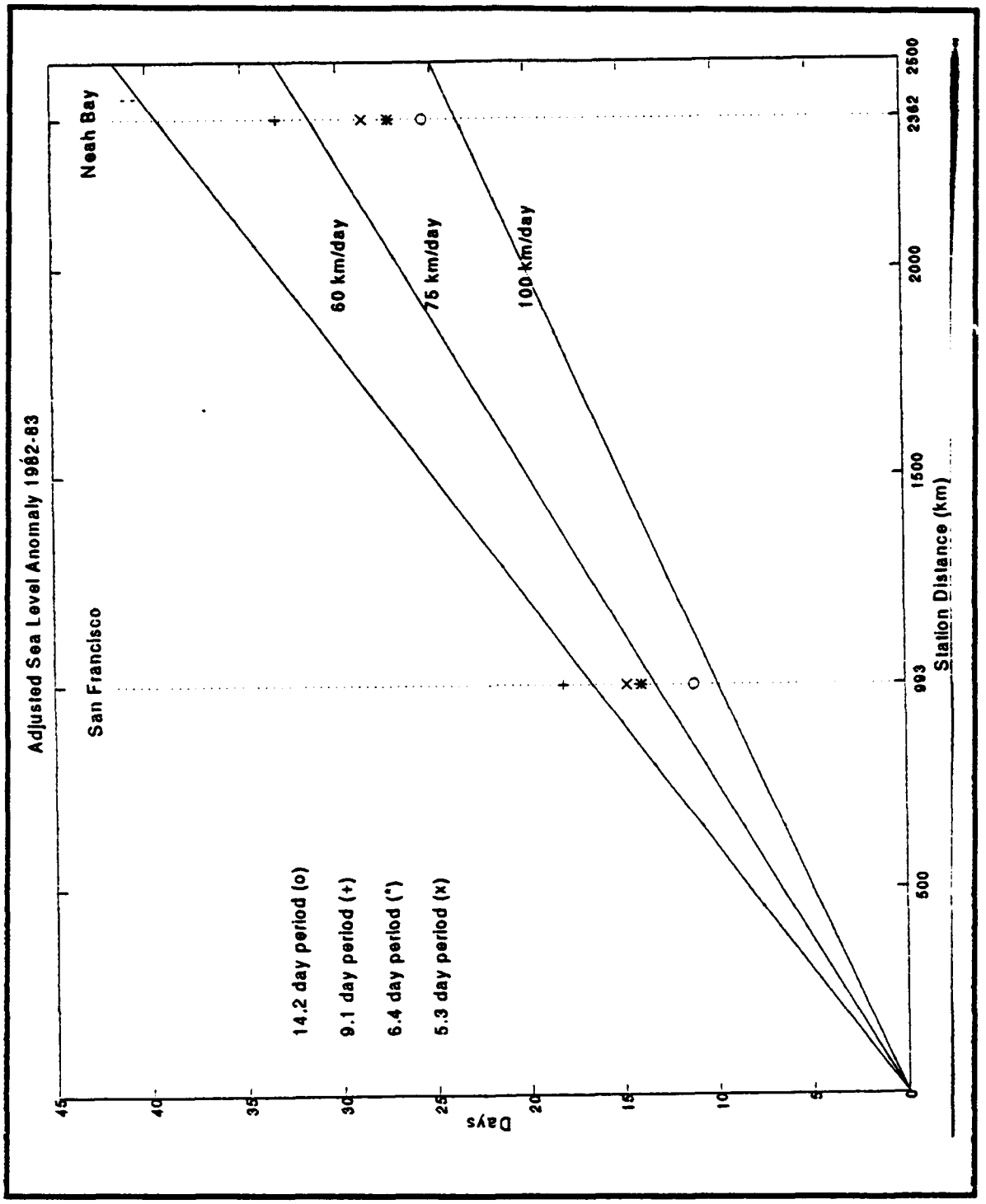

Figure 16. 1982-83 Adjusted Sea Level Anomaly Phase Travel Times from La Jolla to the OtherStations for Selected Periods.

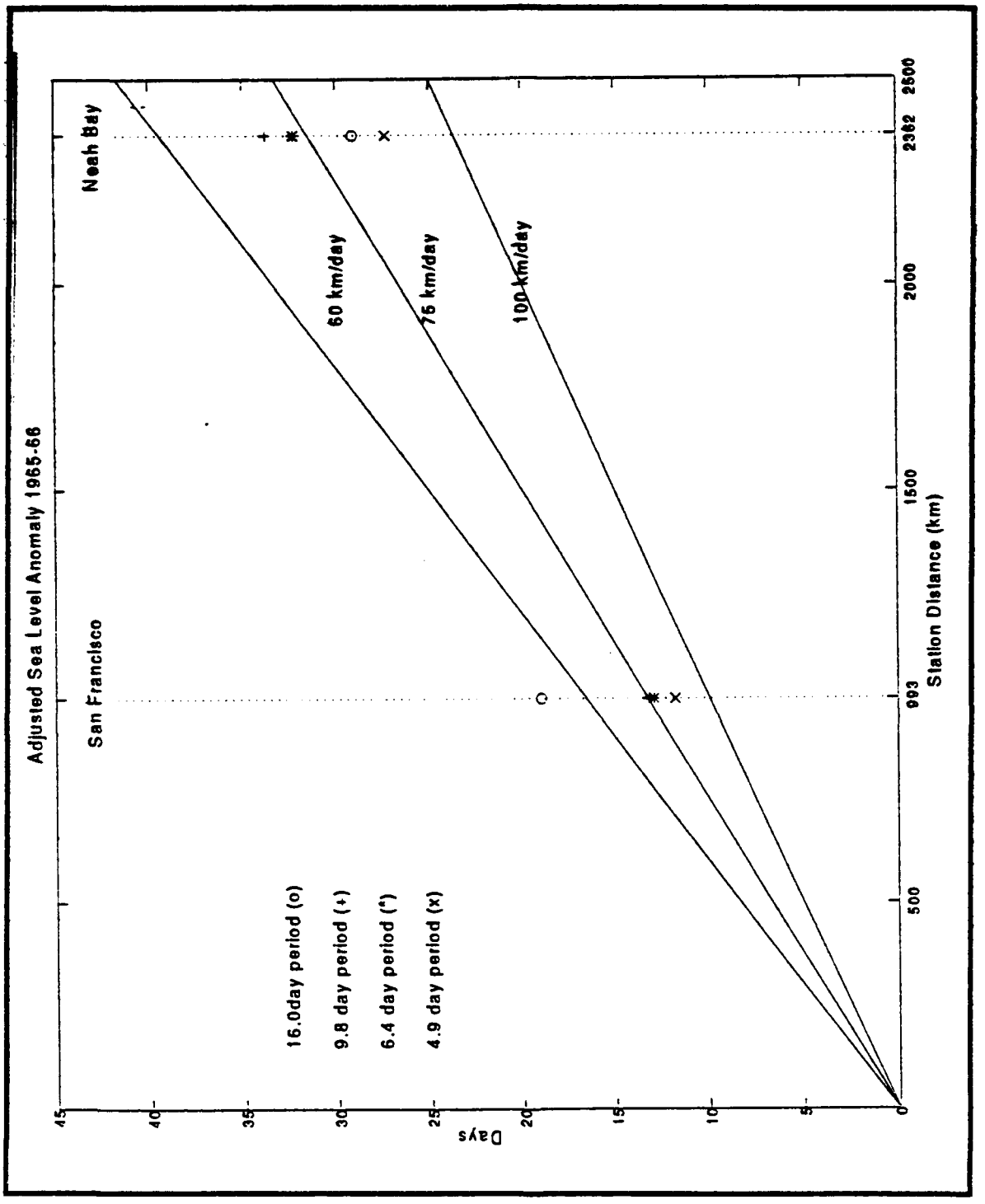

Figure 17. 1965-66 Adjusted Sea Level Anomaly Phase Travel Times from La Jolla to the OtherStations for Selected Periods.

Mean and standard deviation wavenumbers for each frequency were also calculated for the adjusted sea level anomaly in the same manner as for surface temperature anomaly. The dispersion diagram for 1982-83 is shown in Figure 18. Phase speeds fall between 60 and 100 km/day except at low frequencies, where phase speeds appear slower but not significantly so. The adjusted sea level wavenumbers collaborate with surface temperature and illustrate the 75 km/day phase speeds, and the non-dispersive nature of these waves. A regression $\left(r^2 = 0.97\right)$ was performed and the slope of the least squares fit line is 74.3±4.6 km/day with a y-intercept of 0.001±0.009 cpd.

The dispersion diagram for 1965-66 (Figure 19) is similar to 1982-83. The points fall between the phase speed lines of 60 and 100 km/day. A regression $\left(r^2 = 0.97\right)$ was performed and the slope of the least squares fit line is 83.8±4.9 km/day with a y-intercept of -0.011±0.009 cpd. This plot also supports these waves being non-dispersive.

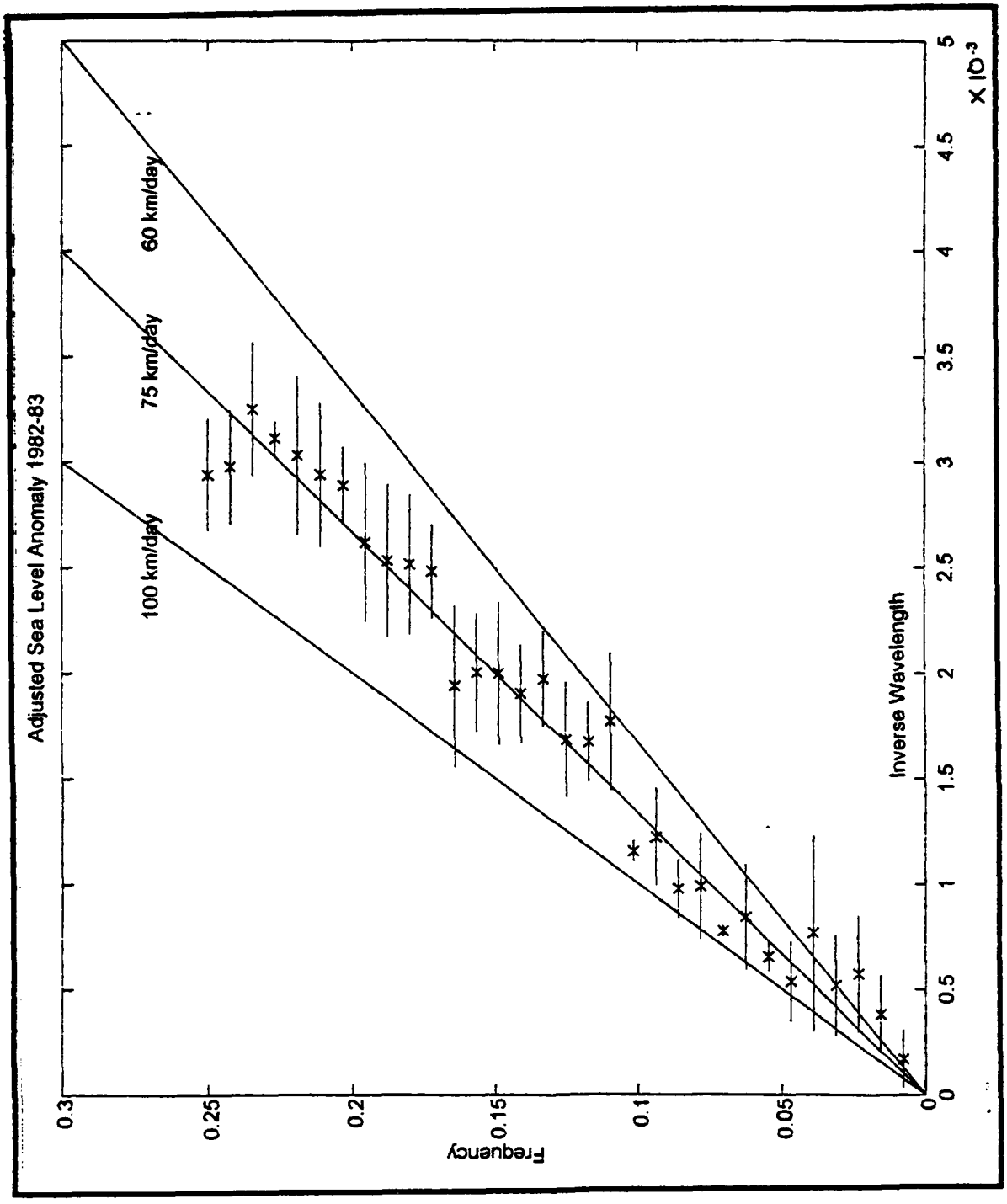

Figure 18. 1982-83 Adjusted Sea Level Anomaly Dispersion Diagram.
Frequency (ω) has units of (cpd), and the wavenumber (k) or inverse wavelength has units of (km^{-1}). The errorbars correspond to the standard deviation of the wavenumber.

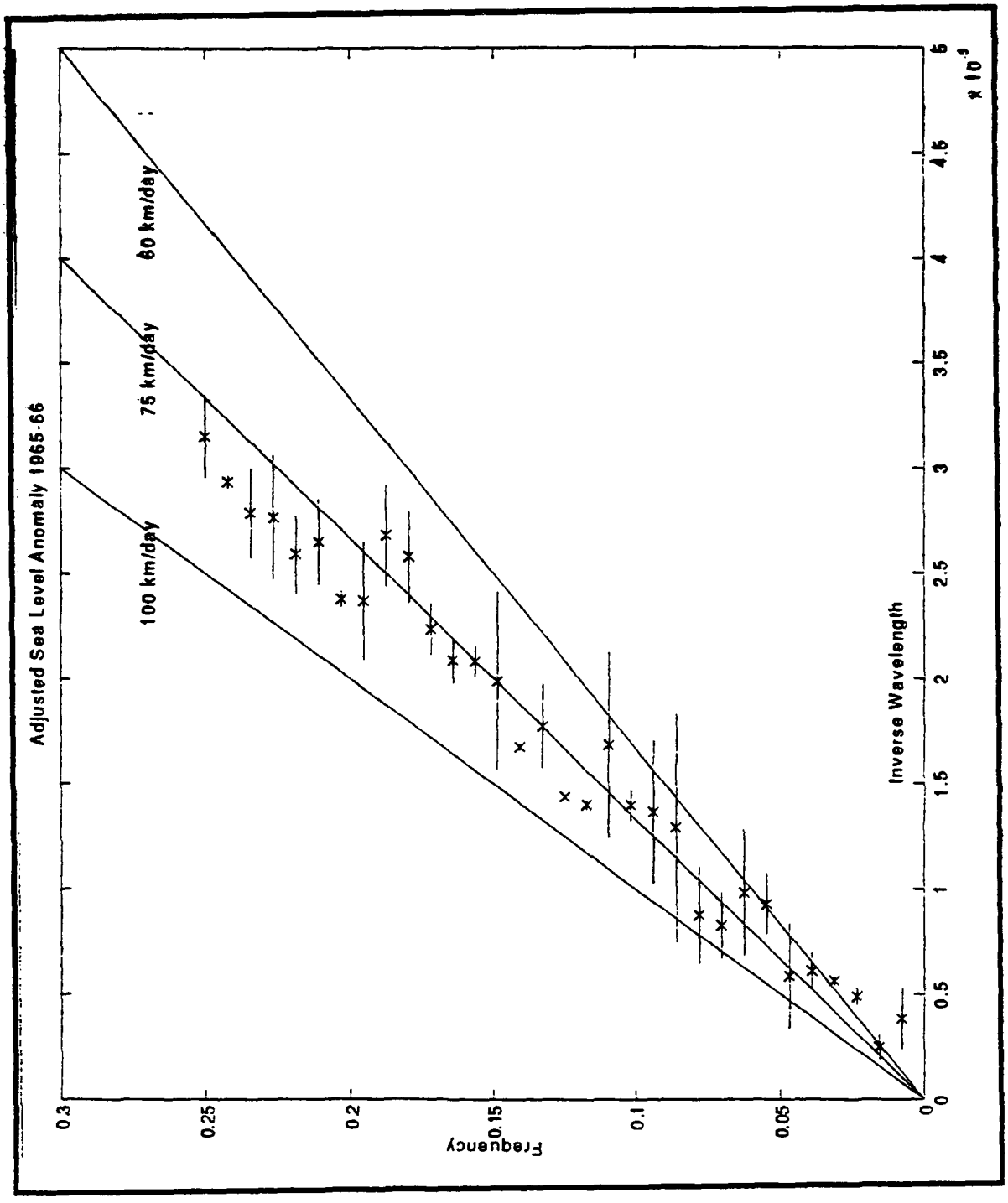

Figure 19. 1965-66 Adjusted Sea Level Anomaly Dispersion Diagram.
Frequency (ω) has units of (cpd), and the wavenumber (k) or inverse wavelength has units of (km^{-1}). The errorbars correspond to the standard deviation of the wavenumber.

IV. DISCUSSION OF RESULTS

The ENSO signal is transferred from its origin in the western Pacific by equatorially trapped Kelvin waves to the west coast of the Americas, (*Enfield*, 1989). Two responses occur at this boundary. Some of the wave energy is reflected back across the Pacific in the form of a westward propagating baroclinic Rossby wave, that may act to "turn off" the ENSO, and the rest of the energy is transmitted poleward in the form of the coastally trapped internal Kelvin waves (*Enfield and Allen*, 1980). The lower frequency waves tend to become the Rossby waves, but some of this energy may propagate poleward in both hemispheres as coastally trapped internal Kelvin waves (*Cane and Sarachik*, 1977). For an equatorially trapped Kelvin wave of frequency ω, the resulting wave will be the reflected Rossby wave if the Coriolis parameter f is less than f_o, where $f_o = \frac{1}{2}\beta c/\omega$ for a two-layer model on a β-plane with internal Kelvin wave phase speed c (*Enfield and Allen*, 1980). For $f > f_o$, the resulting wave is the coastally trapped internal Kelvin wave.

Along the west coast of the United States, internal Kelvin waves are one of the many types of subinertial coastal waves that can exist. The type of wave that dominates the coastal wave field is dependent on the latitude, stratification and bathymetry.

Using a continuously stratified model, a stratification parameter, called the Burger number, S, (*Mysak*, 1980) is given by $S = \frac{H^2 N_o^2 / f^2}{L^2}$, where H is bottom depth, N_o is the maximum of the Brunt-Väisälä frequency, L is the horizontal length (shelf width), and f is the Coriolis parameter. Two limiting cases of subinertial waves apply. For the case $(S \to 0)$, stratification is small and barotropic shelf waves dominate. For $(S \to \infty)$, stratification is strong and internal Kelvin waves dominate (*Huthnance*, 1978). For tne

purpose of this study, $S>>1$ implies internal Kelvin waves dominate over the barotropic shelf waves. For reasonable west coast values, H=1 km, $N_o^2 = 3x10^{-5}s^{-2}$, $f = 10^{-4}s^{-1}$, L=20 km, so S=7.5, with an internal Rossby radius of 55 km.

Using a two-layer model, internal Kelvin wave phase speed c can be estimated using

$$c = \left[\frac{g(\rho_2 - \rho_1)}{\rho_2} \cdot \frac{H_1 H_2}{H_1 + H_2} \right]^{1/2}, \quad \text{where} \quad \left[\frac{g(\rho_2 - \rho_1)}{\rho_2} \right]$$ is reduced gravity, and

H_1 , ρ_1 and H_2, ρ_2 are the thickness and density of the surface layer (1) and deep layer (2). For typical west coast values, g=9.81 m/s^2, $\rho_1 = 1025\ kg/m^3$, $\rho_2 = 1026\ kg/m^3$, $H_1 << H_2$, $H_1 = 100$ m, $c = 84.5$ km/day. This value is similar to the value obtained using a similar model by *Enfield and Allen* (1980).

For all the ENSO events in this study except 1982-83, the onset of the ENSO is typically marked by an anomalous westerly component of the zonal winds near the dateline during December prior to the ENSO year (*Enfield*, 1989). By April of the ENSO year, the equatorial Kelvin waves have started to force anomalously warm sea surface temperatures and high sea levels poleward along the equatorial coast of South America. In September, a transition phase occurs that does not have warm sea surface temperature anomalies off Peru, but shows strengthening of the wind and sea surface temperature anomalies in the central Pacific. This pattern continues through the mature phase in January. Coastal sea surface temperatures then drop to anomalously low values in May following the ENSO year (*Enfield*, 1989). In contrast for 1982-83 event, the sea surface temperature anomalies were delayed by six months until October off Peru. The sea surface anomalies near the dateline actually preceded the coastal warming.

For the oceanic teleconnection, the most important feature of the ENSO lifecycle is the formation of the coastally trapped internal Kelvin waves, that start forming when the

warm anomaly commences off Peru. The time delay for the teleconnection poleward to the California, Oregon and Washington stations is between two and three months, assuming these coastally trapped Kelvin waves are the transport medium. The positive surface temperature and sea level anomalies roughly correspond to the time delays inherent in the teleconnection, with the first anomalies occurring in July and August time frame. The end of the event also roughly corresponds to the following June to July time frame. Locally forced events tend to mask the actual onset and end of the ENSO along the west coast. The atmospheric teleconnection also impacts the signal. The observed signature of 1982-83 event off the west coast does not commence substantially later in the year than the other strong events probably due to this partial masking and the atmospheric teleconnection impact.

Simpson (1984a) speculates that the expansion and intensification of the Aleutian Low and the decrease in the strength of the Pacific high during 1982-83 produced an anomalous atmospheric condition which coupled directly with the large-scale oceanic circulation to produce the California ENSO of 1982-83. The existence of high sea surface temperature and sea level anomalies were attributed to the onshore transport of subarctic water and not due to internal Kelvin waves, which cannot by their nature move water cross-shelf (*Gill,* 1982). *Simpson* (1984a and 1984b) and *Enfield and Allen* (1980) focus on the climatology of the ENSO and not on an event scale as does this study.

This study focuses on internal Kelvin waves from propagating events, which may have been oceanically forced from the equator or meteorologically forced from the coast of the Americas. Two mechanisms seem applicable to the surface temperature and sea level changes. Poleward advection of warm water causes the high surface temperature and sea level anomalies to be in phase. For an existing vertical thermal structure, surface temperature and sea level changes are out of phase, where the internal Kelvin wave

displaces the thermocline, producing increased temperature at the surface and a set down in sea level. Cross-spectral results in general show surface temperature leads sea level, but are not conclusive for determination of the dominant mechanism.

During an ENSO compared with non-ENSO years, the surface temperature and adjusted sea level anomalies do appear elevated and more spatially coherent between stations along the west coast of the United States. This is especially true of the strong events. A general warming or sea level rise has occurred, onto which higher frequency events are superimposed. These higher frequency events do not have a distinct, unvarying pattern between stations or between events for a single station, but are useful in tracking propagation.

1972-73 has interesting characteristics, that are unique in terms of recent ENSO events. This ENSO is not reflected by the time series at Neah Bay, or other Northwest Pacific stations as a positive temperature or sea level anomaly (*Schwing*, 1993). The poleward teleconnection is lost prior to reaching these stations. The 1972-73 event along the west coast is best described as an oceanic ENSO, without the atmospheric teleconnection. It is the best recent example of sole oceanic tropical to mid-latitude teleconnection. Sea surface temperature provides the best contrast between ENSO years for this determination in our analysis. *Norton et al.* (1985) found the positive anomaly for this event similar to the 1982-83 event for subsurface temperature and sea level, but was attenuated by the CCS for surface temperature. Without the atmospheric teleconnection, or Pacific Northwest Anomaly (PNA) atmospheric adjustment (*Norton et al.* 1985), the oceanic teleconnection is negated by locally forced processes.

Cross-spectral analysis of surface temperature and adjusted sea level anomalies for La Jolla versus each of the other stations provides a mechanism to quantify the propagation of events at all frequencies. The results show features propagating poleward in both data

sets at phase speeds of 60-100 km/day. Two different ENSO years were analyzed with the same results for both parameters. These phase speeds are consistent with phase speed estimated for coastally trapped internal Kelvin waves.

Enfield and Allen (1980) focused on interannual events as precursors to the actual ENSO event and developed phase speeds for the propagation of these forcing events. This analysis focuses on the features imbedded within the ENSO event and determines the phase speeds of these features. The physics of the forcing should be consistent with the physics of the maintenance of the ENSO event, so the phase speeds can be compared for these non-dispersive internal Kelvin waves.

The source of these internal Kelvin waves has not been found in this analysis. The source could be from the equator or from off the coast of Mexico (*Murphree, T.*, personal communication) due to a disruption of the waveguide by the Gulf of California. Further research is required for resolution of the actual source.

V. CONCLUSIONS AND RECOMMENDATIONS

Two basic conclusions can be drawn from these time and frequency domain analyses of daily surface temperature and adjusted sea level data:

(1) During ENSO episodes, strong warm surface temperature anomalies exist along the west coast and are supported by high adjusted sea level anomalies.

(2) Warm and cool events at periods of 4-20 days are superimposed on warm surface temperature anomalies for strong ENSO years. These events propagate to the north with phase speeds consistent with internal Kelvin wave theory. Their existence is supported by similar propagating features in the sea level anomaly records.

All ENSO years at all stations selected, except 1972-73 at Neah Bay, exhibited warm surface temperature anomalies and high sea level anomalies. The strong ENSO years of 1957-58 and 1982-83 most closely resembled each other and generally had the largest anomalies. The moderate ENSO years showed great variability in the duration and strength of the anomaly allowing no conclusion on the nature of the signal for the moderate event other than variable. The ENSO of 1972-73 did not extend to Neah Bay, since the ENSO was of the oceanic variety and was not atmospherically teleconnected to these latitudes.

During the strong ENSO years, short duration warm and cool events at less than annual frequencies corresponding to 4-20 day periods, such as those found off Peru by *Smith* (1978), propagate poleward. The phase speed of these propagating events was found in the range of 60-100 km/day. For 1982-83 and 1965-66 surface temperature anomalies, the phase speeds were found to be 65.7±8.2 km/day and 86.2±4.5 km/day, respectively. For 1982-83 and 1965-66 adjusted sea level anomalies, the phase speeds

were found to be 74.3±4.6 km/day and 83.8±4.9 km/day, respectively. These phase speeds are consistent with the phase speeds of internal Kelvin waves for the west coast of the United States, based on theory and other observations. Coastally trapped internal Kelvin waves can transmit the ENSO signal from the equatorial region poleward (*Enfield and Allen*, 1980; *Chelton and Davis*, 1982).

Monthly averaged data have traditionally been used in the analysis of long-term patterns of coastal phenomena. Sea level, due to its steric properties, is employed most extensively. Daily data sets have not been used as frequently due to concern about the "noise" of high frequency events and inherent daily variability through both natural processes and human sampling error. However, the monthly average loses information when it is averaged and lacks adequate temporal resolution for time-dependent calculations such as phase speed. The 180±100 km/day phase speed, using monthly averaged sea level data (*Enfield and Allen*, 1980), is an example of this temporal uncertainty. Proper filtering of the daily data allows for improved temporal resolution without inordinate biasing of the data by high frequency "noise". Daily sea surface temperature provides effective analysis with the same quality of results as the adjusted sea level data for this study. Sea surface temperature is also useful because of the availability of good quality long term data sets.

Recommendations for future research are:

(1) Perform analysis for the 1991-93 ENSO.

(2) Perform analysis for additional North American stations, and representative South American stations.

(3) Perform supportive analysis using salinity data.

The 1991-93 ENSO event is unique and impressive for its strength and duration. Extension of the analysis to this event allows for investigation of any dissimilarities and possible extension of the conclusions from the present analysis.

Adding equatorial and other South American data could show the teleconnection of internal Kelvin waves from an equatorial source to the California stations, and a corresponding teleconnection in the Southern Hemisphere. Increasing the spatial separation for the analysis and providing mirrored teleconnection for the Southern Hemisphere would allow for a lagged cross-correlation phase speed calculation. The resolution using daily data would likely be better than 180±100 km/day that was found from monthly average sea level data (*Enfield and Allen*, 1980). Extension north along the Canadian coast would help define the impact of the Aleutian Low and the actual extent of the oceanic teleconnection. Further analysis of data from additional stations on the coast of the United States to further support these findings would also be useful.

Salinity analysis could be used to corroborate with the surface temperature analysis, since the internal Kelvin wave would carry a strong salinity anomaly signal.. Salinity data is available for the stations currently used in this study and along the west coast of Canada.

APPENDIX A - FARALLON ISLANDS TEMPERATURE FILLED BY BODEGA BAY

Farallon Islands surface temperature data set had many short gaps and was generally missing data from January and February, when weather conditions precluded observations. Bodega Bay was used to help fill these gaps, because it is geographically close to the Farallon Islands and has a similar signal. The data were divided into the three-year periods used for analysis as described in section II. A regression was performed for each period to insure the best estimated fit could be produced. If a Bodega Bay value was available, when a gap occured, in the Farallon Islands data, it was multiplied by the slope of the least squares fit between the two series and then the y-intercept was added. This value became the new Farallon Islands value. If no Bodega Bay value was available a linear fit was performed on Farallon Islands. Figures A.1-3 show representative fitting of Farallon Islands. The percentage fit by Bodega Bay and the r^2 value for the regression are shown in Table 5.

TABLE 5. PERCENTAGE FIT BY BODEGA BAY INTO FARALLON ISLANDS SURFACE TEMPERATURE AND r^2 OF THE REGRESSION:

This table lists the percentage fit by Bodega Bay for each three-year period and the associated r^2 of the regression.

Period	Percent Fit	r^2
1956-58	20	0.52
1960-62	94	0.47
1964-66	87	0.26
1971-73	61	0.38
1974-76	70	0.76
1978-80	62	0.63
1981-83	56	0.78
1986-88	36	0.57

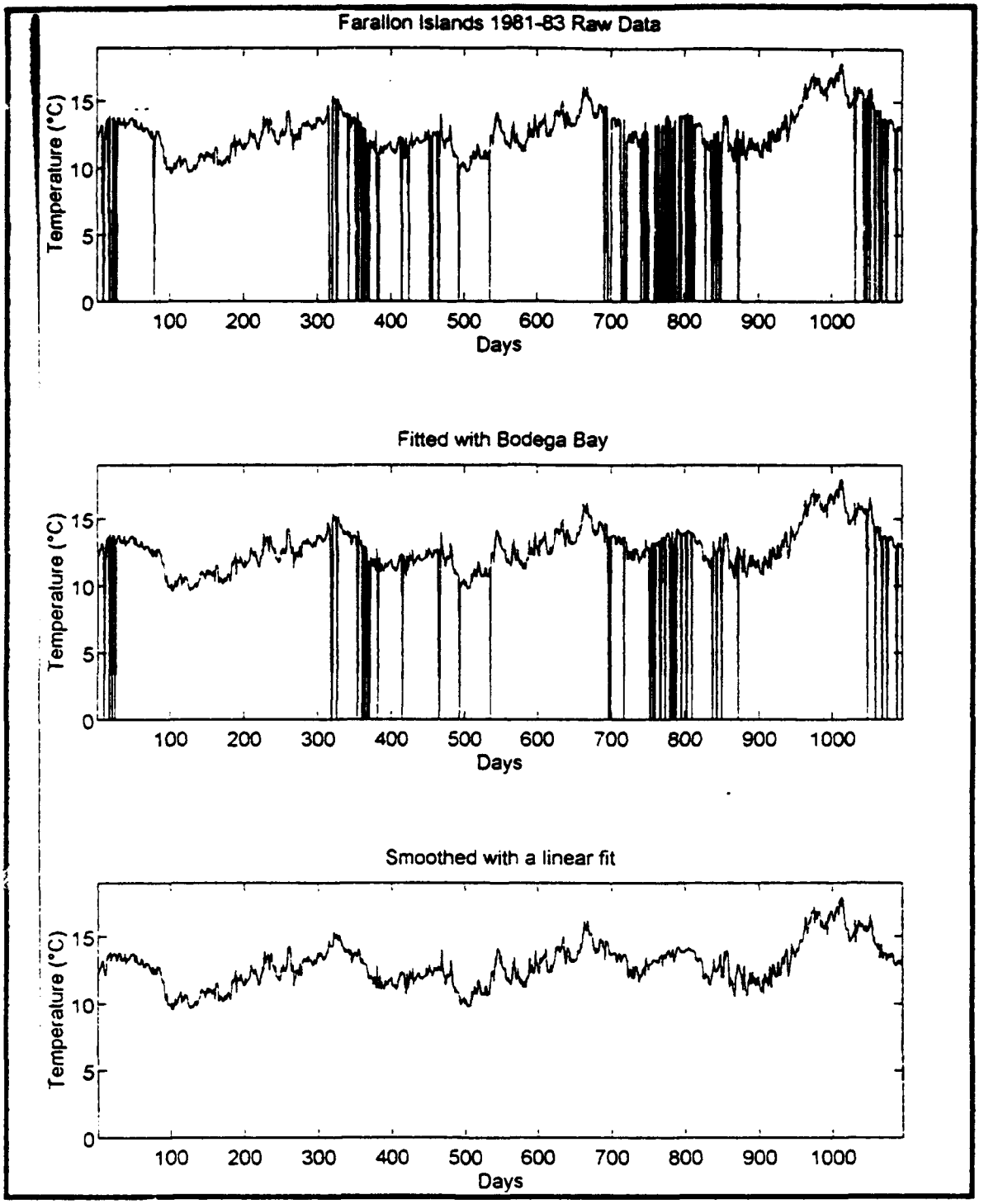

Figure A.1. 1956-58 Surface Temperature Filling of Farallon Islands by Bodega Bay.

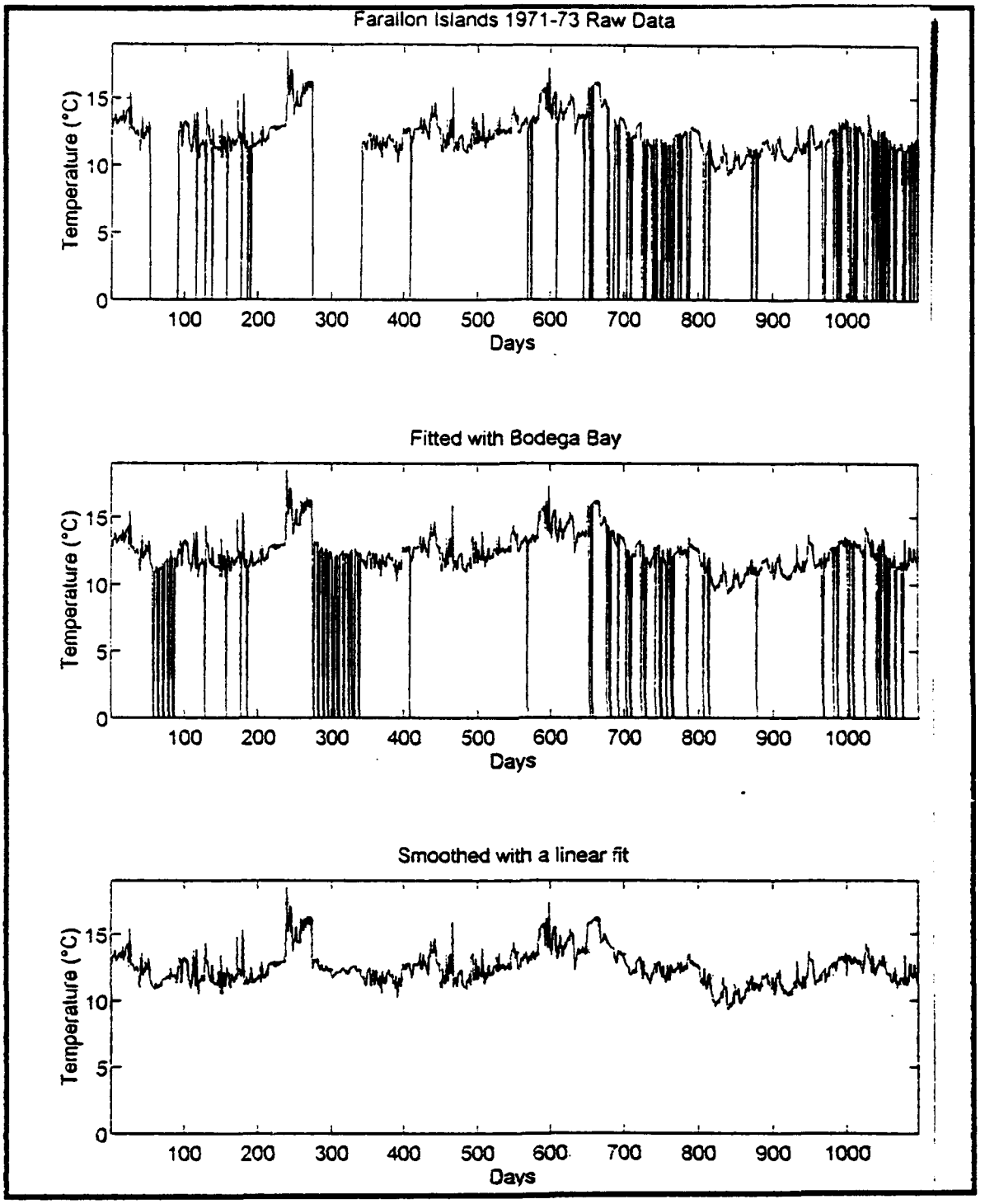

Figure A.2. 1971-73 Surface Temperature Filling of Farallon Islands by Bodega Bay.

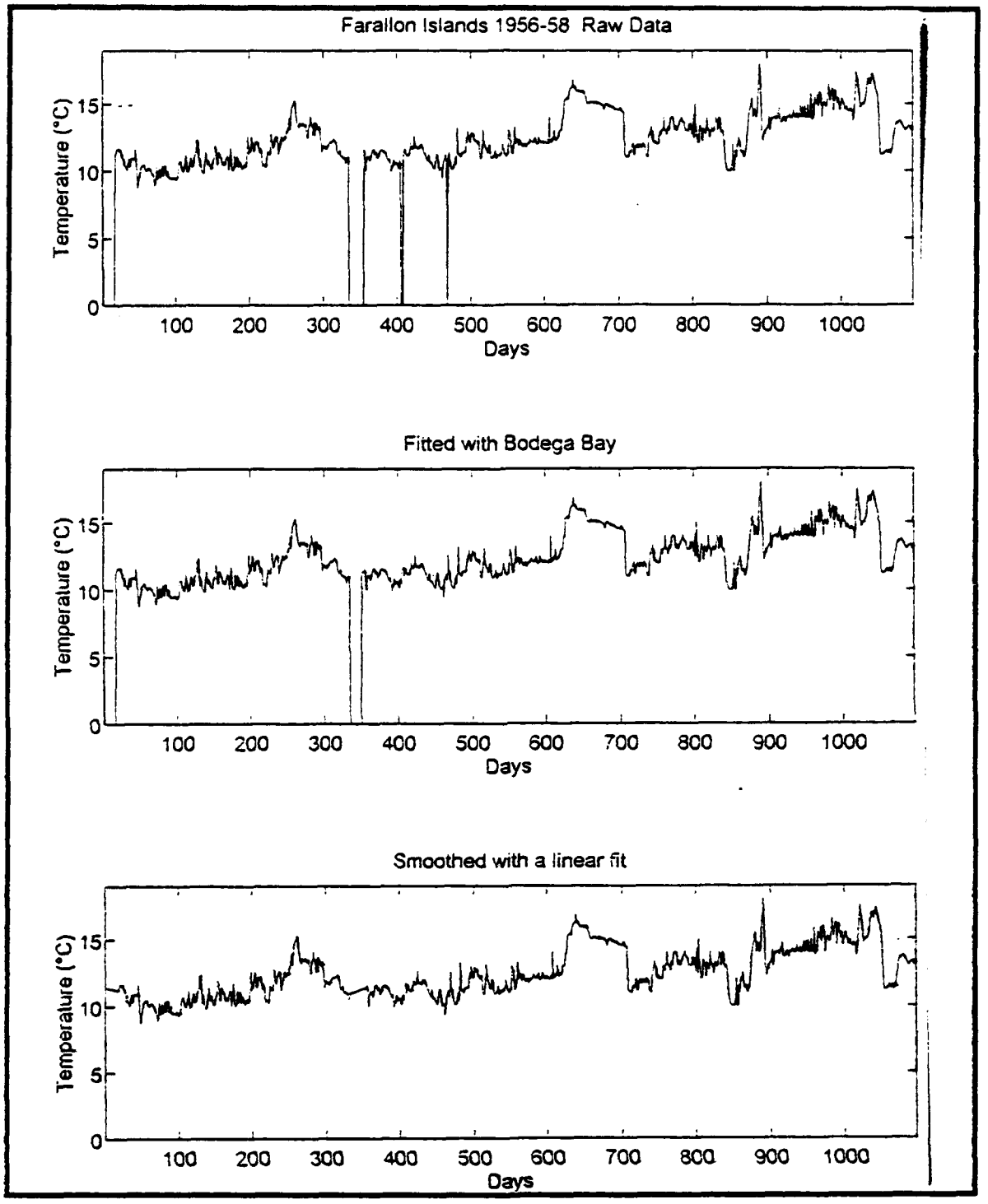

Figure A.3. 1981-83 Surface Temperature Filling of Farallon Islands by Bodega Bay.

APPENDIX B - TEMPERATURE OBSERVATIONS PER MONTH

The daily surface temperature data was initially analyzed to insure sufficient frequency of data collection for any meaningful follow-on analysis. Each station has been displayed as number of observations per month for each month since 1955, or 1966 for Charleston. La Jolla and Balboa are the best stations for consistently high observations per month (Figures B.1). Pacific Grove is also exce t (Figure B.2). Farallon Islands shows the reduction of observations primarily in the w er months (Figure B.2). This is the reason Bodega Bay was employed to help fill. Crescent City and Charleston are not nearly as good quality (Figures B.3). Neah Bay is the best northern region station, but not even close to the southern stations (Figure B.3).

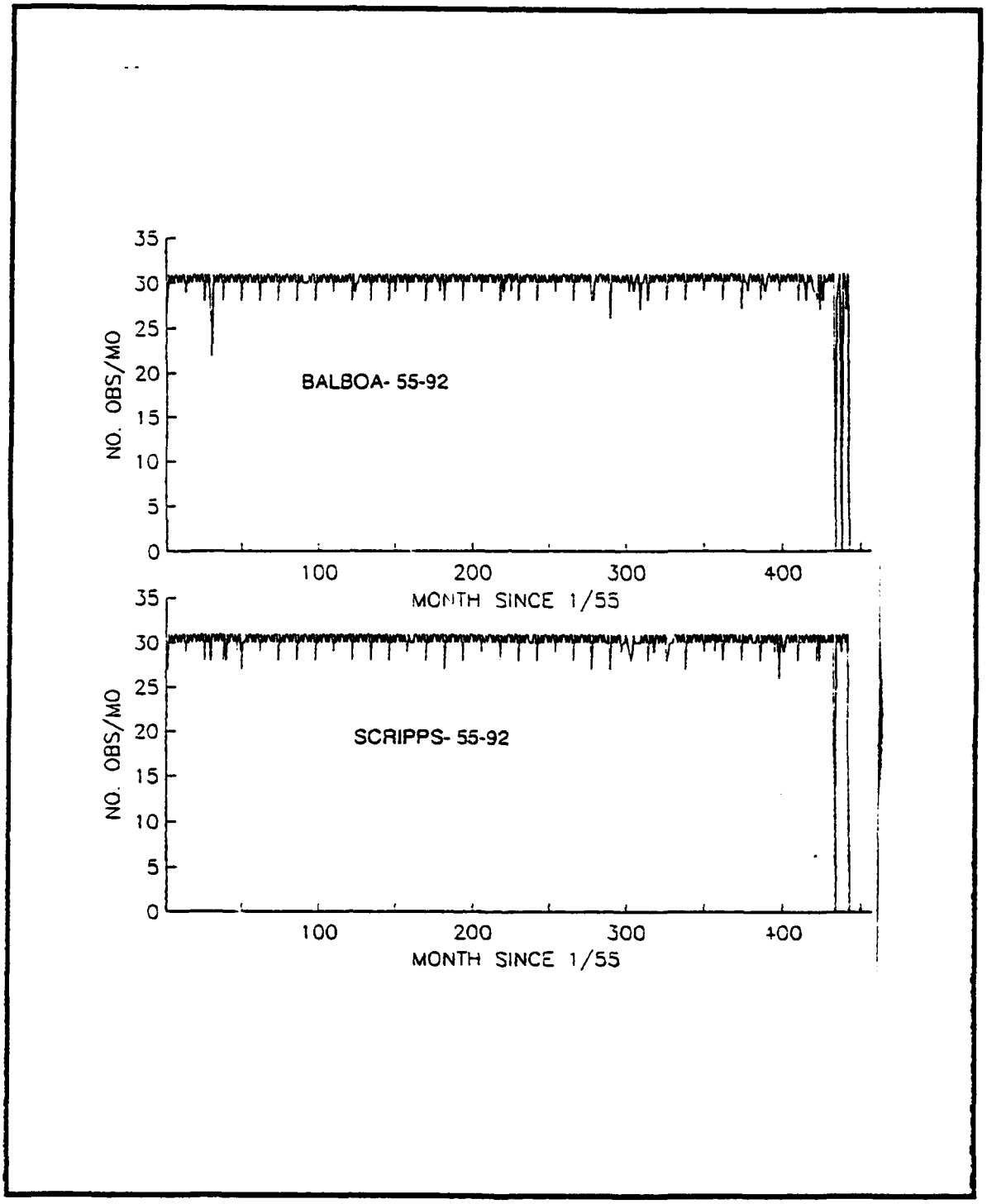

Figure B.1. Monthly Number of Surface Temperature Observations for La Jolla and Balboa.

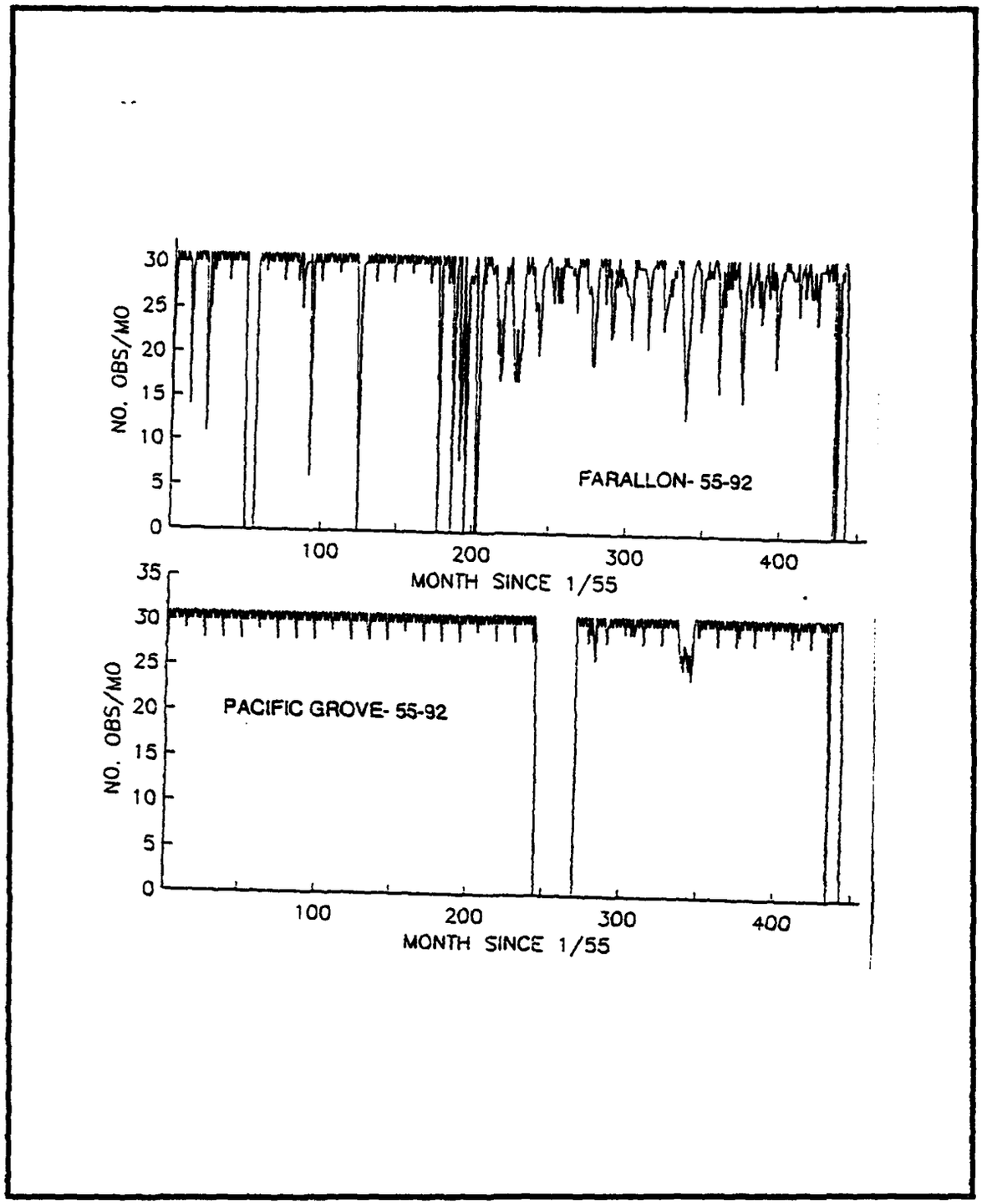

Figure B.2. Monthly Number of Surface Temperature Observations for Pacific Grove and Farallon Islands.

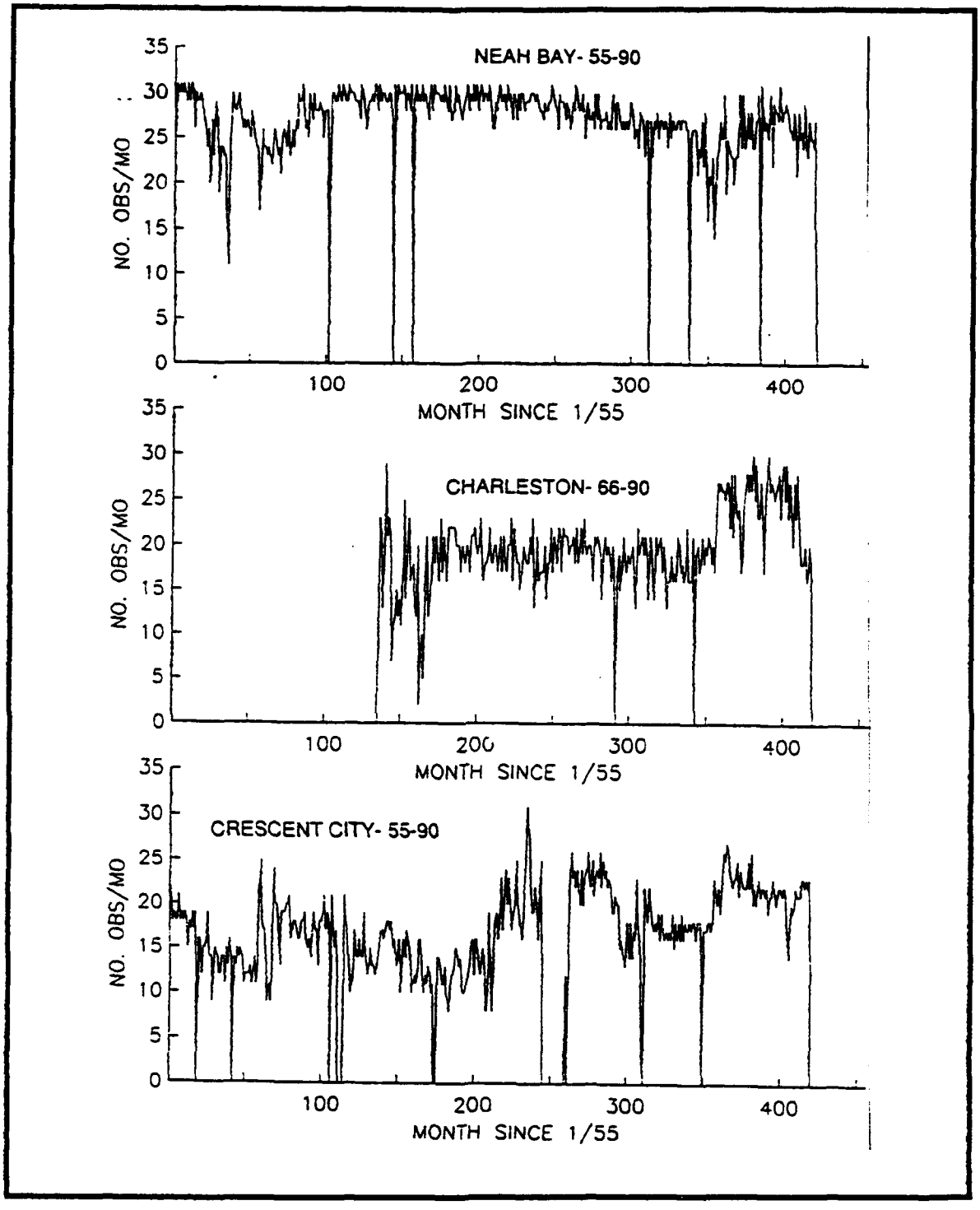

Figure B.3. Monthly Number of Surface Temperature Observations for Crescent City, Charleston and Neah Bay.

REFERENCES

Cane, M. A., and E. S. Sarachik, 1977: Forced baroclinic ocean motions, II, The linear equatorial bounded case, *J. Mar. Res.*, **35**, pp. 395-432.

Cayan, D.R., D. R. McLain, W. D. Nichols, and J. S. DiLeo-Stevens, 1988: Monthly climatic time series data from the Pacific Ocean and western Americas, *USCGS Open File Report*, 379 pp.

Chelton, D. B., and R. E. Davis, 1982: Monthly mean sea level variability along the west coast of North America, *J. Phys. Oceanogr.*, **12**, pp. 757-784.

Clarke, A. J., and K. H. Brink, 1985: The reponse of stratified, frictional flow of shelf and slope waters to fluctuating large-scale, low-frequency wind forcing, *J. Phys. Oceanogr.*, **15**, pp. 439-453.

Denbo, D. W., and J. S. Allen, 1987: Large-scale response to atmospheric forcing of shelf currents coastal sea level off the west coast of North America: May-July 1981 and 1982, *J.Geophys. Res.*, **92**, pp. 1757-1782.

Enfield, D. B., 1989: El Niño, Past and Present, *Rev. of Geophys.*, **27**, pp. 159-187.

Enfield, D.B., and J.S. Allen, 1980: On the structure and dynamics of monthly mean sea level anomalies along the Pacific coast of North and South America, *J. Phys. Oceanogr.*, **10**, pp. 557-588.

Gill, A. E., 1982: *Atmospheric-Ocean Dynamics*, Academic Press, New York, 662 pp.

Hickey, B., 1979: The California current system - hypothesis and fact, *Prog. Oceanog*, **8**, pp.191-279.

Huthnance, J. M., 1978: On coastal trapped waves:analysis and numerical calculationby inverse iteration, *J. Phys. Oceanogr.*, **8**, pp. 74-92.

Huyer, A., and R. L. Smith, 1985: The signature of El Niño off Oregon, 1982-1983, *J.Geophys. Res.*,**90**, pp.7,133-7,142.

Little, J. N. and L. Shule, 1992: *Signal Processing Toolbox, User's Guide,* Math Works, Inc.

Mysak, L., 1980: Recent advances in shelf wave dynamics, *Rev. Geophy. Space Phys.*, **18**, pp.211-241.

Nelson, C.R., 1977: Wind stress and wind stress curl over the California current, *NOAA Technical Report SSRF-714*, U.S. Dept. of Commerce, 87 pp.

Norton, J., D. McLain, R. Brainard, and D. Husby, 1985: The 1982-83 El Niño event off Baja and Alta California and its ocean climate context, *El Niño North: Niño Effects in the Eastern Subarctic Pacific Ocean*. University of Washington Sea Grant, Seattle, pp.44-72.

Oppenheim, A.V. and R.W. Schafer, 1975: *Digital Signal Processing*, Prentice-Hall, 556pp.

Quinn, W. H., V. T. Neal, and S. Antunez de Mayolo, 1987: El Niño occurrences over the past four and a half centuries, *J.Geophys. Res.*, **92**, pp. 14,449-14,461.

Rasmusson, E. M., and T. C. Carpenter, 1982: Variations in tropical sea surface temperature and surface wind fields associated with the Southern Oscillation/El Niño, *Mon. Weather Rev.*, **110**, pp. 354-384.

Robinson, M. K., 1972: The use of a common reference period for evaluating climatic coherence in temperature and salinity records from Alaska and California, *CalCOFI Rep.* 8:121-130.

Simpson, J. J., 1984a: El Niño-induced onshore transport in the California Current during 1982- 83, *Geophys. Res. Lett.*, **11,** 233-236.

Simpson, J. J., 1984b: A simple model of the 1982-83 California "El Niño," *Geophys. Res. Lett.*, **11,** 237-240.

Smith, R. L., 1978: Poleward propagating perturbations in currents and sea levels along the Peru coast, *J. Geophys. Res.*, **83**, pp.379-391.

Schwing, F. B., 1993: Long-term and seasonal patterns in coastal temperature and salinity along the North American west coast, 1993 PACLIM Proceedings, in press.

Wooster, W.S., and L. Fluharty (Eds.), 1985: *El Niño North: Niño Effects in the Eastern Subarctic Pacific Ocean,* 312 pp. University of Washington Sea Grant, Seattle.

INITIAL DISTRIBUTION LIST

		Number of Copies
1.	Defense Technical Information Center Cameron Station Alexandria, VA 22304-6145	2
2.	Librarian, Code 52 Naval Postgraduate School 411 Dyer Rd Rm 104 Monterey, CA 93943-5101	2
3.	Oceanography Department Code OC/CO Naval Postgraduate School 833 Dyer Rd Rm331 Monterey, CA 93943-5122	2
4.	Meteorology Department Code MR/HY Naval Postgraduate School 589 Dyer Rd Rm 252 Monterey, CA 93943-5114	1
5.	Dr. F.B. Schwing Pacific Fisheries Environmental Group PO Box 831 Monterey, CA 93942	1
6.	Dr. L. K. Rosenfeld Code OC/RO Naval Postgraduate School 833 Dyer Rd Monterey, CA 93943-5122	1

7.	Captain C.S. Nelson Deputy Director, Office of Ocean and Earth Sciences National Oceanic and Atmospheric Administration 1305 East-West Highway, Station 10116 Silver Springs, MD, 20910	1
8.	Commanding Officer Naval Oceanographic Office Stennis Space Center, MS 39529-5001	1
9.	Lt. John B. Skillman, USN 1521 St. Luke Dr. Beavercreek, OH 45432	1
10.	Prof. Tom Royer Department of Oceanography University of Alaska Fairbanks, AK 99709	1
11.	Library Scripps Institution of Oceanography P.O. Box 2367 La Jolla, CA 92037	1
12.	Library Royal Roads Military College FMO Victoria, B.C. Canada VOS IBO	1